Cortical motor network modulation:

Common mechanisms parallel efficient motor integration in implicit motor learning in healthy subjects and subthalamic neurostimulation in Parkinson's disease

Inaugural-Dissertation

zur Erlangung des Doktorgrades

der Medizin

der Medizinischen Fakultät

der Eberhard Karls Universität

zu Tübingen

vorgelegt von

Klotz, Rosa

2014

Dekan: Professor Dr. I. B. Autenrieth

1. Berichterstatter: Professor Dr. R. Krüger

2. Berichterstatter: Professor Dr. C. Braun

To my family

Table of contents

List of abbreviations

AD	Alzheimer’s disease
CMC	Corticomuscular coherence
CNS	Central nervous system
DBS	Deep brain stimulation
ED	Extensor digitorum
EEG	Electroencephalography
EMG	Electromyography
ERD	Event-related desynchronization
ERS	Event-related synchronization
ERSP	Event-related spectral perturbation
FD	Flexor digitorum
HC	Healthy control
LED	L-Dopa equivalent dosage
MEG	Magnetoencephalography
MRD	Movement-related desynchronization
MRI	Magnetic resonance imaging
MRS	Movement-related synchronization
PD	Parkinson’s disease
PET	Positron emission tomography
PSD	Power spectral density
SM1	Primary sensory motor cortex
SMA	Supplementary motor area
SRTT	Serial reaction time task
[StimOff]	Subthalamic stimulation off

[StimOn]	Subthalamic stimulation on
STN	Subthalamic nucleus
STN-DBS	Deep brain stimulation of the subthalamic nucleus
TMS	Transcranial magnetic stimulation
UPDRS	Unified Parkinson's Disease Rating Scale

List of figures

List of tables

1 Introduction

"…we still haven't unlocked the mystery of the three pounds of matter that sits between our ears. But today, scientists possess the capability to study individual neurons and figure out the main functions of certain areas of the brain. But a human brain contains almost 100 billion neurons making trillions of connections…

…So there is this enormous mystery waiting to be unlocked, and the 'BRAIN' Initiative will change that by giving scientists the tools they need to get a dynamic picture of the brain in action and better understand how we think and how we learn and how we remember…

…So it won't be easy. Think about what we could do, once we do crack this goal. Imagine if no family had to feel helpless watching a loved one disappear behind a masking, Parkinson's, the struggle in a grip of epilepsy. Imagine if we could reverse traumatic brain injury or PTSD…"

President Obama in the White House
on April 2, 2013, when unveiling the
American 'BRAIN' Initiative

1.1 Parkinson's disease

1.1.1 Overview

Both Europe and the US have recently started impressive initiatives in neuroscience. Europe introduced the 'Human Brain Project' and the US the

‘BRAIN’ Initiative. These initiatives may revolutionize our understanding of the human mind and uncover new ways to treat, prevent, and cure brain disorders. The present work shares two of these timely issues in addressing these two major interests, i.e. the large-scale network mechanisms of learning and PD pathophysiology.

PD is the second most frequent degenerative disorder of the central nervous system (CNS) after Alzheimer’s disease (AD). The incidence is rising with increasing age. In Germany, 100-200/100 000 inhabitants live with this disease and the number is growing since the population is aging and patients with PD live longer due to improved therapy (Diener, 2012). The overall prevalence in persons 65 years of age and older is 1.8 % (De Rijk et al., 1999; Diener, 2012). Accordingly, PD and related neurodegenerative disorders represent a mounting burden on the health care system. This raises economic-political reasoning and translates into the current scientific big data initiatives.

The most obvious symptoms of PD are motor-related and include rigidity, resting tremor (at approximately 4-6 Hz), brady- and hypokinesia and postural instability (Jankovic, 2008). The bradykinesia is particularly pronounced in fast movements that change directions back and forth, they become slow (brady-diadochokinesia) and uncoordinated (dysdiadochokinesia). The non-motor facultative attendant symptoms are very variable and reflect the fact that the cell death in PD affects many different functional circuits of the brain beyond striatal dopaminergic neurodegeneration (Del Tredici et al., 2002). Vegetative symptoms (such as constipation, ptyalism, and sleep disorders), cognitive symptoms (such as bradyphrenia and dementia), sensory disorders (for instance hyposmia and pain) as well as psychiatric symptoms (for example depression and hallucinations) plus many more may occur (Poewe, 2008).

Up to now, the pathophysiology of the cell death is still under investigation and may be multifactorial. Pathohistologically, intracytoplasmatic inclusion-bodies consisting of protein aggregates (mainly alpha-synuclein), the so-called ‘Lewy-bodies’, are found in PD patients (Gibb and Lees, 1988; Hughes et al., 2001). Possibly, following a dysfunction of protein metabolism and provoking cell

death, they are seen as a cause of the neurodegeneration. A multifactorial etiology with a combination of genetic factors and environmental impact contributing in varying degrees is likely (Sulzer, 2007; Warner and Schapira, 2003). As environmental factors, oxidative stress (Jenner, 2003), mitochondrial dysfunction (Burbulla et al., 2014; Swerdlow et al., 1996), the mechanisms of toxic substances such as pesticides (Betarbet et al., 2000; Sherer et al., 2003) and inflammatory processes in the CNS (Hunot et al., 2001) have been investigated.

Especially, the progress in neurogenetic research over the last 15 years with the identification of familial forms of parkinsonism was a major step for the understanding of the pathomechanism of the disease. The first gene identified to be definitely associated with familial PD was the α-*synuclein* gene (Park 1, (Polymeropoulos et al., 1997)). However, variations in the *α-synuclein* gene were very rare in a mutational screening in a large cohort of PD patients (Berg et al., 2005; Sulzer, 2007). Approximately 10 % of all PD patients present with a positive family history following a Mendel's law of inheritance. A systematic overview of the different genes and their potential relation to idiopathic PD with special consideration of clinical phenotype and neuropathology was given by Schiesling and colleagues (Schiesling et al., 2008).

1.1.2 Pathophysiology

The main neuropathological finding in PD is the degeneration of the dopaminergic neurons in the substantia nigra projecting into the striatum which leads to a lack of the neurotransmitter dopamine and the resulting motor inhibitory effect. Two dopamine dependent projections in the ganglia-thalamo-cortical circuits are defined: the direct and the indirect pathway.

The direct pathway involves inhibitory putaminal influence on both the internal part of the globus pallidus and the substantia nigra pars reticulata. Both nuclei project to the motor thalamus, which then leads to the cortical motor regions. Thus, over a cascade of activity modulations in the basal ganglia, L-Dopa leads to an excitatory effect to the motor system.

The indirect pathway leads GABAergic neurons from the substantia nigra pars compacta to the putamen with a loop way over the globus pallidus externus and inhibits the subthalamic nucleus (STN). The STN activates the globus pallidus internus and the substantia nigra pars reticulata which then again project over the thalamus to the cortex.

To summarize, the neurodegeneration of dopaminergic neurons in the substantia nigra pars compacta leads to an overinhibition of the thalamo-cortical-basal ganglia motor output, which is clinically reflected by bradykinesia and akinesia.

1.1.3 Therapy: Medication and deep brain stimulation

The essential basis of PD therapy with L-Dopa, dopaminergic agonists, Catechol-O-methyl-transferase-inhibitors or Monoamine-oxidase-B-inhibitors is the pharmacological compensation of the reduced dopaminergic supply in the synaptic gap.

When clinical fluctuations with uncontrolled off-phases and dyskinesias occur in the advanced stage of disease, deep brain stimulation (DBS) therapy may improve motor symptoms and quality of life (Deuschl et al., 2006; Krack et al., 2003; Schuepbach et al., 2013). Surgical treatment of PD started more than 50 years ago when different functional targets within the basal ganglia were lesioned. After multiple different approaches (e.g. resection of parts of the motor and premotor cortex, transsection of ansa lenticularis) with relatively high complication rate and morbidity, Prof. Benabid was the first to introduce a chronic electrical high-frequency stimulation of the ventral intermedial nucleus of the thalamus contralateral to the tremor dominant hand in PD (Benabid et al., 1987; Benabid et al., 1989). Until today, DBS evolved as a common therapy in movement disorders.

In PD, the STN appears to be the most effective basal ganglia nucleus (Boucai et al., 2004; Krack et al., 1998) and provides an evidence-based therapy (Deuschl et al., 2006; Kleiner-Fisman et al., 2006; Rodriguez-Oroz et al., 2005; Schuepbach et al., 2013; Weaver et al., 2009). A large randomized multi-center

study confirmed that STN-DBS is even more effective than medical treatment alone and improves motor outcome and quality of life (assessed by the Parkinson's Disease Questionnaire summary index (PDQ-39) and the Unified Parkinson's Disease Rating Scale (UPDRS) II (Deuschl et al., 2006). Recently, a multi-center study proved that STN-DBS is superior to medical therapy in PD patients with beginning motor complications (Schuepbach et al., 2013).

High-frequency STN-DBS (e.g. 130 Hz) ameliorates the segmental motor symptoms (bradykinesia, tremor and rigidity) including motor fluctuations and may also improve balance, posture instability to a smaller degree (Limousin et al., 1998; Rocchi et al., 2002). However, disease progression in PD (including patients with primarily effective DBS) is evident as aggravation of cognitive and axial motor symptoms (Nutt et al., 2011). Unfortunately, these symptoms show limited response to both dopaminergic medication and STN-DBS (Castrioto et al., 2011), whereas the segmental motor functions respond better to STN-DBS (Weiss et al., 2012). Therefore, a novel approach was put forward by the Tübingen group, i.e. co-stimulation of the substantia nigra pars reticulata and the STN (Weiss et al., 2013). Advanced programming with so-called 'interleaved pulses' allows independent stimulation of contacts with different amplitudes and pulse widths at a common frequency (Weiss et al., 2013). This combined stimulation of STN and substantia nigra pars reticulata might specifically improve freezing of gait and, therefore, provides a valuable add-on reprogramming technique to the standard STN stimulation (Weiss et al., 2013).

High-frequency stimulation may mimic the functional effects of structural lesioning in the respective brain structure. The stimulated nucleus shows decreased activity resulting in a suppressing effect on efferent projections. In the case of neurostimulation of the STN (STN-DBS) this leads to a decreased firing rate in the direction of the substantia nigra pars reticulata (Benazzouz and Hallett, 2000; Tai et al., 2003).

After all, there are competing models to explain the mechanisms behind the convincing therapeutic effects of STN-DBS. Four main hypotheses to explain the mechanisms of DBS have been discussed (McIntyre et al., 2004): local

mechanisms such as *(i)* a transient depolarization blockade of voltage gated ion channels in subthalamic neurons (Beurrier et al., 2001), *(ii)* jamming of information by imposing an efferent stimulation-driven high-frequency pattern (Garcia et al., 2003; Hashimoto et al., 2003), *(iii)* synaptic inhibition (Dostrovsky et al., 2000), and *(iv)* large-scale network modulation effects- beyond the local influences of DBS. In this view, a decrease of STN overactivity may strengthen the cortical control in parallel to improved motor function (Kuhn et al., 2008a; Montgomery and Baker, 2000; Ozkurt et al., 2011; Salenius et al., 2002; Weiss et al., 2012). This integrates the fact that local cell degeneration results in abnormal neuronal long-range synchronization and pathological connectivity of the functional motor network. This is of special interest since a close correlation between abnormalities in neuronal long-range synchronization and cognitive dysfunction in almost all neuropsychological diseases has been shown (Uhlhaas and Singer; Uhlhaas, 2013).

1.2 Neuronal synchronization

In his book ‘The organization of behavior’ combining his knowledge about brain surgery and human behavior, Donald O. Hebb, who laid the foundation of the concept of neuronal synchronization, wrote the following: “When an axon of cell A is near enough to excite cell B and repeatedly or persistently takes part in firing it, some growth process or metabolic change takes place in one or both cells such that A's efficiency, as one of the cells firing B, is increased.” (Hebb, 2002). Paraphrased as “Neurons that fire together wire together”, this sentence is often referred to as Hebb’s Law. He postulated that repetitive synchronous neuronal activation is an important correlate of learning and memory building.

Increases in activation at the level of local cortical neuronal populations are evident as increases in electroencephalography (EEG) power. However, cognitive processing is not implemented in one single circumscribed area but communication of spatially distributed neuronal groups and cell populations provides the basis for integration of complex information. Thus, different brain areas may remotely interact even if widely separated. Functional coupling of

distant neuronal ensembles arises from synchronized activation. Accordingly, when two separate populations of neurons A and B synchronize with each other, the correlation of their activity may indicate their coherence as a measure of synchrony. In general, synchronization can be characterized in terms of frequency, amplitude and phase. Synchronization may underlie dynamic adjustments and emerge in distinct time and frequency windows relative to a cognitive program. Short-range synchronization between closer neuronal groups present rather (but not exclusively) with higher frequency bands (beta and gamma band) and more distant neuronal groups rather with long-range synchronization present with lower frequencies (theta and alpha band) (von Stein and Sarnthein, 2000). Moreover, oscillatory synchronization within and between cortical areas is increasingly recognized as a key mechanism in motor organization (Gerloff et al., 1998a; Serrien and Brown, 2002).

The synchronization of local neuron populations can be noninvasively evaluated by multichannel surface EEG. Synchronization occurs for instance when a local group of neurons synchronizes its activation by reacting together on the same auditory stimulus and form a functional ensemble (von der Malsburg and Schneider, 1986). We distinguish a phasic and regionally localized decrease (event-related desynchronization, ERD) or increase (event-related synchronization, ERS) of activity of the underlying neuronal cells relative to a specific event. ERD and ERS enable us to study the dynamics of cortical activation in a very high time resolution using EEG with a high sampling rate and time-locked event-related analyses. ERD parallels not only the perception of stimuli, but a variety of different sensory, cognitive and motor tasks can interrupt or desynchronize the ongoing alpha activity in a time-locked way (Berger, 1929; Dujardin et al., 1995; Pfurtscheller and Berghold, 1989).

A cortex in an idling state is represented by local alpha activity, whereas when a stimulus occurs, neurons start to work and desynchronize. Accordingly, an ERD embodies an electrophysiological correlate of an active cortical network involved in processing of incoming information or production of motor behavior (Neuper and Pfurtscheller, 2001).

In studies with go/ no go trials one has argued that ERD may represent both corticospinal excitation (contralaterally), but also ‘active’ inhibition (ipsilaterally) preventing action occurring (Leocani et al., 2001b). With movement mu ERD was shown to be most prominent over sensorimotor areas contralateral to movement execution and extends bilaterally with movement initiation (McFarland et al., 2000). In PD patients, local field potentials of the STN have been recorded showing a beta band desynchronization both with movement and in a task with only imagined and not executed movement. Thus, the ERD during movement might be related to the feedforward organization of movement (Kuhn et al., 2006).

In contrast, an ERS characterizes a brain area in an idle state associated with rest generated by a large area of highly synchronous neuronal firing in the absence of any input (the so-called idling hypothesis, (Pfurtscheller, 1992). With quick simple unilateral movements as in externally paced finger movements, beta ERS can be observed in the post-movement phase and is sometimes called post-movement beta rebound (Jurkiewicz et al., 2006; Neuper and Pfurtscheller, 1996). Although, in general, the ERS is believed to reflect a neuronal deactivation, the post-movement beta rebound that follows movement termination may also represent an active inhibition of the motor cortex to prevent a planned movement (Salmelin et al., 1995) or a sensory reafference and somatosensory processing (Cassim et al., 2001).

Generally, with movements we expect three types of event-related synchronization/desynchronization phenomena: the mu and beta ERD (before and during phasic movement), the beta ERS (14-18 Hz, maximum post-movement) and the gamma ERS (36-40 Hz, maximum short before and during execution of movement (Pfurtscheller and Andrew, 1999).

1.3 Abnormal neuronal synchronization in PD

Pathological synchronization in functional large-scale motor networks is a pathophysiological characteristic in PD. Perioperative recordings of local field potentials from STN macroelectrodes revealed strong beta band

synchronization of the STN which was reduced with movement (Williams et al., 2005), L-Dopa (Kuhn et al., 2006) and STN-DBS (Eusebio et al., 2011; Kuhn et al., 2008a). This reduction correlated with clinical improvement (Kuhn et al., 2008a; Kühn et al., 2006). In addition, externally imposed synchronization through direct stimulation of the STN at 20 Hz slows movement in PD. Even if this slowing is only modest, it supports the fact, that beta synchrony within the basal ganglia-cortical loop may contribute to the slowing of movements in PD (Chen et al., 2007).

But pathological neuronal alterations in PD exceed local STN circuits. Local cortical oscillatory activity in relation to movement is abnormal: ERD of mu activity with voluntary movement is delayed and lower in amplitude in PD patients than in healthy controls (HCs). Both delay and attenuation have been shown to correlate with bradykinesia (Brown and Marsden, 1999; Wang et al., 1999), to be accompanied by a decrease of motor cortical activity (Defebvre et al., 1999) and to be partially reversed by treatment with L-Dopa (Magnani et al., 2002) or STN-DBS (Devos et al., 2004). Also, post-movement beta synchronization is remarkably smaller in PD patients compared to HCs (Pfurtscheller et al., 1998a) and was correlated with bradykinesia and partially restored by L-Dopa or STN-DBS (Devos et al., 2003a; Devos et al., 2003b).

Besides, abnormal resting state corticocortical beta band coherence correlates with the severity of parkinsonism and its reduction by L-Dopa and STN-DBS leads to clinical improvement (Brown, 2007; Silberstein et al., 2005).

Furthermore, corticomuscular coherence (CMC) is altered in PD: In HCs corticomuscular motor integration during weak to moderate isometric contractions occurs predominantly in the beta frequency range (Gross et al., 2000; Halliday et al., 1998; Kristeva et al., 2007; Salenius et al., 1997), likely originating from the primary motor cortex (Gerloff et al., 2006). However, in PD patients this 15-30 Hz coherence is deregulated and CMC is dominated by low frequencies below 10 Hz (Salenius et al., 2002; Weiss et al., 2012). This pathological CMC correlates with bradykinesia scores in the UPDRS (McKeown et al., 2006). Dopaminergic medication may partly restore physiological beta

activity (Salenius et al., 2002) and STN-DBS also leads to an increase of efferent drives from cortex to muscle together with improved motor performance (Weiss et al., 2012).

In HCs, motor units (e. g. active agonistic muscle pairs of the hand and forearm) synchronize at 15-30 Hz during weak isometric contractions in a task requiring precision grip of two spring-loaded levers, whereas intermuscular coherence was absent during movement (Kilner et al., 1999). In PD patients, this intermuscular coherence of cocontracting distal arm-muscles is relatively absent (Marsden et al., 2001). STN-DBS is able to increase the level of intermuscular coherence between agonistic muscles correlated with improvements in bradykinesia (Brown et al., 2001). As this synchronization results from oscillatory corticomuscular drives, these data suggest that the basal ganglia modulate oscillatory activity in the motor cortex.

In summary, synchronization in subthalamo-cortical, corticocortical, corticomuscular and intermuscular loops is altered in PD. These alterations correlate with clinical symptoms and can be modulated by L-Dopa and STN-DBS.

1.4 Cognitive impairment in PD

As mentioned above, PD is clearly associated with a variety of alterations in emotional, initiative, and cognitive functioning contrary to James Parkinson's original descriptions about "the senses and intellect being uninjured" (Parkinson, 1817). Cognitive deficits are very frequently observed in PD. 93 % of PD patients were shown to be impaired in memory, visual-spatial perception and psychomotor speed (Pirozzolo et al., 1982). Cognitive impairment starts with subtle changes such as fatigue, mild forgetfulness and decreased mental flexibility. In a neuropsychological test battery newly diagnosed untreated PD patients had significantly greater difficulty in shifting conceptual sets and produced more perseverative errors (LEES and SMITH, 1983).

Furthermore, PD patients struggle with the performance of dual motor tasks (Chawla et al., 2014; Schwab et al., 1954; Troche et al., 2014). Accordingly, PD patients have great difficulty performing learned movements automatically which was shown when patients were asked to perform a learned sequential movement simultaneously with a letter counting task as compared to healthy subjects (Wu, 2005)). In the functional magnetic resonance imaging (functional MRI), PD patients had greater activation in multiple brain regions including the bilateral cerebellum, bilateral premotor area, bilateral parietal cortex, bilateral precuneus and bilateral dorsolateral prefrontal cortex. In healthy subjects, activation decreased after training in the bilateral premotor area and others compared with the before-training stage. These results suggest that PD patients might require more brain activity to compensate for basal ganglia dysfunction in order to perform automatic movements (Wu, 2005).

Moreover, there is evidence that the ability of implicit motor learning is decreased: Non-demented PD patientes are able to achieve implicit motor learning in the serial reaction time task (SRTT) but to a smaller degree than age-matched HCs possibly due to some deficit in the formation of new associations (Ferraro et al., 1993). PD patients performed specifically worse at longer sequence lenghts and results were not significantly affected by L-Dopa (Jackson et al., 1995; Pascual-Leone et al., 1993).

1.5 Implicit motor learning

1.5.1 Overview

We are constantly surrounded by new information that needs to be perceived, processed and stored. Learning is one of the most essential aspects of the human mind and the extraction and the following adaption to repetitive patterns in our environment facilitate our daily activities. Motor skill learning refers to the process by which a sustained change in motor performance (faster and more accurate) is achieved resulting from practice (Willingham, 1998). Two different types of motor learning are distinguished: Learning processes can occur either

implicitly (=subconsciously) or explicitly with awareness of the underlying structural patterns that can be verbalized and reported.

There are different phases in the multistep course of implicit motor learning: the initial short-term learning in the first training-sessions occurs with a rapid improvement of performance in speed and accuracy and allows the acquisition of a task-relevant routine (Karni et al., 1995). After that, consolidation of the task by time (Hotermans et al., 2008) and/or sleep (Diekelmann and Born, 2010) takes place. Consolidation is defined as the progressive stabilization of a recently acquired memory (Dudai, 2004). Then a slower long-term process with quantitatively smaller behavioral gains than those during fast learning follows by which the skill becomes more permanent. Then possibly another learning phase takes place when the task is practiced again in the next training-session and reconsolidated afterwards again.

Together, motor skills are typically learned with fast progress in the beginning, and then learning slows over multiple training sessions until performance improvement reaches nearly asymptotic levels (Dayan and Cohen, 2011). All these phases together lead to a long-term retention of the skill gains (Romano et al., 2010). The duration of the different phases of implicit motor learning depends on the task complexity, for instance learning how to perform simple button presses might take only several minutes, whereas learning how to play a difficult piano piece might take months. In our study, we planned to assess the initial short-term phase of implicit motor learning with rapid performance improvements.

1.5.2 Serial reaction time task

Implicit motor learning has been in the focus of neuroscientific and psychological research for several decades and it has been investigated by numerous different paradigms such as the SRTT. The SRTT was developed by Nissen and Bullemer (Nissen and Bullemer, 1987) and is one of the most frequently used paradigms to study implicit motor learning; it follows, unbeknownst to the subjects, an underlying regularity of the stimuli.

Performance measures such as decreased reaction times in sequential trials relative to randomly ordered trials are then attributed to implicit motor learning when there is no explicit awareness of the underlying sequence.

In the original series of experiments by Nissen and Bullemer in experiment I two groups of subjects performed the SRTT. On each trial, a light appeared at one of four locations. Subjects were instructed to press the one corresponding key out of a set of four keys as fast as possible. One group received a repeating 10-trial sequence of positions through a continuous series of trials. In the other group, the positions were determined randomly. Nissen and Bullemer compared the response latencies of both groups. They hypothesized that, if the reduction in reaction time only occurs in the group receiving the repeating sequence, it reflected implicit motor learning, whereas a reduction of reaction time in both groups was due to a more general motor skill. Indeed, reaction time decreased dramatically in the sequence group and only sparsely in the group receiving random sequences. However, in this original experiment improvements in performance were both due to implicit and explicit learning because 11 of the 12 subjects in the study achieved awareness of the sequence after some blocks.

Three groups of participants were tested in Nissen and Bullemer's experiment II: The first performed the SRTT alone as in experiment I (single-task group). The other two groups performed a dual task: the SRTT and a secondary tone-counting task concurrently. For one of the dual-task groups, the SRTT followed a 10-position sequence again (dual-task sequence group) while the other group obtained randomly presented targets (dual-task random group). The single-task group was significantly faster than the dual-task groups, but the dual-task sequenced and dual-task random group did not differ significantly. This indicates that participants were not able to learn the sequence when they could not fully attend to the SRTT because of the other distracting task. Since implicit motor learning also involves activity of subcortical brain areas, it is possible that with substantially more training, the dual-repeating group would have revealed more convincing evidence of learning. This possibility is suggested by the fact that, even though dual-task sequenced and the dual-task random groups did

not differ significantly in reaction time, the mean reaction time of the dual-repeating group already tended to be shorter.

Today, most groups use the SRTT in a way that the participants perform both blocks with random trials and blocks with sequential trials and the different blocks within the group are compared instead of a between group comparison as in Nissen and Bullemer's experiments (Nissen and Bullemer, 1987). Besides, the structure of the sequences used in the task has been under ongoing discussion. Originally, Nissen and Bullemer employed a 10-position sequence in which some positions occurred more often than others. Therefore, effects attributed to sequence learning might also be explained by learning simple frequency information rather than the sequence structure itself. So frequency information should be carefully controlled and each location should occur equally often.

Not only have the types of sequences been variable and improved over time but also the measures of explicit knowledge within the task. Even with optimized SRTT designs, explicit knowledge might still occur. Some studies trusted in verbally questioning subjects about their explicit knowledge after the task. Some groups used recognition questionnaires in which subjects had to identify pieces of the applied sequences (Frensch et al., 1998). Others used free-generation tasks: subjects were instructed to generate the sequence by pressing the buttons used in the SRTT (Schwarb and Schumacher, 2010).

1.5.3 Neuronal correlates of implicit motor learning

1.5.3.1 Involved neuronal structures

Motor skill learning is supported by a broad neuronal network that includes cortical areas, the basal ganglia and the cerebellum (Floyer-Lea and Matthews, 2004; Pascual-Leone et al., 1995; Pascual-Leone et al., 1996; Seitz et al., 1990; Yang and Lisberger, 2013).

In the early short-term phase of motor learning, which was assessed in our study, the primary sensorimotor cortex (SM1) was the key brain region involved

in motor skill learning: During the initial stages of implicit motor learning in mice performing an accelerating rotarod task, substantial recruitment of neurons in the primary motor cortex occurred as measured by microelectrode arrays (Costa et al., 2004). In accordance with this finding, anodal transcranial direct current stimulation of the SM1 area during the SRTT improved performance (by enhancing its excitability) whereas anodal stimulation of the premotor cortex and the dorsolateral prefrontal cortexes showed no effect (Nitsche et al., 2003). As mentioned above, the SM1 is known to be involved in the initial phase of implicit motor learning, whereas the prefrontal cortex is mainly involved in later stages of learning namely information storage and retrieval (Honda et al., 1998).

During early implicit motor learning, reorganization in the primary motor cortex area has been described using transcranial magnetic stimulation (TMS) following the technique described by Wassermann (Wassermann et al., 1992): While subjects performed the SRTT cortical output maps to the muscles involved in the task became progressively larger until, when explicit knowledge was achieved, the primary motor cortex map size returned to its baseline topography (Pascual-Leone et al., 1994).

In another study assessing a later phase of implicit motor learning accompanied by long-term changes of the brain, mice that were trained in a motor skill for 11 days revealed significantly higher fractional anisotropy in the postmortem diffusion MRI. Myelin staining in the white matter underlying motor cortex in the hemisphere contralateral (but not ipsilateral) to the trained limb also increased for the skilled learning group versus the control groups. Both increased fractional anisotropy and increased myelin staining correlated significantly with the learning rate (Sampaio-Baptista et al., 2013).

All these studies provide evidence that implicit motor learning induces structural changes in task-relevant pathways and alters the pattern of neuronal activation.

In addition to TMS, transcranial direct current stimulation, electrophysiological studies (EEG, MEG), and neuroimaging methods such as functional MRI and positron emission tomography (PET), are often used to investigate brain plasticity during learning. In favor of a high spatial resolution, time resolution is

worse in MRI and PET than in electrophysiological methods. When investigating learning processes in the MRI, increased activation may reflect the recruitment of additional cortical units with practice. Decreasing activation can be correlated with learning as the task becomes less effortful, it can be carried out more automatically and fewer neuronal resources are needed (Poldrack, 2000).

In a PET study, different forms of motor learning were compared: On the one hand, an implicit visuomotor procedural learning task consisting of the movement of the right hand with an adaptation to a rotated display was associated with activation of the right posterior parietal cortex. This cortical area plays an important role in visuomotor coordination receiving converging proprioceptive visual and vestibular inputs. On the other hand, explicit learning of new sequences presented with activations in the anterior cingulate cortex and the dorsolateral prefrontal cortex which was found to be active in most sequence learning studies (Ghilardi et al., 2000) above there are also multiple studies in the context of implicit motor learning showing modulation both in the cortex and in subcortical areas: In the SRTT the dorsolateral prefrontal cortex with its important function in spatial working memory, the striatum, and the cerebellum play important roles in improving performance (Floyer-Lea and Matthews, 2004; Robertson et al., 2001; Torriero et al., 2004). Increased activity was observed in the left pulvinar thalamus (Grafton et al., 1992), in the left putamen and the left globus pallidus (Seitz and Roland, 1992), and in the right cerebellar dentate nucleus (Floyer-Lea and Matthews, 2004). These wide-spread modulations of basal ganglia activity during implicit motor learning suggest that they play an important functional role in motor programming (Marsden, 1982) and implicit motor learning. The putamen for instance has a specific function in the timing of the movement (Nenadic et al., 2003). The striatum is supposed to be critical for the long-term storage of well-learned movement sequences (Doyon and Ungerleider, 2002). Corticosubcortical networks involving the cerebellum and the basal-ganglia are involved in ‘automatic’ movements (Floyer-Lea and Matthews, 2004). In conclusion, it is not surprising that basal ganglia diseases such as PD are associated with deficits in implicit motor learning as described above.

1.5.3.2 Event-related desynchronization

Self-paced finger movements commonly present with a circumscribed ERD in the upper alpha band (mu-rhythm from approximately 10 to 12 Hz (Pfurtscheller and Aranibar, 1979)) and the beta bands (12-20 and 20-30 Hz (Pfurtscheller, 1981; Toro et al., 1994)) that is predominant in the central areas. It begins around 1 - 2 s prior to movement over the contralateral SM1, becomes bilateral just before onset of the movement and ends with a stronger ERD on the ipsilateral than on the contralateral cortex approximately 2 s after movement onset (Derambure et al., 1997; Guieu et al., 1999; Toro et al., 1994). Preceding or during movement, maximum ERD was observed in most cases in central-vertex regions (Pfurtscheller and Aranibar, 1979).

Subdural electrodes overlying sensorimotor representations for the upper extremity presented with the largest ERD during contralateral self-paced finger movements. Alpha ERD (8-10 and 10-12Hz) presented more restricted, with a more specific topographical pattern for different body parts than beta ERD (12-20 and 20-30Hz). Beta ERD presented wider spread over other sensorimotor representations including for instance more than only the hand areal in a hand movement task (Toro et al., 1994). The duration of the ERD differed upon distinct frequencies: beta ERD reversed within approximately 1 s after movement onset and returned to baseline power in a more rapid way than alpha ERD (Toro et al., 1994). Besides, the beta ERD presented slightly more anterior than the alpha ERD likely being generated rather in the premotor regions whereas the alpha ERD originated mainly from the SM1 (Pfurtscheller and Lopes da Silva, 1999).

Not only self-paced, but also visually and auditory cued finger movements were accompanied by a 10 Hz ERD over the contralateral sensorimotor hand area (Rappelsberger et al., 1994). In accordance to the above mentioned findings with self-paced finger movements, beta ERD similarly occurred with externally-paced finger movements with some special characteristics: it started earlier and recovered faster than alpha ERD. However, in controversy to the above, beta ERD presented more focused to a specific cortical area than alpha ERD in a

study with subdural electrode grids and a visually cued motor task in which the motor response consisted of sustained muscle contractions of different body parts such as tongue protrusion, fist clenching, or foot dorsiflexion (Crone et al., 1998).

In summary, beta ERD presented with a shorter latency and a faster recovery than alpha band ERD in both internally and externally paced movement. Topographic distribution of the ERD was more specific in alpha band in a study with self-paced finger movement, whereas higher specificity of the beta band ERD was found in a study with externally paced phasic movements.

The existence of premovement mu desynchronization seems to be a more general motor phenomenon independent of the forthcoming type of movement and is similarly observed during thumb, index finger or hand movements (Pfurtscheller et al., 1998b). Hence, premovement mu ERD may reflect a general readiness or presetting of sensorimotor neurons, needed to execute a forthcoming movement (Pfurtscheller et al., 1998b). In contrast, duration and amplitude of the beta desynchronization is affected by some characteristics of the movement itself (brisk or slow self-paced finger-movements, dominant or non-dominant hand (Stancak and Pfurtscheller, 1996a; Stancak and Pfurtscheller, 1996b).

However, in which way is the ERD modulated by different tasks? First of all, larger cortical cell assemblies involved in a task produce a stronger ERD. Increasing task complexity with an increased cognitive load leads to a longer alpha ERD with increased amplitude (Boiten et al., 1992). Higher amplitude of alpha ERDs was found in good task performers compared to less efficient ones (Sterman et al., 1996). Accordingly, a higher attentional load in the task causes stronger ERDs (Dujardin et al., 1993).

ERD has also been investigated during rapid consecutive finger tapping in reaction time tasks: In a study with different reaction time tasks with acoustic stimuli (simple reaction time task, choice reaction time task, go/no go reaction time task) bilateral 20 Hz ERD occurred with movement and also with no-go trials over the bilateral hand sensorimotor areas. It began around 150-200 ms

after stimulus for the simple reaction time task and 300-400 ms for the choice and go trials (Leocani et al., 2001b). From these findings it was argued that the ERD is compatible with both corticospinal activation and inhibition (not requiring movement execution and proprioceptive afferences).

The performance of brisk finger movements following different prelearnt sequences according to a metronome tone is accompanied by alpha and beta band ERD prominently over central and parietal areas contralateral to the movement and weaker on the ipsilateral side and over frontal regions. Increased sequence complexity resulted in increasingly large power decrease in terms of spatial extent and magnitude (Manganotti et al., 1998). Sequence complexity was varied as the length of the nonrepeated sequence units was increased. In the simplest sequence, this unit contained a combination of 4 movements before this exact sequence was repeated again. There was a combination of 8 movements in sequence 2, 12 movements in sequence 3, and 16 movements in sequence 4 before repetition.

In an SRTT paradigm, a progressive development of a localized 10 Hz ERD over SM1 was observed and facilitated within the process of implicit motor learning until subjects achieved explicit knowledge (= peak of ERD). In the ‘after-learning’ stage the ERD declined from peak to baseline, which might parallel more automatic finger movements (Zhuang et al., 1997).

Taken together, movement-related desynchronization may represent a neuronal state of both maximal readiness and information processing capacity (Thatcher et al., 1983).

1.5.3.3 Event-related synchronization

The ERD is generally followed by the ERS, i.e. a sharp recovery and rebound of alpha and beta band power.

The latency of the ERS depends on the frequency band: With self-paced finger-movements the 10 Hz ERS starts 2 s after EMG onset whereas the 18–22 Hz ERS occurs 0.75 s after EMG onset (Leocani et al., 1997). Accordingly, in a study with externally paced wrist movements the 16-20 Hz ERS starts earlier (at

approximately 2 s after EMG onset) than the 10 Hz ERS (at approximately 4 s after EMG onset; (Pfurtscheller et al., 1996). In the same study the topography of ERD and ERS was investigated: Postmovement beta ERS was found predominantly over the contralateral hemisphere with a focus slightly anterior to the focus of the largest mu desynchronization (somatosensory area vs. motor area) with self-paced movements. With externally paced movements a bilateral symmetrical ERD during movement was found and after movement a beta ERS occurred more pronounced over the contralateral side.

In a work with TMS on the SM1 the time course of corticospinal excitability before and after brisk thumb abduction movements in a reaction time task was studied (Chen et al., 1998). A reduced excitability compared to baseline (300-100ms before EMG onset) was found from 550 to 1000 ms after EMG offset in simple reaction time movements, which likely corresponds to the beta ERS reaching values above the reference power at 0.9 and 1.1 s after movement onset (Pfurtscheller et al., 1995). Thus, ERS may reflect attenuation of corticospinal activation or inhibition resulting in an inactive, idling state of the motor cortex (Leocani et al., 2001a).

1.5.3.4 Coherence

Coherence provides the basis for successful neuronal communication leading to an optimally timed synaptic input from one neuronal group to its target group within the excitability peak (Volgushev et al., 1998; Womelsdorf et al., 2007). Distant neuronal pools either between two cortical areas, between cortex and subcortical brain areas or between cortex and spinal neurons can synchronize. CMC correlates with effective corticospinal motor integration and motor performance (Hummel and Gerloff, 2006; Weiss et al., 2012).

In a study with isometric contractions, beta band CMC between the sensorimotor cortex and the contralateral hand and forearm muscles was most pronounced during the steady hold period of this task (Kilner et al., 2000). The level of compliance in this precision grip task influenced the extent of CMC with a stronger CMC in a more compliant condition in which subjects moved the levers against a spring-like load. So CMC was abolished during the phasic force

recalibration and greatest during steady hold periods just after movements (Baker et al., 1997; Kilner et al., 2000). Accordingly, in a study comparing a force tracking task with a natural combination of index and middle fingers and an unnatural combination of the two fingers MEG and EMG (i.e. simultaneously producing equal force strength in index and middle finger) were recorded with the following results: The ‘natural’ task induced a beta band CMC whereas the ‘unnatural’ task produced a both beta and low gamma CMC, which was also stronger. Hence, more corticomuscular interaction is needed for the unnaturally coordinated fingers (Wu et al., 2013).

In an isometric visuomotor task in which subjects had to compensate target forces with predictable or unpredictable frequencies performance, CMC, cortical power, and the ERD were assessed. The unpredictable condition was associated with worse performance, lower cortical power, stronger ERD and lower CMC. Thus, the unpredictable modulation of the force is likely to lead to a decrease in corticospinal synchrony and to worsen performance (Mendez-Balbuena et al., 2013).

Specifically, the strength of gamma band (40 to 70 Hz) coherence between motor cortex and spinal motor neurons parallels subjects’ readiness to respond in a simple reaction time task (Schoffelen et al., 2005). Again, this coherence contributes to an effective corticospinal interaction and shortened reaction times. There is another study to be mentioned supporting this theory of gamma band coherence as a sign of readiness on the level of corticocortical synchronization: Neuronal coactivation in frontal and central cortex was examined during a visual oddball task with a random mix of 15% oddball targets and 85% frequent non-target letters. Increased corticocortical gamma coherence appeared to be related to increasing expectation of the oddball, i.e. the longer the series of frequent trials extended the greater it became (Qassim et al., 2013).

In line with these results in an MEG study individuals with higher coherence in attention networks exhibited a visual oddball task faster: The strength of high gamma imaginary coherence between the left middle frontal gyrus and left

intraparietal sulcus, between the left middle frontal gyrus and the right middle frontal gyrus, and the high gamma power in the left thalamus predict the speed of target detection (Akimoto et al., 2013).

CMC in phasic movement has also been investigated: Subjects performed a voluntary right index finger movement every 12–25 s and presented with low frequency (5 Hz) coherence with movement onset followed by beta band coherence between the primary motor cortex and premotor areas and muscle after movement termination, lasting for 1-2 s (Feige et al., 2000).

As described above, CMC is altered in PD: Beta CMC is deregulated and CMC is dominated by low frequencies below 10 Hz (Salenius et al., 2002; Weiss et al., 2012), correlating with bradykinesia scores in the UPDRS (McKeown et al., 2006). Physiological beta CMC can be restored partly by L-Dopa (Salenius et al., 2002) and STN-DBS (Weiss et al., 2012).

1.5.4 Conclusions for implicit motor learning

In summary, the following principles about neuronal synchronization during implicit motor learning and phasic movement have been substantiated before: *(i)* The motor cortex serves as the core processor of the first rapid phase of implicit motor learning supported by the dorsolateral prefrontal cortex. When learning continues, additional contributions come from the supplementary motor area (SMA), parietal regions, the basal ganglia and the cerebellum (Floyer-Lea and Matthews, 2004); *(ii)* Externally paced finger movements as performed in the SRTT present with a premovement mu and beta ERD and a postmovement beta ERS; *(iii)* ERD is enhanced with increasing task complexity, higher efficiency in task performance and higher attention; *(iv)* CMC is an important mediator of human motor control and may support effective task performance (Schoffelen et al., 2005; Weiss et al., 2012).

1.6 Purpose of the study

Event-related modulations in oscillations of local cortical neuronal populations can be seen as changes in EEG activity (ERD and ERS) and quantified as

‘event-related spectral pertubation’ (Delorme and Makeig, 2004). Neuronal synchronization between the oscillations of distant neuronal pools can be expressed as coherence both during stationary conditions as ordinary coherence or during dynamic processes in the time-frequency domains. There is ample evidence that coherence promotes similarly efficient communication between neuronal pools as during integration of complex information and motor programs.

Here, we tested PD patients with STN-DBS and HCs on the SRTT. This test contained a baseline of 4*96 random stimuli (blocks) and consecutive 8 blocks in which the motor learning took place. This data set allowed us to analyse two core issues:

As first issue, we aimed to analyze the motor network substrate of PD motor impairment and its modulation with STN-DBS, i.e. stimulation off [StimOff] vs. stimulation on [StimOn] (*Analysis 1*). As second issue, we aimed to study the cortical correlate of implicit motor learning in HCs and PD patients (*Analysis 2*).

In *Analysis 1,* we characterized the cortical activation and corticomuscular synchronization pattern in PD. Importantly, we characterized the comprehensive and wide-spread cortical and corticomuscular network effects of STN-DBS treatment in externally paced movements for the first time. Therefore, we analyzed electrophysiological EEG and EMG data on externally paced finger movement in PD patients comparing [StimOff] and [StimOn].

In the light of the mentioned previous data, we tested the following main hypotheses:

- Clinical motor impairment (UPDRS scores) and reaction times improve with STN-DBS
- Premovement mu and beta movement-related desynchronization (MRD) can be strengthened (increased in amplitude, temporally and topographically) by STN-DBS treatment
- The MRD correlates with the clinical state

Moreover, we explored the role of CMC. Given only sparse previous work on CMC in dynamic motor processing, we assumed that CMC is suppressed during motor output similar to HCs (Kilner et al., 2000). Therefore, the PD patients in [StimOff] condition might present with hindered CMC suppression during motor output and be relieved with stimulation.

In *Analysis 2* we aimed to address the cortical processing during the early phase of implicit motor learning in HCs and PD patients with both [StimOff] and [StimOn]:

Improvements of motor skills are achieved in terms of implicit motor learning and can be quantified with the SRTT. Externally paced finger movements (as in the SRTT) present with MRD. We took advantage of mu and beta band MRD to monitor the cortical network mechanism during implicit motor learning in the SRTT.

In the course of implicit motor learning:

- We hypothesized that reaction times decrease over the sequence blocks with decelerated reaction times in the random blocks
- We expected PD patients to be impaired in implicit motor learning with [StimOff] and improvement of learning performance with [StimOn]
- We hypothesized that the PSD increases in learning blocks over for implicit motor learning relevant structures, mainly SM1 and dorsolateral prefrontal cortex in this early phase of learning
- We hypothesized that alpha and beta band MRD is present during the SRTT and most pronounced over the contralateral SM1 area
- We hypothesized that the MRD increases over learning blocks compared to [BL]

2 Material and methods

2.1 Subjects

All experiments were conducted with written informed consent and the approval of the ethical committee of the University of Tübingen.

2.1.1 HCs

HCs were recruited among the university hospital staff and among family members of the PD patients. 15 HCs took part in the study. Inclusion criteria were right-handedness approved by the Edinburgh Handedness Inventory (Oldfield, 1971) as well as an age over 18 years. Out of all HCs, three had to be excluded from *Analysis, two of them* due to explicit knowledge of the sequence, which is further explained below. Cognitive impairment (Mini Mental State Examination Score < 24 (29.0 ± 1.0)) and depression (Becks Depression Inventory Score < 12 (3.7± 3.0)) were defined as exclusion criteria. The remaining subjects (6 male, 6 female) had an average age of 58.8 ± 8.5 years (mean ± standard deviation). 2 subjects had to be excluded only from the electrophysiological analyses due to insufficient electrophysiological data.

2.1.2 PD patients

Inclusion and exclusion criteria of the study were equivalent as described above for the HCs. Moreover, all idiopathic PD patients had undergone surgery for STN-DBS in Tübingen. Medtronic quadripolar macro electrodes type 3389 and either ACTIVA PC® or Kinetra® impulse generators were implanted (Medtronic, Neurological Division, Minnesota, USA). Patients were recruited from the Department for Neurodegenerative Diseases, University of Tübingen. Of the 24 PD patients included in the study, four patients were excluded from the final analyses due to reduced EMG data quality (n = 2), inability to adhere to the paradigm (n = 1), and inability to tolerate the study-related DBS reprogramming and discontinuation (n = 1). These four patients are not considered in the following.

Finally, we tested 20 PD patients with a mean age of 58.6 ± 9.4 years (15 male, 5 female). The mean disease duration from diagnosis was 15.7 ± 5.3 years and the mean time range since implantation of the DBS electrodes was 3.0 ± 1.6 years. The patients had a mean Hoehn & Yahr Score of 2.7 ± 0.9 and a Schwab and England Activities of Daily Living Scale of 73.5 ± 13.5 %. Mean UPDRS I was 2.1 ± 1.5, mean UPDRS II was 14.5 ± 6.1, mean UPDRS IV was 3.3 ± 3.2. The average Mini Mental State Examination Score was 29.3 ± 1.0 and the average Becks Depression Inventory Score was 7.9 ± 4.0. Individual clinical features of all patients are described below (Table 1).

Table 1 Clinical features of patient cohort.
Note: LED = L-Dopa equivalent dosage [mg] (calculation described below), M = male, F = female, age, duration of disease and time from DBS implant [years]

Patient	Age	sex	Duration of PD	Duration of DBS	Hoehn & Yahr	LED
PD1	51	M	11	2	2.5	400
PD2	64	F	16	1	2.5	1210
PD3	52	M	15	3	2.0	520
PD4	58	M	11	4	2.0	350
PD5	60	M	15	4	2.0	150
PD6	55	M	10	1	2.0	300
PD7	59	M	17	2	3.0	630
PD8	77	M	7	2	1.5	300
PD9	71	F	26	1	4.0	200
PD10	53	M	13	4	2.0	700
PD11	62	F	18	2	4.0	300
PD12	52	M	16	4	2.0	300
PD13	52	M	11	1	3.0	870
PD14	58	M	20	6	4.0	530

PD15	71	F	22	4	4.0	750
PD16	51	M	14	5	2.0	500
PD17	40	M	7	2	2.0	450
PD18	50	F	21	3	4.0	680
PD19	75	F	22	6	2.0	150
PD20	60	M	22	2	4.0	910

2.1.2.1 Medication

Patients took part in the study after overnight withdrawal of all dopaminergic medication which generally leads to a reliable clinical off-state in advanced disease stages and therefore is the gold standard for ‘off testings’ (George et al., 2013; Weiss et al., 2013). However, it should be kept in mind that overnight withdrawal of dopaminergic medication is not expected to result in a complete wash-out of dopaminergic medication, particularly due to long-acting preparations like dopamine agonists (such as Ropinirole, Pramipexole, Rotigotine). We expressed individual daily medications as L-Dopa equivalent dosage (LED) as recommended previously (Deuschl et al., 2006) and as implemented in the guidelines of the German Society for Neurology. The mean daily LED was 510 ± 280 mg.

Accordingly, 100 mg daily dose of standard L-Dopa are clinically equivalent to

- 100 mg L-Dopa and 25mg Benserazide, 100 mg L-Dopa and 25 mg Carbidopa
- 133 mg of controlled-release L-Dopa
- 75 mg of L-Dopa plus Entacapone or Tolcapone
- 1 mg of Pergolide, Pramipexole, Lisuride, or Cabergoline
- 5 mg of Ropinirole
- Rotigotin-patch 8mg/24h

- 10 mg of Bromocriptine or Apomorphine
- 20 mg of Dihydroergocriptine

2.1.2.2 Stimulation parameters

Every patient was stimulated with his/her best individual stimulation parameters without inducing side effects in [StimOn]. In patients with chronic monopolar stimulation (negative electrode contact polarized against the generator case) stimulation parameters were reprogrammed to bipolar settings (two adjacent electrode contacts polarized against each other) to reduce the stimulation artifact in the EEG recordings (Silberstein et al., 2005; Weiss et al., 2011). To maintain a similar clinical effect the amplitudes were increased by approximately 30 % compared to the individual monopolar parameters for the study testing. Regular hardware function was ensured (testing of impedances on active electrode contacts, battery status) prior to the recordings. The DBS conditions [StimOff] or [StimOn] were introduced at least 20 minutes before the testing. If a clear clinical effect occurred promptly after changing the therapeutic condition (UPDRS III change of at least 30%), we eventually reduced this period for clinical and ethical reasons, particularly if the patient reported unpleasant off motor symptoms. With this approach we achieved a reliable difference between the [StimOff] and [StimOn] motor scores in the UPDRS III of a mean improvement of 60.7 ± 14.5% (for individual subject level see Table 6, more than the average improvement of UPDRS III with DBS-STN of 41% as reported elsewhere (Deuschl et al., 2006).

Table 2 Individual stimulation parameters during the study

PD	STN left (contacts, amplitude, pulse width, frequency)	STN right (contacts, amplitude, pulse width, frequency)
PD1	3-2+, 4.5 V, 60 µs, 130 Hz	7-6+, 4.0 V, 60 µs, 130 Hz
PD2	2-3+, 3.5 V, 60 µs, 130 Hz	6-7+, 4.2 V, 60 µs, 130 Hz
PD3	1-2+, 4.3 V, 90 µs, 130 Hz	6-7+, 3.2 V, 90 µs, 130 Hz

PD4	3-2+, 4.8 V, 60 µs, 130 Hz	7-6+, 4.2 V, 60 µs, 130 Hz
PD5	2-3+, 5.0 V, 90 µs, 130 Hz	5-6+, 3.5 V, 60 µs, 130 Hz
PD6	2-1+, 3.5 V, 60 µs, 130 Hz	6-5+, 4.5 V, 90 µs, 130 Hz
PD7	1-2+, 4.6 V, 60 µs, 120 Hz	5-6+, 4.6 V, 60 µs, 120 Hz
PD8	2-1+, 6.0 V, 60 µs, 180 Hz	6-5+, 3.0 V, 60 µs, 180 Hz
PD9	2-3+, 6.5 V, 90 µs, 130 Hz	4-5+, 4.5 V, 60 µs, 130 Hz
PD10	1-3+, 3.5 V, 60 µs, 130 Hz	6-7+, 2.5 V, 60 µs, 130 Hz
PD11	2-3+, 5.0 V, 90 µs, 120 Hz	6-7+, 4.5 V, 90 µs, 120 Hz
PD12	2-3-1+, 4.6 V, 120 µs, 180 Hz	6-5+, 4.0V, 90 µs, 180 Hz
PD13	2-3+, 4.2 V, 120 µs, 130 Hz	6-7+, 3.9 V, 120 µs, 130 Hz
PD14	2-3+, 2.5 V, 60 µs, 130 Hz	6-5+7+, 2.6 V, 120 µs, 130 Hz
PD15	3-2+, 2.0 V, 120 µs, 125 Hz	7-6+, 2.8 V, 90 µs, 125 Hz
PD16	1-3+, 4.9 V, 90 µs, 130 Hz	6-7+, 5.2 V, 90 µs, 130 Hz
PD17	0-3+, 5.6 V, 60 µs, 130 Hz	5-7+, 3.5 V, 120 µs, 130 Hz
PD18	2-3-1+, 2.7 V, 60 µs,130 Hz	6-7+, 3.9 V, 90 µs, 130 Hz
PD19	2-3+, 3.3 V, 120 µs, 125 Hz	6-7+, 3.3 V, 120 µs, 125 Hz
PD20	3-2+, 4.2 V, 60 µs, 130 Hz	6-7+, 3.5 V, 60 µs, 130 Hz

2.2 Experimental design: Formal test procedure of the SRTT

As described in the introduction, the SRTT is a paradigmatic procedure to study implicit motor learning introduced by Nissen and Bullemer (Nissen and Bullemer, 1987).

In our study, the SRTT was structured as follows: The presenting screen showed four horizontally arranged red circles, which lightened up randomly. Each circle corresponded to one of four ergonomically arranged buttons that were pressed by the respective fingers two to five: index finger for button I, middle finger for button 2, ring finger for button 3, and little finger for button 4 (Figure 1 shows the presenting screen and the key box with the buttons). Whenever one of the circles lightened up, the subjects had to press the corresponding button as fast and correct as possible.

The paradigm started with the Baseline [Bl] (used for *Analysis 1* and *2* as described in the following) in which the stimuli came up in random order. Thus, there was a lack of any underlying pattern and each stimulus had an equal and independent probability of occurring next. With any pressed button - correct or wrong finger - the stimulus disappeared.

In absence of any motor reaction, the trial was timed-out by stimulus withdrawal after 1.0 s. The interstimulus interval was 1.5 s. The [Bl] consisted of four blocks each consisting out of 7*12 (84) trials, one trial meaning one stimulus and the following (right, wrong or missing) response, were performed; each block was followed by a break of 20 s to prevent fatigue. The reaction time was calculated for each block including correctly answered trials only.

After the [Bl], all HCs and if possible depending on sufficient cooperation PD patients were tested in the next task (relevant for *Analysis 2*) including random and sequential blocks: This task started with two ‘random blocks’, followed by four ‘sequence blocks’, then another ‘random block’, a ‘sequence block’ again and a last ‘random block’ (Table 3). Stimuli were not presented randomly in the ‘sequence blocks’ (as in the baseline and in the ‘random blocks’) but with a sequential pattern. In the ‘sequence blocks’ stimuli were arranged in a repeating sequence of cue locations unknown by the subject.

Whereas in the ‘random blocks’ the reaction time is assumed to be constant, a decrease of reaction time in the ‘sequence blocks’ will reflect implicit motor learning presumably (at least in part) because participants benefit from implicit knowledge of the sequence.

Table 3 Elements of the SRTT paradigm
[BL] = baseline, four ‘random blocks’, also used for *Analysis 1* as explained above. [Ra] and [Rb] = two additional ‘random blocks’ at the beginning of the SRTT. [Sa] to [Se] = five ‘sequence blocks’. [Rc] and [Rd] = ‘random blocks’. b = block

[Bl]	[Ra]	[Rb]	[Sa]	[Sb]	[Sc]	[Sd]	[Rc]	[Se]	[Rd]
4 b	2 b	1b	1 b	1 b	1 b	1 b	1 b	1 b	1 b

Note that this whole composition from [Ra] to [Rd] (excluding [Bl]) was performed once with [S1] and once with [S2], as described in the following. We generated two independent 12-trials sequences with a custom-made Matlab script ([S1], [S2], Table 3) respecting previous sequence criteria (Willingham, 1998): *(i)* no direct repetition of the same button, *(ii)* no repetitive pattern of two stimuli twice after each other/ back-and-forth movements, *(iii)* no enumerative pattern of more than two stimuli, *(iv)* all four possible stimuli should occur equally often so that the sequence cannot be learned on the basis of frequency information, *(v)* no overlap between the two sequences ([S1] vs. [S2]) of more than three stimuli in a row.

Table 4 Sequences of SRTT paradigm
Index finger for button I, middle finger for button 2, ring finger for button 3, and little finger for button 4

S1	4	2	1	3	1	4	2	3	2	4	1	3
S2	2	4	3	1	2	1	4	3	4	2	3	1

All participants of the study (both HC and PD) performed the [Bl]. The PD patients were tested once in each of the two following conditions:

- Condition I: [StimOff]
- Condition II: bilateral [StimOn] (parameters in Table 2)

Before starting the task in a new condition the UPDRS III score of each patient was assessed. For PD patients the order of stimulation condition ([StimOff] versus [StimOn]) and for all participants in the task of *Analysis 2* the order of sequences ([S1] versus [S2]) were randomized. The paradigm was performed with two sequences for two reasons: *(i)* to stabilize the variance of the behavioural and spectral data and *(ii)* to compare the behavioural and spectral data of PD patients in the two conditions [StimOff] versus [StimOn]. 10 of the 21 PD patients were able to perform more than the baseline in [StimOn] and out of these 10 PD patients 7 were able to perform everything also in [StimOff].

After completion of both runs, we asked the subjects in the following order, *(i)* if they had perceived anything peculiar during the task, *(ii)* whether they had noticed a repeating sequence of stimuli locations, and if so *(iii)* to recall it, or if not *(iv)* to guess a sequence. Accordance of more than four consecutive stimuli per sequence led to rejection of the subject from *Analysis 2* to prevent confounding of our implicit motor learning analysis with explicit contributions. This procedure is considered conservative since D. Willingham had calculated random-control scores for a free recall task by rescoring each subject's recall as if the sequence seen during training had been some other, randomly selected pattern (Willingham, 1998). Thus, they obtained a mean guessing performance of 4.6 out of twelve trials. In their study the implicit motor learning group showed an average recall of 5.3 out of 12 trials.

Subjects received short breaks of 20 s between blocks and a larger break of 15 min between the two sequence runs to prevent fatigue. The whole test procedure including preparation time took 2-3 hours.

2.3 Experimental set-up

2.3.1 Subject's position

A 15.4 inch screen presented the visual stimuli. The subjects sat on a chair with back- and armrest to ensure a comfortable arm position with relaxed arm muscles and one meter distance to the presentation screen. The right arm was

adducted in the shoulder joint and the elbow was flexed in 90°. The subjects rested their right forearm on a pillow and finger 2 to 5 of the hand on the four keys of the button pad.

Subjects were instructed to give short brisk downward taps on the response box without active finger extension and to relax their fingers between two consecutive finger taps as complete as possible. Motor performance and signal quality were monitored throughout the whole experiment by the investigator.

2.3.2 EEG and EMG

The electrophysiological data flow was synchronized to motor performance. All electrophysiological data were recorded and monitored online with the Brainvision Recorder (Brain Products version 1.20, MES Electronics, Gilching, Germany) and sampled at 1 kHz. The impedance of all electrodes was kept below 15 kΩ.

We used a 64-channel EEG according to the international 10-20 system with a frontal ground (FPz) referenced to combined earlobes with an Easy cap #80 (EASYCAP GmbH, Herrsching, Germany) with Ag/AgCl sintered ring B10-S-# electrodes (EASYCAP GmbH, Herrsching, Germany).

In order to study the agonist-antagonist reciprocal interplay bipolar surface, EMG of the right FD and ED muscles were recorded. We used bipolar Ag/AgCl surface electrodes with a standardized 22 mm interelectrode spacing (Norotrode 20 Bipolar SEMG Electrodes, Myotronics-Noromed Inc., Tukwila, WA, USA). The separate EMG ground was located on the right processus styloideus radii.

Table 5 EEG channel locations
Theta: vector (in degrees) of polar angles of the electrode locations, radius: vector of polar-coordinate radii (arc-lengths) of the electrode locations

Channel number	Polar angle (theta)	Polar radius (radius)	Channel label	Channel number	Polar angle (theta)	Polar radius (radius)	Channel label
1	17.926	0.515	Fp2	33	90.000	0.133	C2
2	-17.926	0.515	Fp1	34	0.000	0.000	Cz
3	35.858	0.522	AF8	35	-90.000	0.133	C1
4	22.461	0.421	AF4	36	-90.000	0.267	C3
5	0.000	0.380	AFz	37	-90.000	0.400	C5
6	-22.461	0.421	AF3	38	-90.000	0.533	T7
7	-35.892	0.522	AF7	39	108.110	0.532	TP8
8	53.313	0.660	F10	40	110.670	0.408	CP6
9	53.867	0.528	F8	41	117.570	0.288	CP4
10	49.405	0.431	F6	42	135.070	0.181	CP2
11	39.897	0.345	F4	43	180.000	0.127	CPz
12	23.493	0.279	F2	44	-135.070	0.181	CP1
13	0.000	0.253	Fz	45	-117.570	0.288	CP3
14	-23.493	0.279	F1	46	-110.670	0.408	CP5
15	-39.947	0.345	F3	47	-108.050	0.532	TP7
16	-49.405	0.432	F5	48	126.130	0.528	P8

17	-53.913	0.528	F7	49	130.600	0.431	P6
18	-53.313	0.660	F9	50	140.100	0.345	P4
19	71.607	0.665	FT10	51	156.510	0.279	P2
20	71.948	0.532	FT8	52	180.000	0.253	Pz
21	69.332	0.408	FC6	53	-156.510	0.279	P1
22	62.425	0.288	FC4	54	-140.050	0.345	P3
23	44.925	0.181	FC2	55	-130.600	0.432	P5
24	0.000	0.127	FCz	56	-126.090	0.528	P7
25	-44.925	0.181	FC1	57	144.140	0.522	PO8
26	-62.425	0.288	FC3	58	157.540	0.421	PO4
27	-69.332	0.408	FC5	59	180.000	0.380	POz
28	-71.948	0.531	FT7	60	-157.540	0.421	PO3
29	-71.607	0.665	FT9	61	-144.110	0.522	PO7
30	90.000	0.533	T8	62	162.070	0.515	O2
31	90.000	0.340	C6	63	180.000	0.507	Oz
32	90.000	0.267	C4	64	-162.070	0.515	O1

2.3.3 Behavioral triggers

The behavioral triggers (visual cues, motor responses) were registered simultaneously to EEG and EMG through a parallel-port interface. Experimental setup and data transmissions are illustrated in Figure 1.

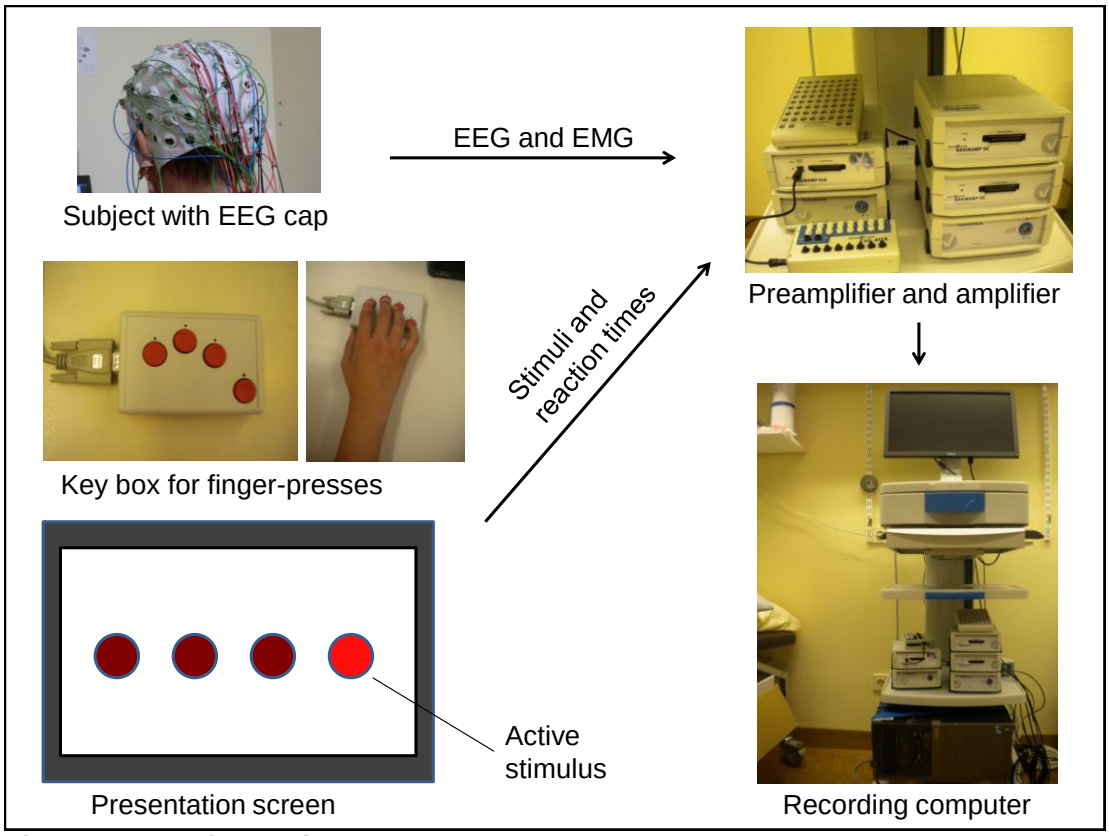

Figure 1 Experimental set-up
EEG, EMG and performance data (both stimuli and finger presses) were transferred over the preamplifier and the amplifier to the recording computer and recorded with the Brainvision Recorder.

2.3.4 Preprocessing

We employed custom routines under Matlab 7.14 (TheMathWorks, Natick, MA, USA), utilizing the EEGLAB v9.0.2.3b toolbox (Delorme and Makeig, 2004) for data preprocessing, spectral analysis, and two-dimensional topographic plots and the FieldTrip toolbox for statistical data analysis on the time-frequency series and three-dimensional data plotting (Donders Institute for Brain, Cognition and Behaviour, Radboud University Nijmegen, The Netherlands (Oostenveld et al., 2011)).

After band-pass filtering, the EEG data from 0.5-200 Hz and the EMG data from 10-300 Hz, we full-wave rectified the EMG data. Then, we visually inspected the data and rejected episodes with artifacts from facial muscles, movement artifacts and vertical or horizontal eye movements by visual inspection.

Subsequently, principal component analyses, a well-established procedure detailed previously (Delorme and Makeig, 2004), was performed. We removed principal components attributable to artifacts, such as motion-related signals, temporal or facial muscle artifact, eye blinks, eye movements, line noise and cardiovascular artifacts. We carefully inspected the topographical maps, the time activations and the activity power spectrum of each component. An example of eye blinking artifacts is given in Figure 2 and was rejected from the data.

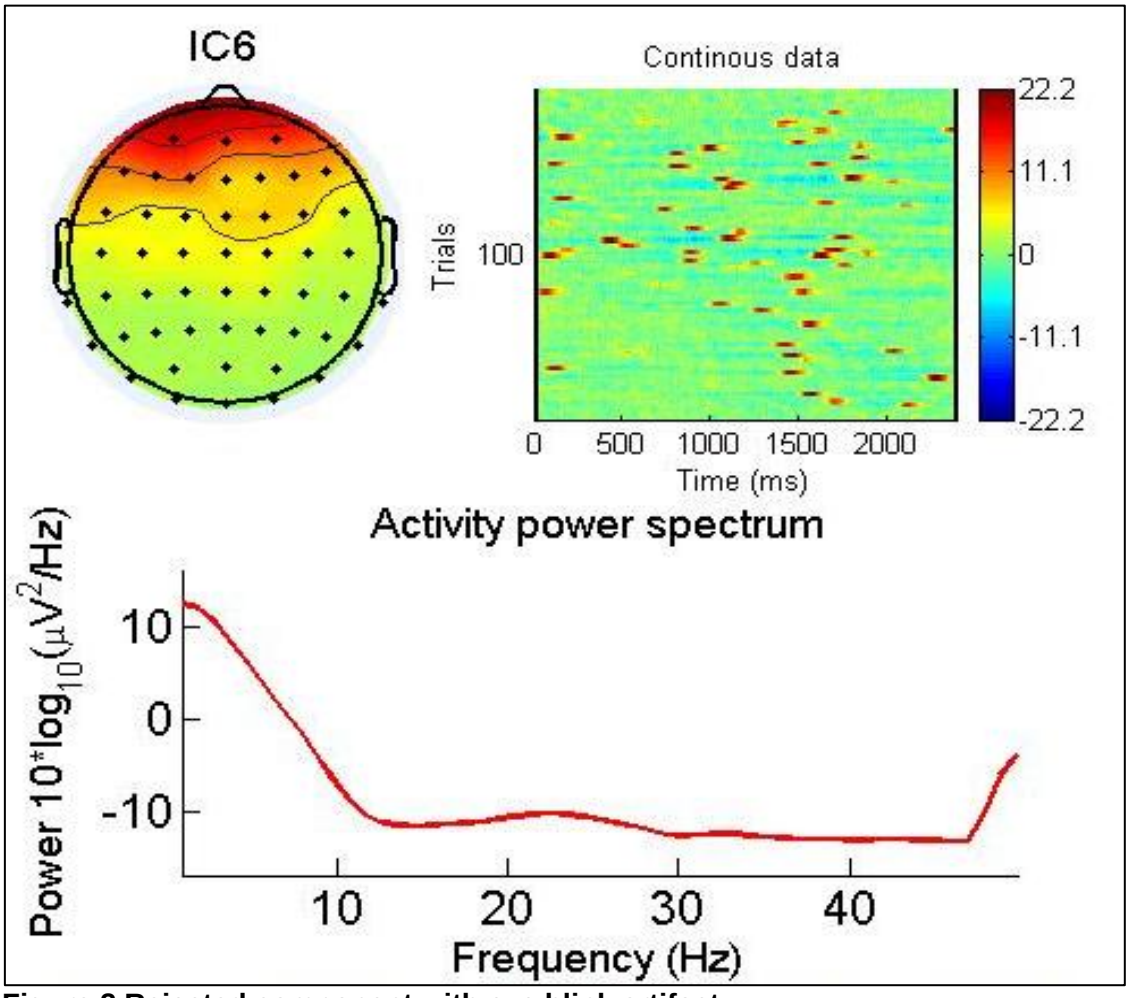

Figure 2 Rejected component with eye blink artifact
At the top left: topographic plot with selective fronto-polar high power projection; at the top right: time activations with distinct eye movements visible as red spots, on the bottom: activity power spectrum

Components with selective activity in the higher frequency bands in single channels in peripheral locations were considered as muscle artifacts. See Figure 3.

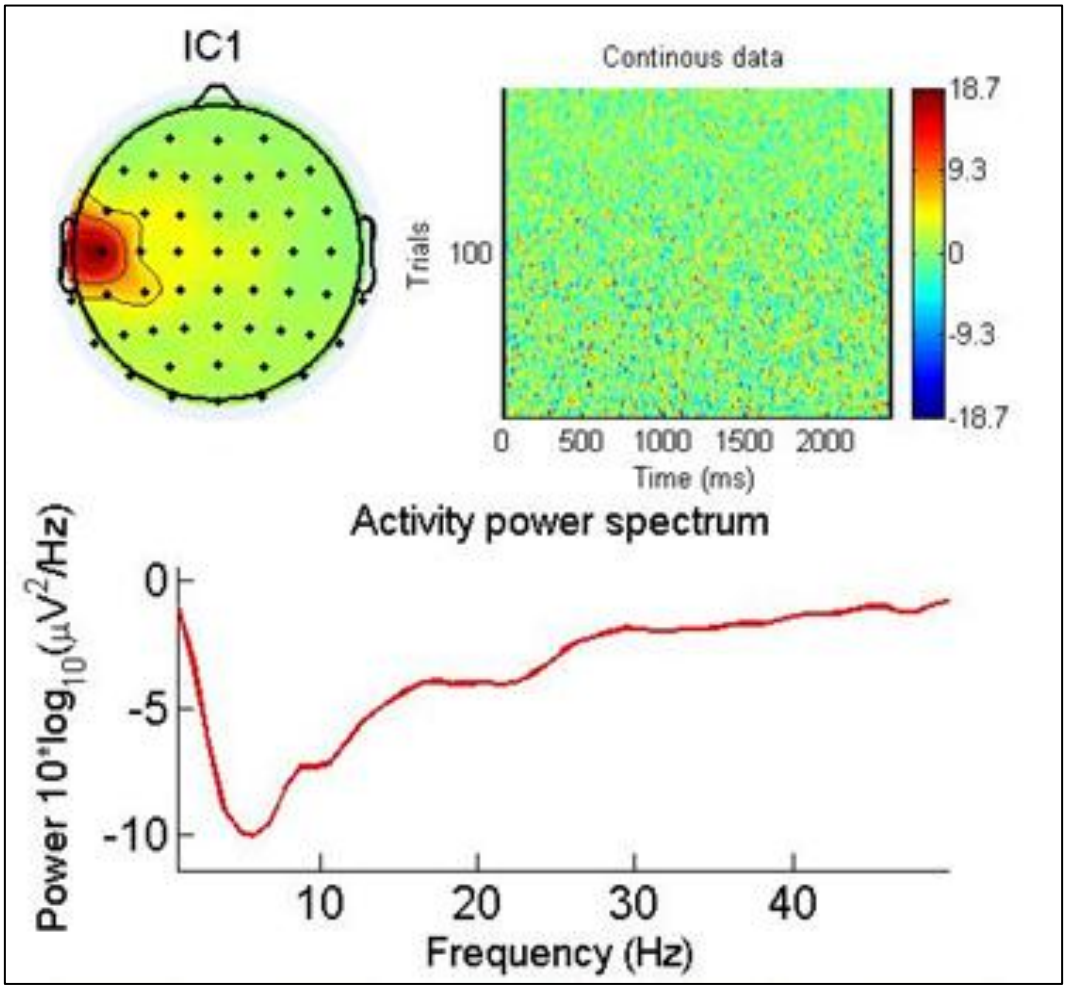

Figure 3 Rejected component with muscular artifact.

The regular cardiovascular artifacts can easily be seen by scrolling through component activation (time series). We removed the components that were affected by artifacts. Afterwards, the remaining components were transformed back to the time domain. Finally, the same procedure was performed on a second principal component analysis on the pruned data to clear residual artifacts as recommended previously by Delorme (Delorme et al., 2007). We rejected the breaks and cut the data in single epochs of 1200 ms (800ms before and 400ms after button press).

We obtained reference-free EEG data using Hjorth's source derivation, a recording technique for EEG tracings, which provides an increased ability to isolate activity localized around an electrode. It leads to a better reduction of artifacts and higher degree of topographical clarity (Hjorth, 1980).

2.4 Definition of dependent variables

2.4.1 Performance data: UPDRS III and reaction time

Before starting the task in a new condition ([StimOn] versus [StimOff]), clinical motor symptoms in terms of the UPDRS III score were assessed. To measure segmental symptoms items 20 to 26 of the UPDRS III were used.

The reaction time was computed as the time between onset of the stimulus (lightening up of one circle) on the screen and correct finger press by the subject. Wrong finger presses and implausibly short reaction times (< 200 ms) were rejected from the data analyses. We defined an error ratio of 10% per person and round as exclusion criteria for the SRTT which is in line with the common standard according to other SRTT studies with HCs, e.g., in Romano's study subjects were asked to focus more on accuracy after every round with an accuracy level fewer than 91% (Romano et al., 2010).

2.4.2 Event-related muscular and cortical time-frequency power spectra

Event-related muscular and cortical time-frequency power spectra reflect regional oscillatory activity of neuronal assemblies related to a specific event or task, in our case the button press. To visualize the mean event-related changes in spectral power, we computed the event-related (log) spectral perturbation (ERSP), which then indicates the power (in dB) at a given frequency and latency relative to the time-locking event.

For n trials, if $F_k(f,t)$ is the spectral estimate of trial k at frequency f and time t

$$ERSP\ (f,t) = \frac{1}{n}\sum_{k=1}^{n} |F_k|f,t)\,|^2$$

(Delorme and Makeig, 2004).

To compute F, we used a Morlet wavelet algorithm to obtain better frequency resolution at higher frequencies. We computed the ERSP for all cortical and muscular electrodes from - 800 ms to + 400 ms considering a Hanning-tapered sinusoidal wavelet transform to obtain better frequency resolution at higher frequencies. For muscles, we chose a frequency range of interest from 10 to 100 Hz. This resulted in a time window of the time-frequency spectra from -632 ms and +232 ms relative to the button press at time '0'. For event-related cortical time-frequency power spectra, we chose a frequency range of interest from 8 to 100 Hz. This resulted in a time window of the time-frequency spectra from -591 to +192 ms relative to the button press at time '0', which again resulted in a time resolution of 4.8 ms and a frequency resolution of 2.0 Hz.

2.4.3 Event-related corticomuscular time-frequency coherence spectra

With the EEGLAB function 'newcrossf', we computed the linear event-related time-frequency coherence spectra. The coherence estimates the extent of a complex linear relationship, respectively the degree of synchronization between two signals. It is an extension of Pearson's coefficient of correlation for complex numbers depending on the frequency of an oscillatory signal and defined by the following formula:

$$Coh_{xy}(f) = \frac{|P_{xy}(f)|^2}{P_{xx}(f)P_{yy}(f)}$$

P_{xx} and P_{yy} represent the respective autospectral densities while P_{xy} is the cross spectral density of the signals x and y. Task-related coherence reflects interregional synchronization of oscillatory neuronal activity. Coherence may range between 0 and 1 with 0 indicating a complete absence of synchronization while 1 indicates perfect synchronization.

We calculated the linear event-related time-frequency coherence spectra between all cortical channels and FD and all cortical channels and ED with particular attention to the channel C3 (SM1 = region of interest) to assess

synchronization in the frequency domain. Again, we used the Morlet wavelet algorithm.

2.4.4 PSD

With the command spectopo we were able to plot the relative topographic distribution of power of all channels at specified frequencies. In contrary to the afore described event-related analyses we computed the PSD on continuous data block-wise separately for each block of the paradigm ([BL], [Sa], [Sb], [Sc], [Sd], [Rc], [Se], [Rd]), a method commonly used in neuroimaging, such as functional MRI. We transformed the data from logarithmic [dB] power scale to linear [µV2/Hz] scale.

We inspected the PSDs as grand averages of all subjects in the following six frequency bands: theta (3.9 – 7.8 Hz), alpha (8.8 – 12.7 Hz), low beta (13.7 – 19.5 Hz), high beta (20.5 – 30.3 Hz), low gamma (31.3 – 44.9Hz) and high gamma (60.5 – 89.8Hz).

2.5 Data evaluation and statistical analyses

The statistical analysis was performed with the software IBM Statistics SPSS version 20 and Matlab 7.14.

Performance data: Reaction times were normalized to baseline reaction time on individual subject level to stabilize interindividual variance of average reaction time (Gomez-Beldarrain et al., 1998). All performance data were normally distributed according to Kolmogorov-Smirnov tests and therefore ANOVAs and parametrical t-tests were performed. In case of deviations from the sphericity assumption according to Mauchly's sphericity test, the Greenhouse-Geisser correction was applied. We computed a three-way repeated measures ANOVA with factors SEQUENCE, ORDER and BLOCK to compare the data from [S1] and [S2] and [O1] (first round) and [O2] (second round) to explore whether there was an effect of sequence or order. Since there was neither an effect of SEQUENCE ($F_1 = 1.617$, $P = 0.259$) nor of ORDER ($F_1 = 1.746$, $P = 0.244$) we

concatenated the two datasets of each subject in order to stabilize the variance of behavioral and spectral measures.

We computed the median of all reaction times out of one block and performed repeated measures ANOVA with factor BLOCK. As a post hoc test [Sa], [Sb], [Sc], and [Sd] were each compared to the pooled data of [BL, Ra and Rb] in a one-tailed paired t-test, and [Se] was compared to the pooled data of [Rc and Rd] in a one-tailed paired t-test. P-values were corrected for multiple testing according to the FDR correction (Benjamini et al., 2001). The significance level was set to alpha < 0.05.

Implicit motor learning was assumed to be reflected by a significant decrease of reaction times in ‘sequence’ compared to ‘random’ blocks as described elsewhere (Cohen et al., 1990; Keele et al., 1995; Nissen and Bullemer, 1987).

Electrophysiological data: Since tonic background activity caused by rigidity interfered with the EMG recordings, we aimed to improve the signal-to-noise ratio. Thus, we masked the muscular time-frequency samples on the 95% bootstrap significance level, i.e. non-significant time-frequency samples of muscular activation and corticomuscular cross-coherence were zeroed out on individual subject level.

We used the time-frequency event-related spectral pertubation to determine the muscular activation onset. To this end, we defined the time point of muscular activation onset on the single subject level when activity first exceeded the bootstrap significance level. Muscular activation onset of FD and ED were then compared between conditions ([StimOff] vs. [StimOn]) with paired samples t-tests. Finally, grand averages of these thresholded individual spectra were built to achieve group level data.

To compare the different treatment conditions or successive blocks, we used a nonparametric framework for comparisons of the cortical event-related spectral pertubation and corticocortical cross-coherence. The Monte-Caro estimates from the permutation distribution were determined. We used the permutation statistics implemented in the Fieldtrip open source toolbox. 1000 random permutations were employed on a dependant samples t-test with an alpha level

of $p < 0.05$ and non-significant features of the output plots were zeroed out and plotted in green. These sample-wise statistics (product of number of channels * times * frequencies, i.e. 64 * 200 * 46) implicate an enormous number of multiple comparisons. Thus, a cluster-based correction method was applied to effectively address this multiplicity problem without losing sensitivity for spectral changes (Maris and Oostenveld, 2007).

Relationship between clinical scores and electrophysiological data: We explored whether the segmental UPDRS motor score improvement (difference between [StimOff] and [StimOn]) as dependent variable can be predicted by the change in MRD using multiple regressions. Therefore, we computed the difference in movement-related power mean of the time-frequency window of interest as derived from the event-related spectral pertubation analyses. We included the regions of interest, i. e. the electrodes of the SM1 regions (C1, C3, C5), premotor area (FC1, FC3, FC5), prefrontal area (F1, F3), and central region including SMA area (Fz, FCz). Colinearities between electrodes used in our model were ruled out which was important because movement-related desynchronization may show similar patterns across neighboring electrodes.

For the PSD, we constructed topographic maps using a statistical nonparametric mapping procedure. Using two-tailed paired-sample t-tests, we performed group-wise comparisons between [BL-Sa], [BL-Sb], [BL-Sc], [BL-Sd] and [pooled data from Rc and Rd - Se]. The null hypothesis of equality was rejected for $alpha < 0.05$ after correction for multiple comparisons using the false discovery rate method (Benjamini and Hochberg, 1995). We plotted the significant t-values; all non-significant t-values were put to 0.

3 Results

3.1 *Analysis 1*: Externally paced finger movements in PD patients

3.1.1 Clinical scores: UPDRS III

As expected, [StimOn] led to a significant improvement of motor symptoms in the total UPDRS III compared to [StimOff] (22.3 ± 9.7 vs. 57.0 ± 13.6; paired-sampled t-test: t_{19} = 14.184, p < 0.001). Similarly, there was a significant improvement of the segmental UPDRS III subscore (8.1 ± 4.6 vs. 20.3 ± 6.7; t_{19} = 10.532, p < 0.001), and each individual patient exhibited a segmental motor improvement of at least 30% (Table 5).

Table 5 Complete UPDRS III and segmental UPDRS III
Note that the segmental UPDRS III consists of items 20-26 of the complete UPDRS.

Patient	UPDRSIII [StimOff]	UPDRSIII [StimOn]	Segmental UPDRSIII [StimOff]	Segmental UPDRSIII [StimOn]
PD1	64	13	26	6
PD2	38	22	14	11
PD3	61	19	25	8
PD4	38	8	11	2
PD5	54	19	24	10
PD6	48	7	12	0
PD7	64	20	17	7
PD8	39	18	15	9
PD9	68	27	29	8
PD10	50	10	18	2

PD11	48	24	22	7
PD12	61	24	17	8
PD13	31	20	7	5
PD14	70	23	24	8
PD15	59	30	17	9
PD16	75	40	32	18
PD17	70	18	24	5
PD18	72	36	25	16
PD19	52	23	18	7
PD20	77	44	29	16

3.1.2 Reaction Times

Including only the correct trials of the [Bl] data of all 20 PD patients reaction time was significantly shorter with [StimOn] compared to [StimOff] (649.7 ± 137.9 ms vs. 712.2 ± 117.0 ms; $t_{19} = 2.308$, $P = 0.016$; one-tailed paired t-test). Error ratio was significantly higher in the [StimOff] condition with 25.21 ± 19.0 % compared to [StimOn] with 14.57 ± 14.9 % ($t_{19} = 2.657$, $P = 0.016$).

3.1.3 Power FD

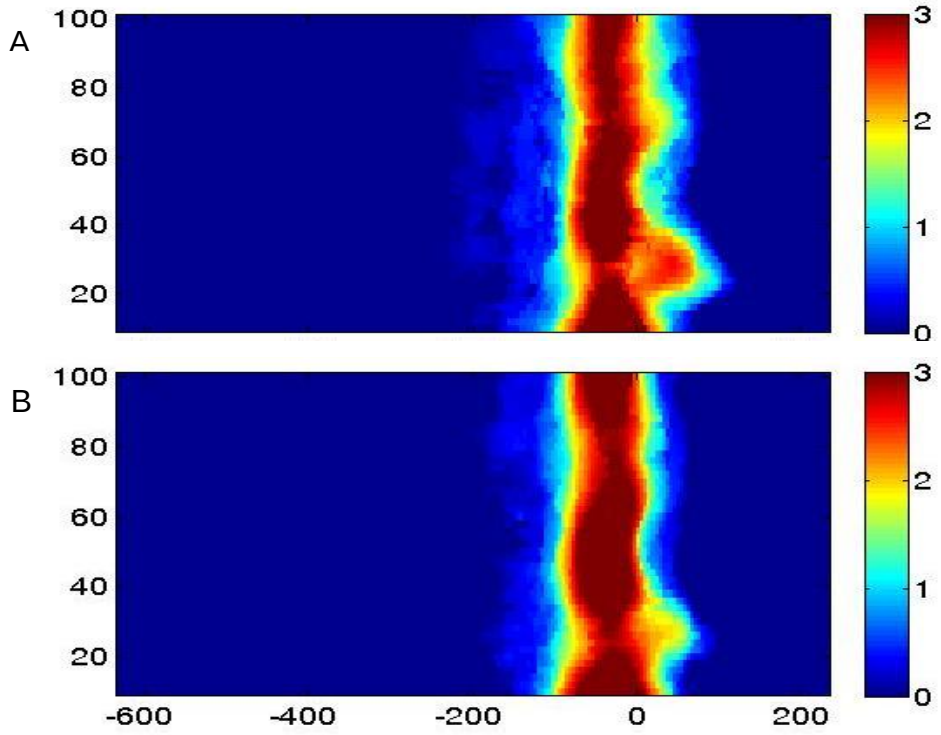

Figure 4 ERSP of FD in PD patients
ERSP plots of the agonistic muscle FD. X-axis: time from -633 to +232 ms around the button press. Y-axis: frequencies from 10 to 100 Hz. The color bar indicates the power in dB. (A) PD [StimOff], (B) PD [StimOn]

In both conditions, the broad band activation of FD started 90-100 ms before button press earliest in alpha band. The main activation outlasted the button press for approximately 40 ms. Highest amplitudes of power were found in alpha (around 12 Hz) and low gamma band (around 40 Hz). Maximal amplitude in [StimOff] was 4.1 dB and in [StimOn] 4.2 dB. The permutations statistics of the time-frequency spectrum including cluster-based correction for multiple comparisons did not show a significant difference of FD activation.

Both [StimOff] and [StimOn] presented with a similar time course of muscular activation: FD activation onset was almost the same in both therapy conditions (-123.5 ± 53 ms in the [StimOff] and -134.7 ± 51 ms in the [StimOn]; $t_{18} = 1.025$, $P = 0.319$; paired samples t-test).

A Pearson product-moment correlation coefficient was calculated to determine the relationship between an individual's onset of FD and their clinical scores in

UPDRS III and segmental UPDRS III. There was no significant correlation between UPDRSIII/segmental UPDRSIII and the onset of FD neither in [StimOff] nor in [StimOn].

Table 6 Pearson correlation coefficient between FD onsets and clinical scores

Condition	Pairs	Correlation coefficient r	Significance
PD [StimOff]	FD onset – segmental UPRDS III	r_{20} = - 0.011	P = 0.965
	FD onset – UPDRS III	r_{20} = - 0.108	P = 0.651
PD [StimOn]	FD onset – segmental UPDRS III	r_{20} = - 0.220	P = 0.365
	FD onset – UPDRS III	r_{20} = - 0.141	P = 0.564

3.1.4 Power ED

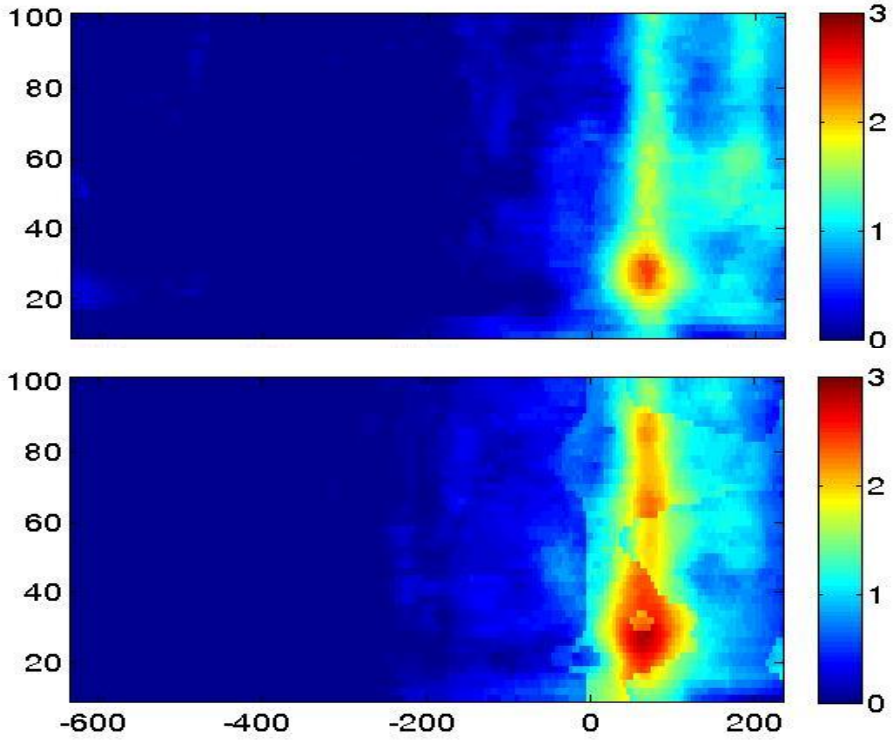

Figure 5 ERSP of ED in PD patients
ERSP plots of the antagonistic muscle ED. X-axis: time from -633 to +232 ms around the button press. Y-axis: frequencies from 10 to 100 Hz. The color bar indicates the power in dB. (A) PD [StimOff], (B) PD [StimOn].

In both conditions, the activation of the antagonistic muscle ED began at about 0-10 ms and ended approximately 120 ms after button press. In the high beta band, power reached the highest amplitudes, up to 2.4 dB in [StimOff] and 2.8 dB in [StimOn]. In [StimOn], activation in the high gamma band was more pronounced than in [StimOff], however, this did not reach statistical significance after pairwise permutation tests and cluster-based correction for multiple comparisons.

Activation started around -11.0 ± 72 ms in PD [StimOff] and - 35.3 ± 92 ms in PD [StimOn]. The difference of onset times in the two conditions did not reach significance (paired-samples t-test PD [StimOn] and [StimOff]: $t_{17} = 1.017$, $P = 0.324$).

Activation onset of FD and activation onset of ED differed significantly in both conditions (Paired-samples t-test, PD [StimOff]: $t_{19} = -7.7$, $P = 0.000$, PD

[StimOn]: t_{17} = -3.3, P = 0.004). The time period between onset of FD and ED is 112.5 ± 65ms in [StimOff] and 97.7 ± 107ms in [StimOn].

To summarize the activation data of FD and ED in both conditions:

- The ERSP of both FD and ED was not modulated with STN-DBS stimulation.
- Activation onsets of both FD and ED did not differ significantly between conditions.

3.1.5 MRD – topographic mapping

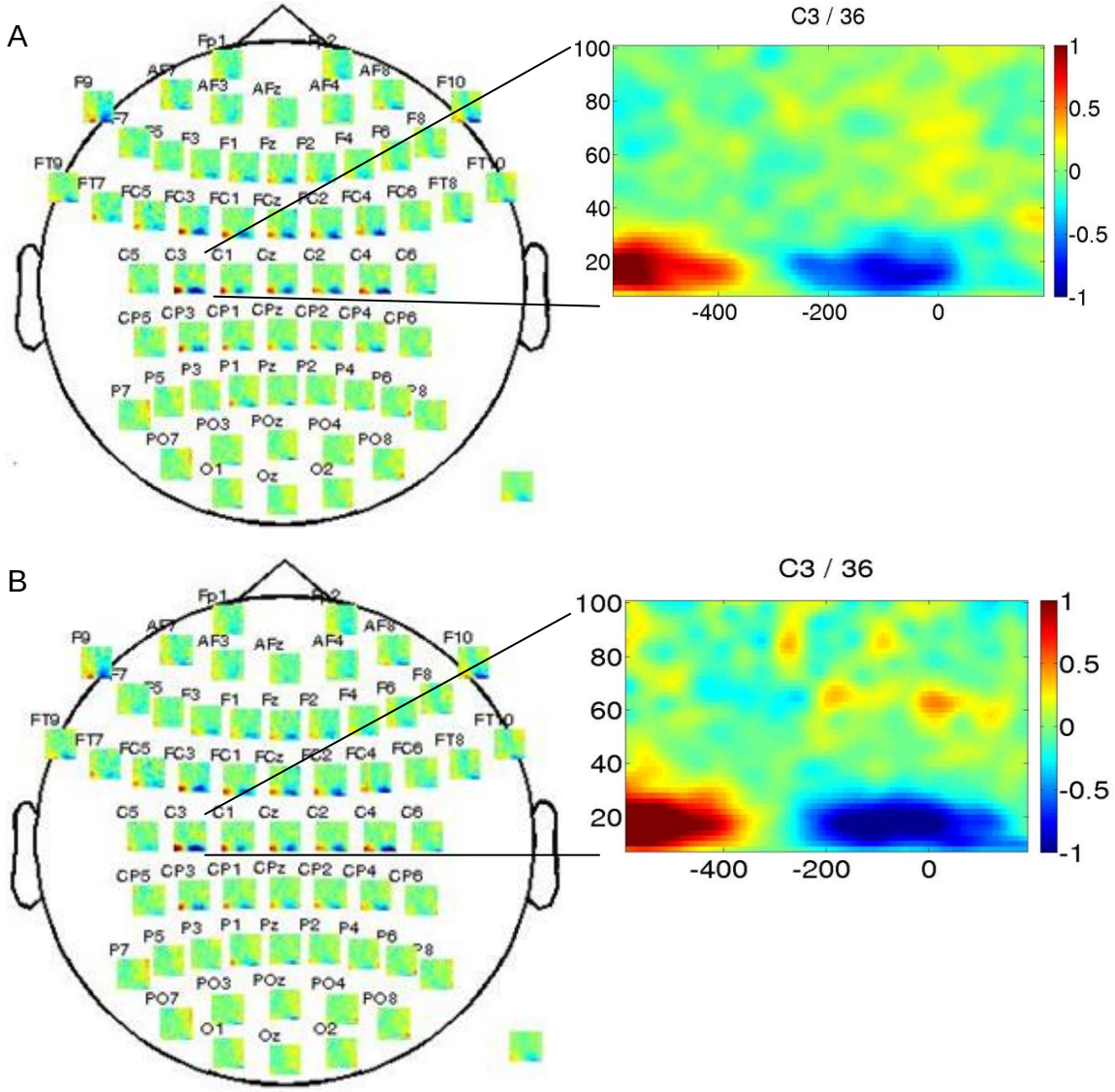

C

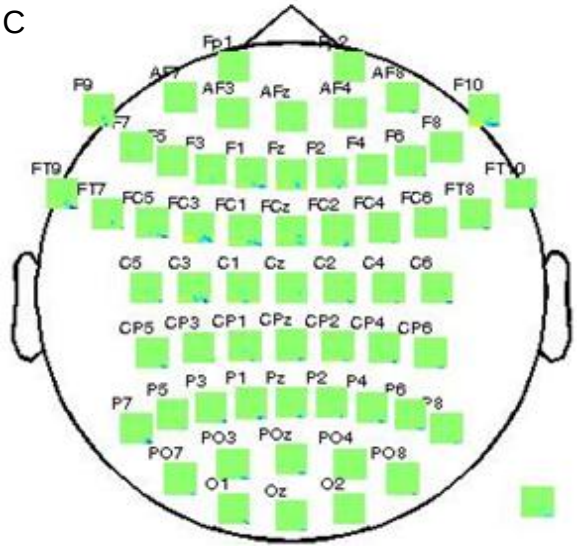

Figure 6 Topographic mapping of ERSP in PD patients
Topographic mapping of ERSP plots on the left and ERSP plot of C3 on the right side. X-axis: time from -591 to +192 ms around the button press. Y-axis: frequencies from 8 to 100 Hz.(A) ERSP [StimOff], (B) ERSP [StimOn], (C) ERSP [StimOn] - [StimOff] including Permutations statistics and cluster-based correction; n.s. time-frequency samples are zeroed out and presented in green

In the [StimOff] condition MRD of alpha and beta band activity was observed with focal pronunciation over the bilateral sensorimotor C3 and C4 electrodes. This also involved the central and (to a lesser degree) the bilateral frontal electrodes (Figure A).

In the left SM1 region of interest (C3 electrode), alpha and beta MRD onset occurred at approximately -250 ms relative to finger tap registration at time ‘0’ and outlasted the finger tap for approximately +40 ms. In [StimOn], MRD covered a wider cortical area including the prefrontal, frontal, fronto-central, temporal, supplemental motor, bilateral centro-parietal and parieto-occipital electrodes (Figure B). There was no significant difference between conditions in gamma band.

With [StimOn], both alpha and to a lesser extent beta band MRD were significantly stronger compared to the [StimOff] condition, mostly pronounced over the left sensorimotor area (Figure 6C).

On the left SM1 region of interest MRD onset occurred at approximately -350 ms with [StimOn] similar to [StimOff], however, outlasted the finger tap for +160 ms and thereby significantly longer compared with [StimOff].

Taken together, the MRD was significantly stronger and outlasted the finger tap longer with [StimOn] in the alpha, low and high beta bands over a wide range of channels. There was no significant modulation of the movement-related activity in the gamma bands.

Next, we analyzed whether clinical improvement could be predicted by MRD differences between [StimOff] and [StimOn]. For the multiple regression model we included electrodes with major MRD modulation when comparing [StimOff] and [StimOn]: left SM1, premotor areas, prefrontal areas, and the central areas including SMA. For the MRD difference ([StimOff] – [StimOn]) we chose the time-frequency window of interest that showed maximum event-related spectral pertubation (frequency range: 14-24 Hz, time range: -198 to -1 ms). The highest coefficient of determination was accomplished when applying five electrodes of interest (F1, FC1, FCz, C1, C5; $R^2 = 0.78$, $F = 4.293$, $P = 0.014$).

Furthermore, we were able to model the reaction time improvement ([StimOff] vs. [StimOn]) (electrodes F1, FC3, Cz, C1, C5; $R^2 = 0.809$, $F = 5.306$, $P = 0.006$).

3.1.6 Event-related time-frequency corticomuscular cross-coherence with FD

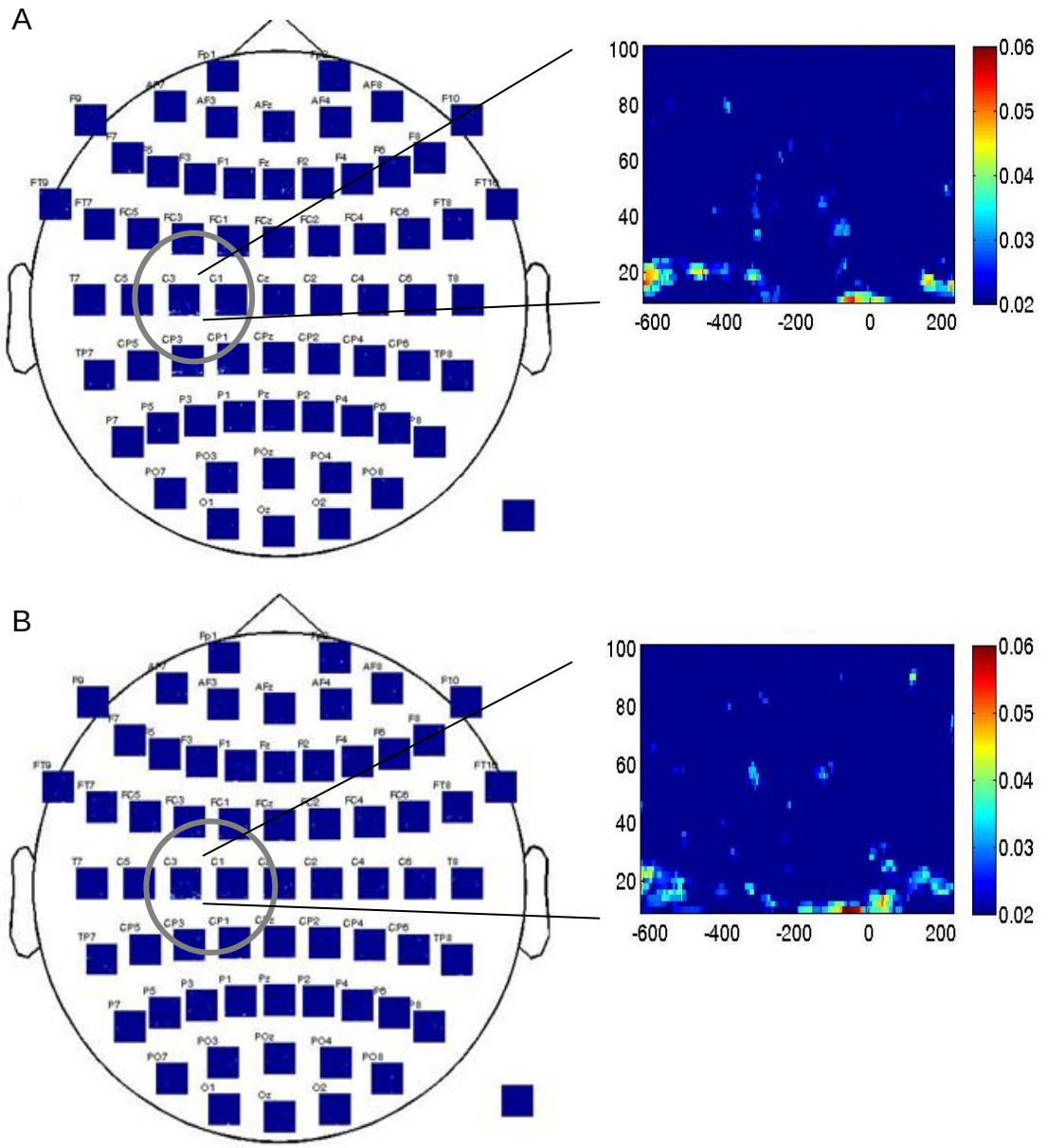

Figure 7 Topographic mapping of event-related time-frequency coherence to FD in PD patients
Topographic mapping of CMC between cortex and FD on the left and CMC between C3 (SM1) and FD on the right side. X-axis: time from -633 to +232 ms around the button press. Y-axis: frequencies from 10 to 100 Hz. The color bar indicates the level of CMC. (A) CMC [StimOff], (B) CMC [StimOn]

Both in condition [StimOff] and [StimOn], CMC to FD was found mainly in alpha and beta band and primarily in the region of interest (SM1, C3), in the channels C1, CP1 and CP3 and only weakly in some frontal and fronto-central channels.

The event-related time-frequency CMC to FD was not modulated significantly by STN-DBS.

Between the left motor cortex and the agonistic muscle FD, we found a weak diffuse beta band CMC in both conditions before finger tapping. This CMC ended approximately 300 ms before and reemerged 150 ms after the button press. Besides, alpha band CMC occurred around the button press which started around 90 ms before and lasted until approximately 60 ms after the button press in [StimOff]. Peak coherence was found 46 ms before button press with 0.05 in [StimOff]. In [StimOn] event-related alpha band CMC lasted longer (from -200 ms until 100 ms) and was more pronounced than in [StimOff]. In [StimOn] peak coherence was found 60 ms before button-press with 0.06.

3.1.7 Event-related time-frequency corticomuscular cross-coherence with ED

A

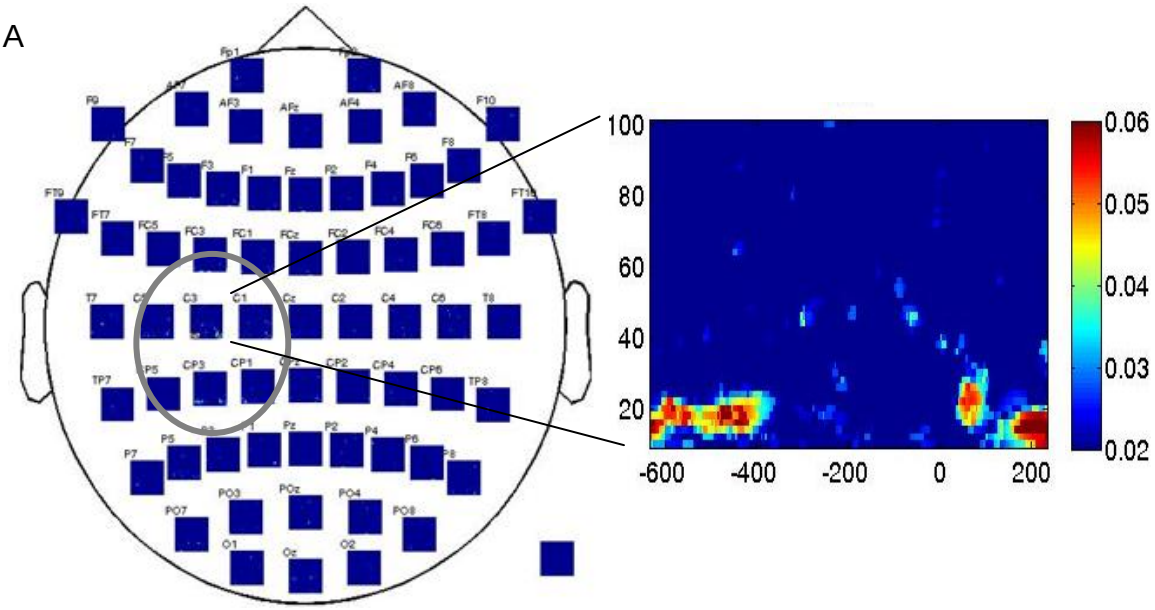

B

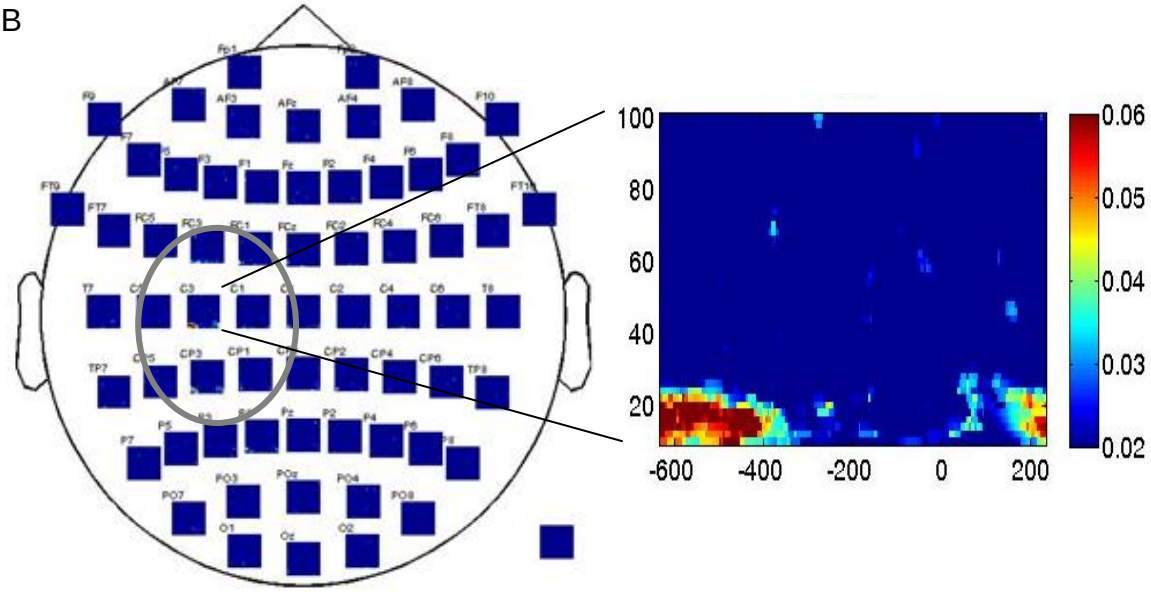

Figure 8 Topographic mapping of event-related time-frequency CMC to ED in PD patients
Topographic mapping of CMC between cortex and ED on the left and CMC between C3 (SM1) and ED on the right side. X-axis: time from -633 to +232 ms around the button press. Y-axis: frequencies from 10 to 100 Hz. The color bar indicates the level of CMC. (A) CMC [StimOff], (B) CMC [StimOn]

CMC to ED was also found mainly in alpha and beta band and primarily in the region of interest (SM1, C3), but also over the channel CP3 and weaker over FC3 in both conditions.

Similar to FD, there was an early beta band CMC between the contralateral motor cortex and the ED in the premovement period. Then coherence was suppressed approximately 350 ms before button press. On individual subject level this early CMC was stronger in [StimOn] than in [StimOff] and it was suppressed during activation of the muscle but for a beta peak of CMC in [StimOff] from 30 to 100 ms which could not be found in [StimOn]. On group level these differences did not reach significance in the permutation analysis after cluster-based correction. Significant CMC reoccurred around 150 ms after the button press.

3.2 *Analysis 2*: Implicit motor learning

3.2.1 Performance data

3.2.1.1 PD patients

20 PD patients performed the [Bl], but only 4 PD patients were able to the complete the whole SRTT paradigm in [StimOff], and 6 PD patients completed the SRTT in [StimOn]. 3 of the 4 patients who performed the task in both conditions had an error ratio of more than 10% in at least one condition (Table 7). In the end, only 1 PD patient performed the task completely in both conditions with an error ratio of less than 10%.

In the PD group *Analysis 2* (assessing implicit motor learning and including the other blocks than the [Bl] of the paradigm) was not performed due to the high drop-out rate of patients and the high error ratio in those PD patients that performed the complete paradigm.

Table 7 PD patients in SRTT: Error ratio in 'sequence blocks'
Concatenated error ratio in % of all 'sequence blocks' [Sa, Sb, Sc, Sd, Se] in the two conditions

* = error ratio > 10%, x = discontinued

PD patient	error ratio in % [StimOff]	error ratio in % [StimOn]
PD4	33.44*	15.48*
PD5	8.33	7.38
PD7	X	5.00
PD9	17.62*	12.33*
PD10	X	4.75
PD12	27.86*	9.53

3.2.1.2 HCs

Data from 3 of 15 HCs were excluded from further analysis due to evidence for explicit learning in these subjects. Consequently, for the performance data in *Analysis 2* we used 12 datasets. The HC group presented with implicit motor learning reflected by a significant decrease in reaction time in the 'sequence blocks' (Figure 11). A repeated measures ANOVA revealed significant differences between blocks (F_7 = 4.256, P = 0.001). In the post-hoc t-tests, [Sa] und [Sb] did not differ significantly from the pooled [BL, Ra and Rb] (Sa: t_{11} = 1.887, P = 0.1147, Sb: t_{11} = 1.257, P = 0.235). [Sc] (t_{11} = 3.102, P = 0.04) and [Sd] (t_{11} = 2.888, P = 0.03) displayed significantly shorter reaction times compared to [Bl]. [Se] was significantly faster than the two last random blocks [Rc and Rd] (one-tailed paired t-test t_{11} = 3.128, P = 0.01). Taken together, motor performance significantly improved in the 'sequence blocks' [Sc], [Sd], and [Se] compared to 'random blocks'.

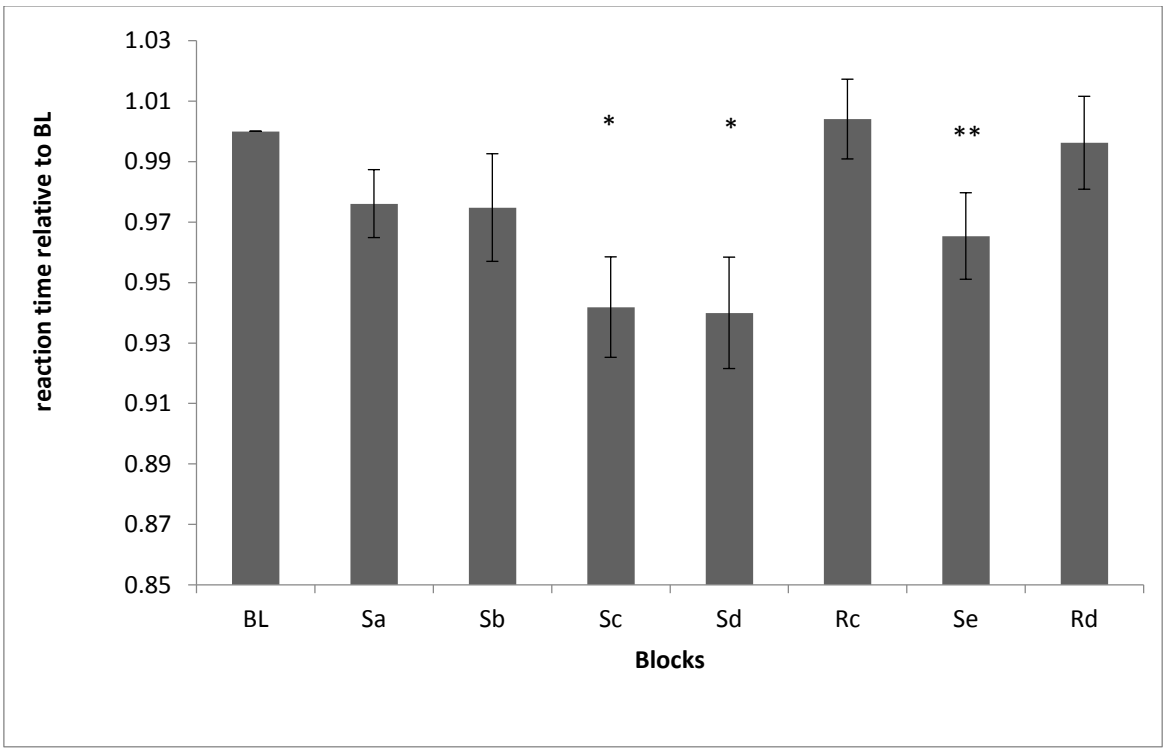

Figure 9 Grand averages of relative reaction times and standard error pooled by blocks during implicit motor learning.
Decreased reaction time in 'sequence blocks', followed by slower reaction times in [Rc and Rd]. [*] = 'sequence blocks' with significantly improved motor performance compared to BL. [**] = 'sequence block' with significantly improved motor performance compared to the two random blocks in the end [Rc and Rd]. X-axis: blocks as

described above (BL= concatenated ‘random blocks’, note that here, the first block consists of 6 ‘random blocks’: [Bl], [Ra], [Rb]; Rc-Rd = ‘random blocks’; Sa-Sd = ‘sequence blocks’). Y-axis: mean reaction time relative to [Bl].

3.2.2 PSD in HCs

We used the PSD analyses to compare the [BL] with the following blocks in all frequency bands in order to find EEG correlates of the process of implicit motor learning. We found significant changes in local activities comparing the [BL] to the following blocks in alpha and low beta band as described here:

Alpha band (Figure 10): When comparing [BL-Sc] we found an increased activation in two electrodes (P4, PO4) over the right posterior parietal cortex region and larger left hemispheric activation over the left lateral centro-parietal and posterio-parietal cortices (C5, CP5, CP3, P7, P5, P3, P1, PO7, PO3, O1). [Sa], [Sb], [Sd] and [Se] did not differ significantly from [BL] in the alpha band.

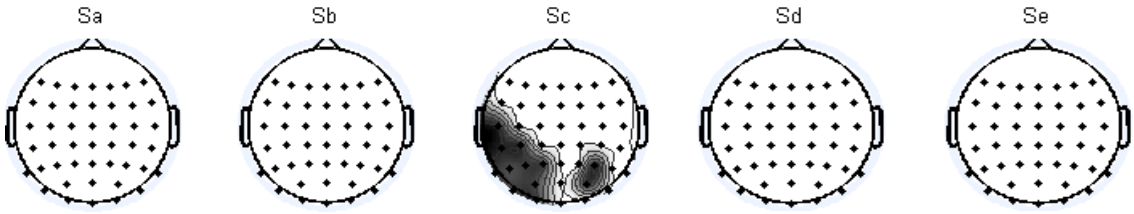

Figure 10 PSD: Topographic maps of t-values in alpha-band
Comparisons: [BL-Sa], [BL-Sb], [BL-Sc], [BL-Sd] and the pooled data [Rc and Rd - Se]. Note that we used a nonparametric mapping procedure and all comparisons were FDR corrected and all non-significant t-values were put to [0]. Grey: significant t-values in [Sc] compared to [BL].

Low beta band (Figure 11): We found an increased activation in various electrodes in [BL-Sa], more dominant on the left hemisphere, including left frontal, left supplemental motor, left premotor, left motor and bilateral posterior parietal cortices (F3, F1, Fz, FC3, FC1, FCz, FC2, C5, C3, C1, Cz, C4, CP5, CP3, CP1, CPz, CP2, P7, P3, P1, P2, P4, PO3, PO4). In [BL-Sc] we found a significantly increased activation in two electrodes (P4, PO4) over the right posterior parietal cortex region which was also described before in alpha band in the same block. [BL-Sd] showed a significantly increased activation in the right posterior parietal region (P2, P4, PO4) and the left temporal region (CP5, P7). [Sb] and [Se] did not differ significantly from [BL] in the low beta band.

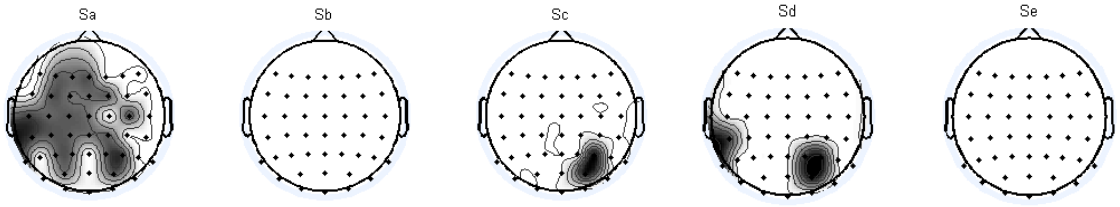

Figure 11 PSD: Topographic maps of t-values in low beta-band
Comparisons: [BL-Sa], [BL-Sb], [BL-Sc], [BL-Sd] and the pooled data [Rc and Rd - Se]. Note that we used a nonparametric mapping procedure and all comparisons were FDR corrected and all non-significant t-values were put to 0. Grey: significant t-values in [Sa], [Sc] and [Sd] compared to [BL].

Theta, high beta, low gamma and high beta band: We found no significant changes in any of the comparisons [BL-Sa], [BL-Sb], [BL-Sc], [BL-Sd] and the pooled data of [Rc and Rd - Se] in local activities in the frequency bands theta, high beta, low and high gamma.

3.2.3 Power FD in HCs

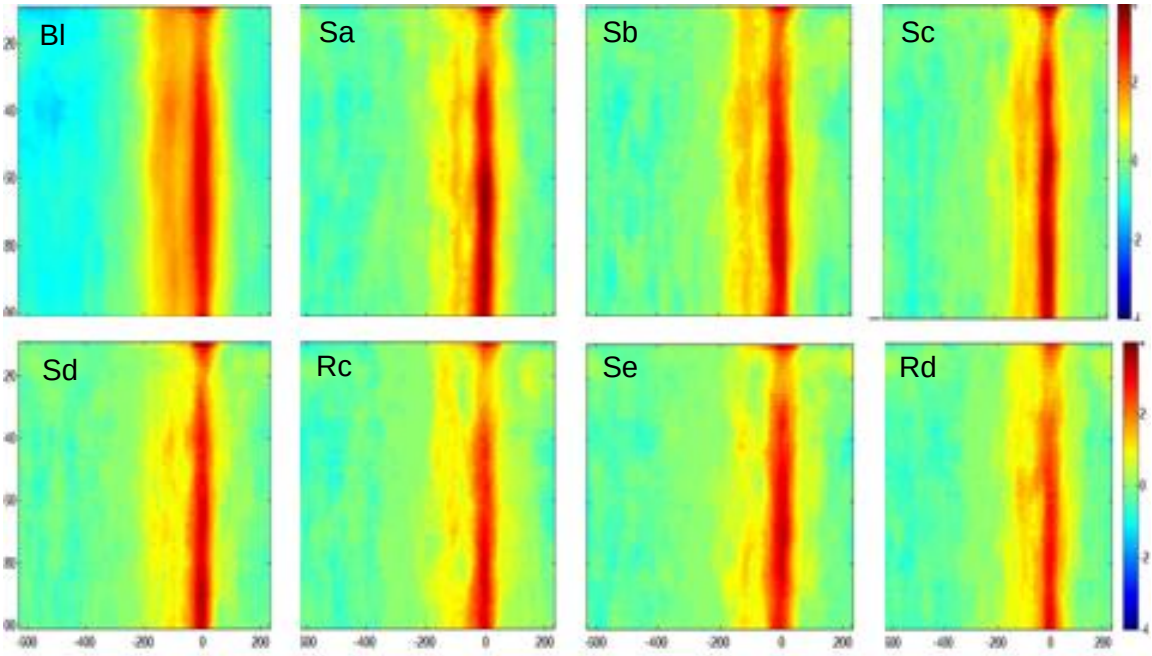

Figure 12 ERSP of FD (block-wise)
ERSP plots of the agonistic muscle FD separately for each block (Bl, Sa, Sb, Sc, Sd, Rc, Se, Rd) in HCs. X-axis: time from -633 to +232 ms around the button-press. Y-axis: frequencies from 10 to 100 Hz. The color bar indicates the power from -4 to 4 in dB.

For the agonistic muscle FD we found activations in all frequency bands starting at approximately -140 ms with a pronounced power in the 50 ms directly before and after the button press in each block. The high gamma band presents with

the strongest power, which varies over blocks: the [BL] power goes up to 3.4 dB, then it increased to a maximum in [Sa] (3.9 dB) over [Sb] (3.5 dB) and [Sc] (3.7 dB), after [Sd] (3.6 dB) it decreases to [Rc] (3.3 dB), [Se] (3.4 dB) and [Rd] (3.1 dB, all peak values). We found no significant modulation of muscle activation over blocks.

3.2.4 MRD in HCs– cortical mapping

A

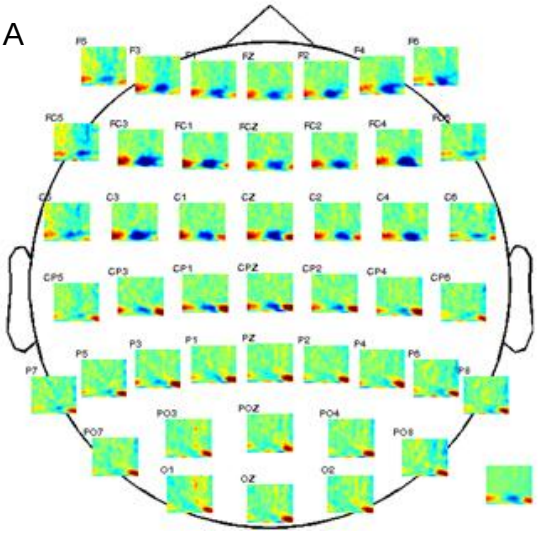

B

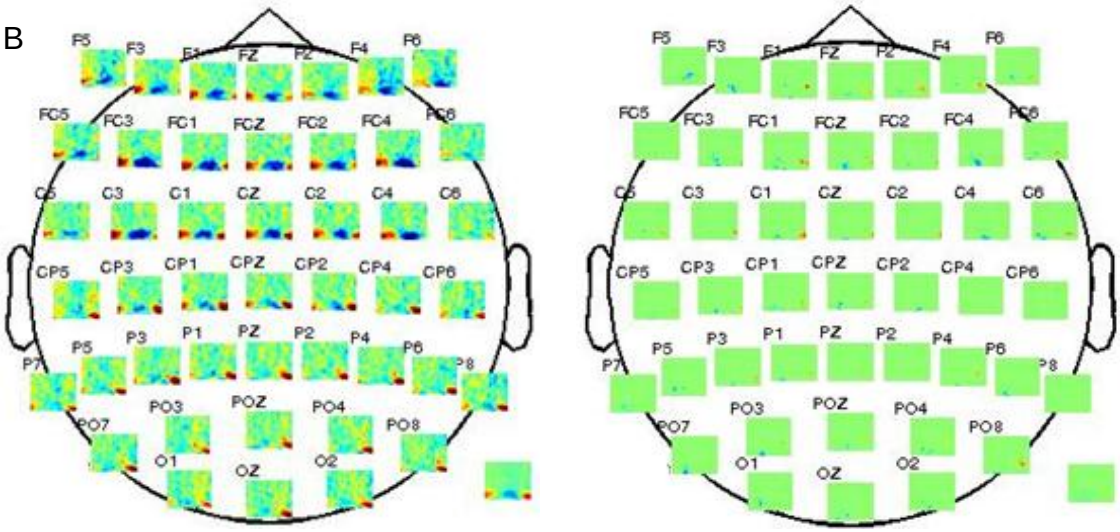

C

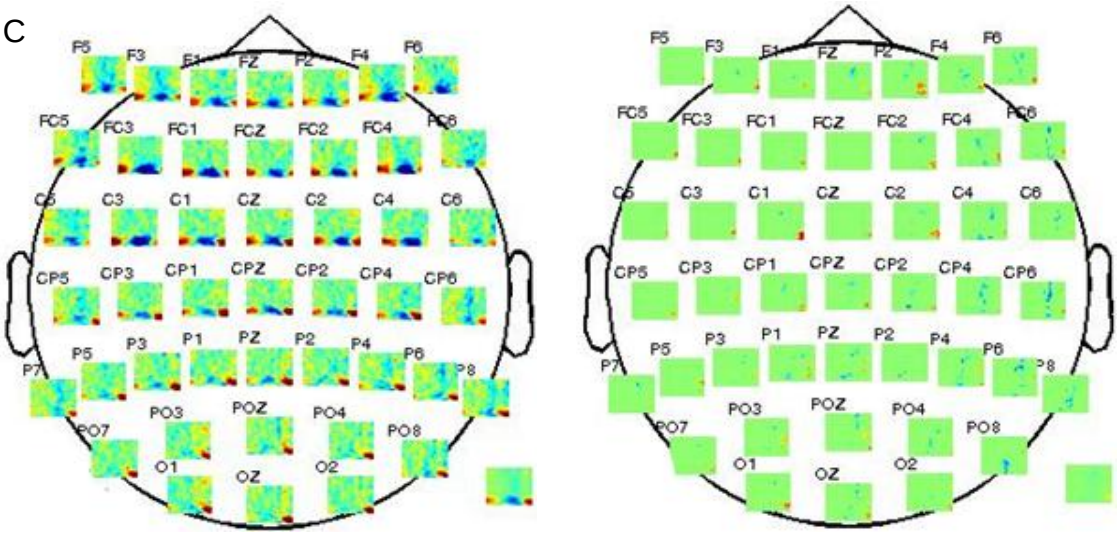
F5 F3 F1 FZ F2 F4 F6
FC5 FC3 FC1 FCZ FC2 FC4 FC6
C5 C3 C1 CZ C2 C4 C6
CP5 CP3 CP1 CPZ CP2 CP4 CP6
P5 P3 P1 PZ P2 P4 P6
P7 P8
PO3 POZ PO4
PO7 PO8
O1 OZ O2

D

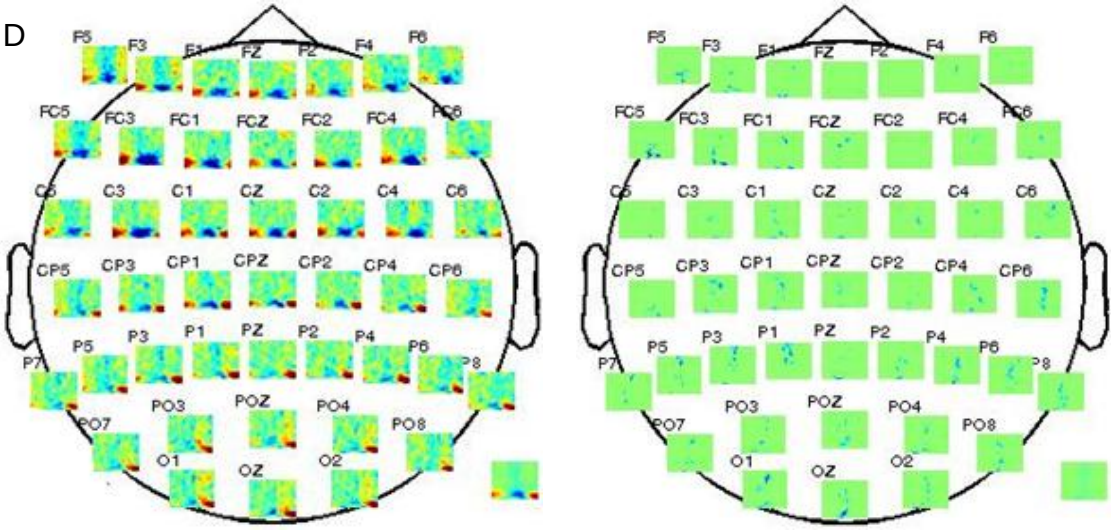
F5 F3 F1 FZ F2 F4 F6
FC5 FC3 FC1 FCZ FC2 FC4 FC6
C5 C3 C1 CZ C2 C4 C6
CP5 CP3 CP1 CPZ CP2 CP4 CP6
P5 P3 P1 PZ P2 P4 P6
P7 P8
PO3 POZ PO4
PO7 PO8
O1 OZ O2

E

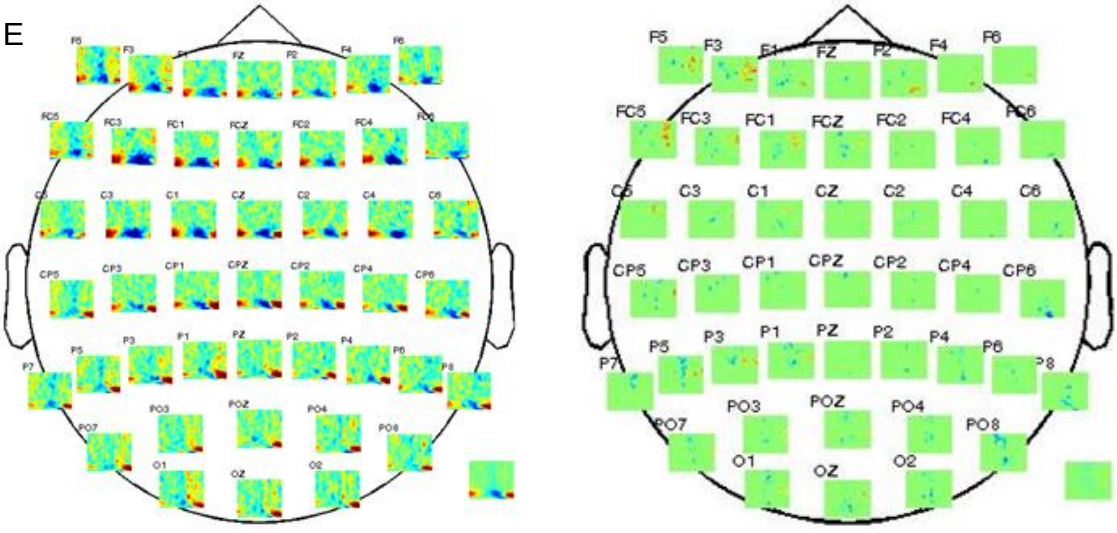
F5 F3 F1 FZ F2 F4 F6
FC5 FC3 FC1 FCZ FC2 FC4 FC6
C5 C3 C1 CZ C2 C4 C6
CP5 CP3 CP1 CPZ CP2 CP4 CP6
P5 P3 P1 PZ P2 P4 P6
P7 P8
PO3 POZ PO4
PO7 PO8
O1 OZ O2

F

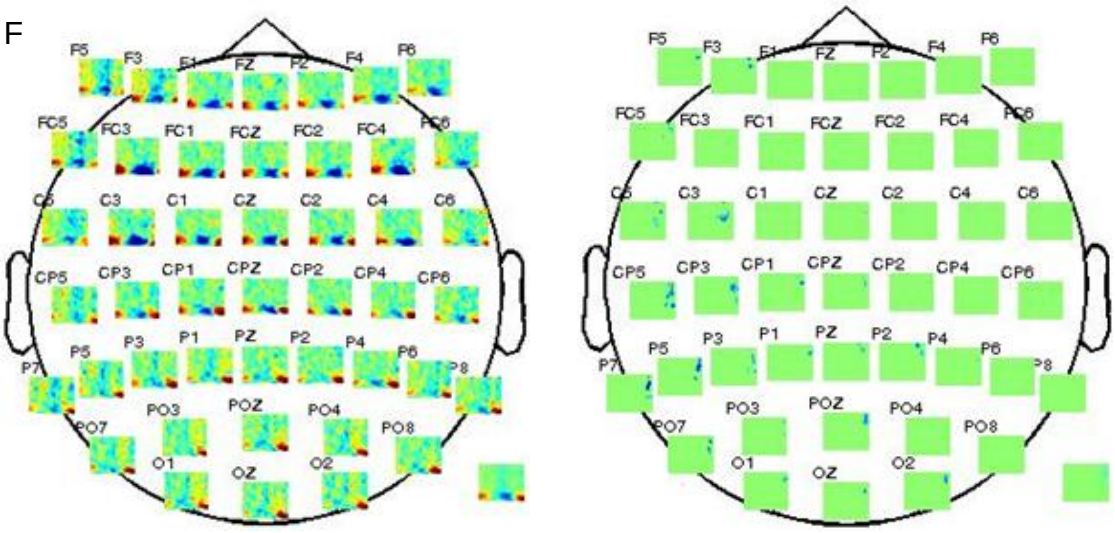

Figure 13 Topographic mapping of ERSP during implicit motor learning
Topographic mapping of ERSP plots in HCs. Left side: original data plots, right side statistical difference plots. X-axis: time from - 607 to 208 ms around the button press. Y-axis: frequencies from 8 to 100 Hz. (A) ERSP [Bl], (B) ERSP [Sa] and ERSP [Bl - Sa], (C) ERSP [Sb] and ERSP [Bl - Sb], (D) ERSP [Sc] and ERSP [Bl - Sc], (E) ERSP [Sd] and ERSP [Bl - Sd], (F) ERSP [Se] and ERSP [RcRd - Se]

We found an MRD in the alpha and beta bands most pronounced over the bilateral prefrontal (specifically the dorsolateral prefrontal cortex), fronto-central and central channels (F-, FC and C-channels) starting approximately 250 ms before and ending about 30-40 ms after button press. FC3, C3, FC4 and C4 showed a distinct pronunciation of MRD in comparison to the surrounding electrodes. The MRD was most pronounced from 8 to 30 Hz. Moreover, higher frequencies also showed a weak MRD. However, over some electrodes such as C2 and C4, the alpha and beta band MRD was paralleled by a simultaneous gamma MRS. After the beta band MRD, which ended between 25 and 75ms after the button press we found an MRS between 10 and 30 Hz. This MRS covered a wider cortical area than the MRD including centro-parietal and parieto-occipital electrodes.

The MRD was modulated significantly over the learning blocks as can be seen in the statistical plots on the right side and shall be described in a comprehensive way as follows:

In [Sa], the MRD increased specifically over frontal, fronto-central and central electrodes (F5, F3, FC3, FCz, FC4, C4) and mildly over left centro-parietal,

parietal and parieto-occipital electrodes. The postmovement MRS was more distinct over central electrodes such as C1 and C3 and some frontal electrodes.

In [Sb], the MRD went back to [Bl] level over those electrodes that presented with increased MRD in [Sa]. The MRD increased mildly over electrodes over the right hemisphere, e. g. FC4, C4 and parietal electrodes. During the button press the gamma band activity was weaker than in the [Bl] mainly on the right side over several electrodes most pronounced over CP4 and CP6. The MRS that we saw in the end of our time window was more pronounced over several electrodes spread over the cortex most distinct over C1.

In [Sc], the MRD presented stronger than in [Bl] over left frontal and fronto-central and bilateral parieto-occipital and occipital electrodes. Besides, we found a gamma band MRD which timely parallels movement and is embedded in the MRD in alpha and beta bands over bilateral parietal and centroparietal channels most pronounced in P1, P3 and P5. On the contrary, over the channel C4 a gamma band MRS parallels the button-press as described before.

In [Sd] the alpha and beta band MRD was not significantly stronger than in [Bl] but for the electrodes FC4, FC6, CP6, P2 and P4. Gamma band activation right after the button press was stronger over left frontal and fronto-central electrodes. Weaker than in [Sc] gamma band MRD presented over parietal channels.

When comparing [Se] to [RcRd] the fewest differences were seen, here the MRD was not modulated. Only in the end of the time window, after the button press the gamma band showed less activation in [Se] than in [RcRd].

4 Discussion

Here, we demonstrate that both subthalamic stimulation as an external stimulus and implicit motor learning as an internal stimulus induce wide-spread movement-related changes in cortical activity. STN-DBS and implicit motor learning facilitate the MRD. Thus, the MRD is a central correlate of both, implicit motor learning and therapeutic neurostimulation.

4.1 *Analysis 1*: Externally paced finger movements

As expected, subthalamic stimulation [StimOn] led to a significant improvement of motor symptoms of more than 30% in each PD patient (mean improvement 60.7 ± 14.5%) measured by the total UPDRS III and improvement of the segmental UPDRS III. This is in line with the internationally approved standard that STN-DBS reduces the UPDRS III motor score by 41% on average (Deuschl et al., 2006). Subsequently, STN-DBS also led to enhanced motor performance in terms of shorter reaction times and a smaller error ratio in the externally paced finger movement task. These results are in accordance with previous studies that confirmed that STN-DBS is an efficient therapy for motor symptoms in PD and improves motor performance (Deuschl et al., 2006; Dujardin et al., 2001; Krack et al., 2003). Our results extend these previous results with the novel finding that the motor performance in our specific serial reaction time task is improved.

STN-DBS did not alter the muscle activation pattern: Time course, amplitude and frequency range of muscle activation were similar in both conditions.

We were able to demonstrate that simple externally paced finger movements are associated with different topographies of cortical activation. The MRD is a well-established and frequently used electrophysiological indicator to describe cortical motor processing in the time-frequency domain including its topography. After careful consideration of all results of *Analysis 1* novel insights on the defective motor-network mechanisms in PD can be delineated:

With externally paced random order finger movements we found an alpha and beta band MRD which presented most pronounced over bilateral SM1, but it

also implicated the bilateral central and frontal electrodes in [StimOff]. With [StimOn] alpha and beta band MRD were significantly stronger compared to [StimOff] most pronounced over left dorsolateral prefrontal cortex (FC3) and bilateral SM1 areas (C3/C4 electrodes). Further cortical areas are involved in this task. Thus, with [StimOn] a wider topographical range of cortical areas were activated including the bilateral frontal, fronto-central, temporal, supplemental motor, and bilateral centro-parietal electrodes (Figure 6).

Furthermore the alpha and beta band MRD lasted longer in [StimOn] (from -250 to +160 ms) than in [StimOff] (from -250 to +40 ms). These differences in MRD between [StimOff] and [StimOn] were correlated with improvements in both segmental UPDRS III, reaction time (as shown in our multiple regression models) and error ratio. Since both the muscle activation pattern and CMC were not modulated by STN-DBS this may lead to the consideration that clinical improvement with STN-DBS is mainly reflected by activity modulations of the cerebral network.

Together, alpha and beta MRD as a surrogate of cortical motor activation were decreased in PD patients and partly restored with STN-DBS.

Our results are in line with previous data, i.e. (Devos et al., 2004), that showed abnormal movement-related cortical oscillatory activity. Similarly, we found that the reduced cortical activation in [StimOff] can be restored by therapy. Nevertheless, our study provides some important progress compared to previous data: *(i)* we achieved a higher topographic resolution by applying a larger set of electrodes (64 electrodes in our study versus 37 electrodes in Devos' study); *(ii)* we used a sophisticated statistical model with nonparametric mapping procedure and applied permutation statistics. A cluster-based correction method effectively addressed the multiplicity problem without losing sensitivity for spectral changes; *(iii)* using multiple regressions we were able to predict the therapeutic outcome from MRD. In our paradigm with externally paced finger movements we found an MRD that was also increased with STN-DBS but started at the same time-point in both conditions and lasted longer in [StimOn] than in [StimOff].

In detail, in Devos' study with self-paced wrist flexions (Devos et al., 2004) an increase of the mu MRD over SM1 and a decrease of the desynchronization latency was found when STN-DBS was introduced in PD patients. In conclusion, in both ours and Devos' study, the MRD was more pronounced with STN-DBS. Thus, in line with Devos, we were able to demonstrate that STN-DBS modulates movement-related cortical reactivity. STN stimulation may therefore partly restore SM1 cortex activation during movement in advanced PD.

Furthermore, in their internally paced wrist movement task (with longer premovement planning phase compared to externally paced movement), Devos and colleagues were able to show that the MRD latencies over the contralateral central region correlated inversely with the UPDRS motor rating. In our study, we were able to show a correlation between MRD strength and both segmental motor UPDRS III and reaction time.

Earlier studies had shown that sensorimotor mu MRD is delayed with voluntary movement and to be lower in amplitude in PD patients which correlated with bradykinesia (Brown and Marsden, 1999; Wang et al., 1999). These alterations could also be partially reversed with L-Dopa (Magnani et al., 2002).

In a PET study, effective bilateral STN stimulation has been shown to significantly increase blood flow over and reactivates different cortical areas such as the SMA, the cingulated cortex and the dorsolateral prefrontal cortex (Brown et al., 1999), which also plays an important role in our study. In our PD patients with [StimOff], the dorsolateral prefrontal beta band activity desynchronizes only sparsely, and this was reversed with [StimOn].

The strengthening of MRD over the dorsolateral prefrontal areas with STN-DBS (probably reflecting a more active state of this cortical area) fits to its executive motor functions such as response selection and in motor programming of new or attention-demanding tasks (Jahanshahi, 2013). Furthermore, in HCs the prefrontal cortex was shown to be closely connected to the basal ganglia, specifically to the striatum. In a recent PET study on motor timing in PD this striato-frontal connectivity was shown to be absent in PD patients 'Off'

medication and improved with the administration of L-Dopa (Jahanshahi, 2013)(Jahanshahi et al., 2013). This is concurring with the idea that in PD ‘Off’ medication the prefrontal cortex is less active because of excessive inhibitory beta band synchronization of the remote cortical and basal ganglia nodes. Thus, this demonstrates again, that dopaminergic deficiency in the substantia nigra pars compacta leads to pathological connectivity and results in changes of activation of distant brain areas, such as the prefrontal cortex. This is in line with another PET study that assessed executive dysfunction of the prefrontal cortex. This study showed that the executive impairment rather relates to an overinhibitory basal ganglia control on prefrontal activity than to intrinsic prefrontal dysfunction per se (Dirnberger et al., 2005).

As STN-DBS reduces beta band desynchronization of the prefrontal cortex, we substantiate the view that prefrontal cortex and subthalamic nucleus are strongly interconnected by beta band rhythms. The attenuation of the exaggerated inhibitory beta band in the STN achieved by STN-DBS (Eusebio et al., 2011; Little et al., 2013) might mediate the attenuation of the overinhibitory prefrontal beta band in PD patients during movement. The reduction of beta band oscillations in the STN was correlated to improvements in rigidity and bradykinesia (Kuhn et al., 2008b).

In addition to the ERD, the gamma event-related synchronization, which occurred approximately - 50 ms before until 70 ms after the button press, was predominantly found over the contralateral SM1 area and less pronounced on the ipsilateral side. It was not modulated significantly between conditions.

Phasic 40-Hz ERS was reported around movement onset embedded in a 10-Hz ERD over contralateral sensorimotor areas with a maximum shortly before movement onset and during execution of movement (Pfurtscheller and Neuper, 1992). As described above, in general, gamma band oscillations in the motor circuit are considered as prokinetic. Both in healthy rats (Brown et al., 2002) and in PD patients with DBS (Brown, 2003) after administration of L-Dopa recordings of local field potentials in the STN showed high gamma oscillations paralleled by a reduction of rigidity and akinesia.

However, in addition to modulations of the clinical scores, of the muscle activation, and of the cortical power during movement, it has been shown that there are corresponding modulations in the strength of coherence between cortex and muscle (Baker et al., 1997; Kilner et al., 1999). Earlier studies have shown that cross-correlation analysis of oscillatory activity in the time domain mirrors a potential mechanism for encoding behavioral parameters in the motor system (Murthy and Fetz, 1992). In case this oscillatory activity has a functional role in motor behavior, it should show systematic variation with specific parameters of the motor task.

In general, coherence between SM1 and the motor units exists during isometric contraction with peak frequencies in the range from 15 to 40 Hz, depending on the contraction strength (Hari and Salenius, 1999). Consistently, in a study with isometric contractions beta band CMC between the sensorimotor cortex and the contralateral hand and forearm muscles was most pronounced during the steady hold period of this task (Kilner et al., 2000). The level of compliance in this precision grip task influenced the extent of CMC with a stronger CMC in a more compliant condition in which subjects moved the levers against a spring-like load. So CMC was abolished during the phasic force recalibration and greatest during steady hold periods just after movements (Baker et al., 1997; Kilner et al., 2000).

In our study, we found significant CMC between the SM1 area and both the agonistic FD and the antagonistic ED muscle in the alpha and low beta bands. The CMC mainly occurred in the premovement period (before muscular activation onset) which might reflect a kind of readiness to respond in the same way as corticospinal coherence was interpreted in another reaction time task study (Schoffelen et al., 2005). One could also infer that this premovement CMC reflects a mechanism of sensorimotor gating (Swerdlow et al., 2000). The premovement CMC to the ED ended 350 ms before button press and reoccurred 150 ms after. It was not modulated significantly with STN-DBS. Thereby, the level of CMC in the steady state before the movement may reflect the resetting of a form of control used by the motor system as it passes through an important change in state: from a flexion movement to a hold position. This

transition must demand an effective corticomuscular communication (Kilner et al., 1999).

Interestingly, in few individual patients a premature rebound of CMC between SM1 and the antagonistic ED occurred about 30 to 100 ms after button press. This was most pronounced in the [StimOff] but not significantly different from the [StimOn]. Given the previous findings of CMC suppression during the phasic movement period, this finding may point to impaired cortical control over antagonistic muscles in PD. Similar evidence comes from studies on reciprocal inhibition of antagonistic muscles via spinal Ia inhibitory interneurons. This reciprocal inhibition of antagonistic muscles was disturbed in PD patients and supraspinal control mechanisms were revealed either on cortical (Bertolasi et al., 1998; Meunier et al., 2000) or subthalamic level (Raoul et al., 2012).

In accordance with these findings previous studies showed that STN-DBS can modulate the CMC: It leads to an increase of efferent drives in the low beta band from cortex to muscle together with improved motor performance (Weiss et al., 2012).

Since CMC is a measure of synchrony between SM1 and the motor unit (Mima and Hallett, 1999), the present data may support that the premature rebound of CMC may play a functional role in motor impairment of PD. This was observed in individual patients but did not reach significance on group level.

4.2 *Analysis 2*: Implicit motor learning

As expected, the behavioral results in the SRTT of the present study indicate that repetitive trials with the same sequence (in our case the sequences [S1] and [S2]) produced implicit motor learning with gradually fastening reaction times over ‘sequence blocks’. This finding reproduced the results of previous studies about implicit motor learning (Nissen and Bullemer, 1987; Willingham et al., 1989).

But how can one distinguish which components of changes in cortical oscillations during the SRTT are linked to the movement itself and which are linked to the implicit motor learning of the sequence? The motor cortex, for

instance, is essential for the integration of movements but it is also supposed to play an important role in implicit motor learning. This makes it complex to disentangle, whether activity changes reflect the motor execution itself and/or relate to sequence learning. It was argued that modulation of neuronal oscillations over the motor cortex can be assigned to sequence learning when it occurs only in the first of the two following contexts: the first context is a movement as part of a sequence and the other one is an isolated movement (Ben-Shaul et al., 2004). Accordingly, we addressed this need by contrasting random trials (as obtained during ‘baseline’) and trials within an underlying sequence to disentangle the two phenomena.

Our electrophysiological data showed the following results: The broad band activation of the agonistic muscle FD was not modulated significantly over the consecutive learning blocks, whereas changes in cortical MRD were observed.

As described in the introduction, several neuronal substrates of implicit motor learning have been identified: In addition to subcortical areas such as the basal ganglia and the cerebellum, a set of cortical regions plays an important role, especially in the initial fast learning phase. Implicit processes originate in the posterior parietal cortex as a perceptual domain and then may propagate from the SM1, as the principal structure, and the dorsolateral prefrontal area to the premotor cortex, SMA, and pre-SMA (as shown in a PET study by Grafton (Grafton et al., 1998) and a review by Ashe (Ashe et al., 2006).

These areas showed increased PSDs in the alpha and low beta band in our electrophysiological study: In the alpha band we found an increased activation over the right posterior parietal cortex region and a broader left hemispheric activation over the left lateral centro-parietal and posterior-parietal cortices in [Sc].

In the low beta band we found an increased activation in various electrodes in several blocks, more dominant on the left hemisphere, including left frontal, left supplemental motor, left premotor, left motor and bilateral posterior parietal cortices. Other frequency bands showed no significant changes in PSD.

The changes over the posterior-parietal cortices may reflect their function in visual perception and the areas that belong to the motor network (SMA, premotor, SM1) play an important role in performing the task. The modulation of oscillatory activity in different frequency ranges may reflect distinct aspects of information processing in a cortical motor network, which need to be further assessed.

After all, there is a good general understanding of the main neuronal substrates associated with implicit motor learning. But although we have an approximate idea of the operations carried out in these areas that relate to sequence control, we lack sufficient detail to really understand the underlying processes.

In our study, we found an alpha and beta band MRD during the performance of the SRTT which presented most pronounced over SM1 and SMA region but also over the bilateral frontal, fronto-central and central channels starting approximately 250 ms before and ending about 30-40 ms after button press. After the MRD we found an MRS between 10 and 30 Hz starting between 25 and 75 ms after the button press. Both MRD and MRS were enhanced in the ‘sequence blocks’ compared to the [Bl] block. Since the MRD reflects an activation of the concerning brain area (Neuper and Pfurtscheller, 2001), its increase mainly over the SM1 and SMA region is related to the process of sequence learning and supports again the conclusion that these cortical areas play an important role in integration of implicit motor learning.

In our task, one would expect that during the first two ‘sequence blocks’ ([Sa] and [Sb]) ‘feature extraction’ occurs, i.e. subjects may implicitly extract the underlying sequence. In this phase, motor learning has started already but performance assessed by the reaction time has not improved significantly, yet. In the very initial phase of learning ([Sa]), the MRD changes especially over frontal, fronto-central and central channels. The frontal cortex and specifically the prefrontal cortex is closely linked to attention during the learning of new sequences (Jenkins et al., 1994). F4 and FC4 electrodes show an increased MRD in both [Sa] and [Sb]. In [Sb] increased MRD, additionally, shows stronger topographic representation over centro-parietal channels. This phase of [Sa]

and [Sb] might already lead to modulation of synaptic efficacy through long term potentiation- and depression-like plasticity. Long-term potentiation has been described before to occur in early cortical reorganization processes and to rely on increasing efficacy of existing synaptic connections (Rosenkranz et al., 2007; Ziemann et al., 2004).

In the next phase of learning during [Sc] and [Sd], which, in general, still belongs to the early and fast phase of implicit motor learning, we were already able to demonstrate a significantly reduced reaction time. In [Sc] the changes of MRD are most pronounced over left frontal and fronto-central and bilateral parieto-occipital and occipital electrodes. Common electrodes of [Sc] and [Sd] with increased MRD are P2 and P4. Potentially, in this phase of learning, the meaning of alpha and beta band MRD decreases. Accordingly, we found a gamma MRD over parietal and centro-parietal channels paralleling the alpha and beta MRD, but also a gamma MRS over C4. Gamma desynchronization, if representing a similar function to gamma coherence, might be associated with higher expectation of the new stimulus (Qassim et al., 2013) and also with readiness to respond (Schoffelen et al., 2005). A distinct gamma MRS over M1 has been described before with simple index finger movement and was suggested to act as a biomarker in the analyses of functional brain activity (Huo et al., 2010). In general, and also in PD (Florin et al., 2013; Litvak et al., 2012) gamma oscillations are related to prokinetic effects (Brucke et al., 2013).

Together, it can be concluded that the MRD is a central correlate of implicit motor learning. Presenting most pronounced over SM1 and SMA region and reflecting their activation, this supports again the conclusion that these cortical areas play an important role in integration of implicit motor learning. In the first two sequential blocks, frontal and fronto-central channels showed a stronger MRD representing attention during the learning of new sequences, later, prokinetic gamma band becomes more important paralleling the fastening of reaction times.

4.3 Methodological considerations of our study

4.3.1 Inability to blind the stimulation condition in PD patients

Blinding the [StimOff] vs [StimOn] condition in PD patients is impossible, since the stimulation condition can be easily perceived by both patient and investigator if stimulation is clinically effective. This may have affected the clinical ratings, whereas the electrophysiological data analysis follows a fully-automated and operationalized procedure that will not be affected by expectation effects. Nevertheless, the clinical efficacy (mean improvement of 60.7 ± 14.5%) was in line with the internationally approved standard that STN-DBS should improve the UPDRS III motor score for at least 30% (Deuschl et al., 2006).

4.3.2 PD patients' motor performance

The three cardinal symptoms of PD are tremor, rigidity and akinesia. Particularly, rigidity led to some interference with our EMG recordings, as some patients showed elevated muscle tone between consecutive finger taps. In line with our observation PD patients may have higher passive stiffness of the muscle belly and tendon than HCs (Marusiak et al., 2011). This elevated background activity may interfere with phasic EMG activation. We found that the most reliable method to detect the EMG onsets was to use a time-frequency spectral decomposition of the muscular time series. Interestingly, we found tonic background activity mainly in the frequency range below 20 Hz and could therefore separate the phasic broad band activation up to 100 Hz as demonstrated in Figure 4. Moreover, a bootstrap significance threshold on the 95% significance level was introduced to mask for constant background activity unrelated to phasic activation. Similarly, the corticomuscular coherence spectra were thresholded on the 95% bootstrap significance level.

The task for *Analysis 2*, the SRTT, lasted longer and accordingly needed more attention and precision than the task for *Analysis 1*. Due to their advanced disease stage, PD patients were in general not able to achieve sustained and reliable performance on the SRTT. However, we achieved a sufficient quantity

of properly performed externally paced movements in the four baseline random blocks to analyze the spectral perturbations outside the learning curve. In doing so, we only considered epochs of a single finger tap, if reaction time, correctness and signal quality of an epoch accounted for our quality standard after careful visual inspection.

4.3.3 Short inter-stimulus interval

In our study, evaluating implicit motor learning, we had to keep the time interval between two consecutive stimuli short to prevent the achievement of explicit knowledge. Therefore, we chose an inter-trial interval of 1.5 s. In general, a time interval of a couple of seconds between two consecutive events is recommended, when assessing MRD and especially MRS in internally generated movements, since both MRD and MRS need time to evolve and to dissolve (Pfurtscheller and Lopes da Silva, 1999). Nevertheless, studies investigating the MRD in the course of implicit motor learning have been successfully conducted, for example with an inter-trial interval of 2.0s (Zhuang et al., 1997), and other work adressed motor integration with even shorter intertrial intervals (Gerloff et al., 1998b; Herz et al., 2013). This demonstrates that evolution, amplitude and topographic representation of the MRD can be assessed reliably as well in externally paced finger-movements.

In general, after movement execution, MRD is followed by MRS. The time of onset of MRS is about 700 - 2000 ms after EMG onset in externally triggered and self-paced brisk movements (Leocani et al., 1997; Pfurtscheller, 1992). Accordingly, in the context of MRS, an inter-stimulus interval of several seconds is favorable. In our study, we were limited in studying the post-movement MRS for two reasons: the short interstimulus interval and the time window that we used to cut the data, i. e. from -800 ms to +400 ms.

4.4 Outlook

In electrophysiological and imaging studies, the relevant anatomical structures for different forms of learning have been identified. However, information on interactions between separate brain regions is still sparse. Learning-related changes in the functional connectivity of the cortical motor network have been investigated using coherence analyses of functional MRI data (Herz et al., 2013; Rappelsberger et al., 1994; Sun et al., 2007): These studies show that motor performance and learning are not only accompanied by local cortical power changes, but also by changes in functional coupling between separate brain areas. Questions about connectivity between different brain regions are on the rise in current neuroscience research. In this spirit, our understanding of the brain's functioning leaves behind the concept that one single, segregated brain area solely holds a specific functioning.

The current understanding is that several areas are connected on both structural (axonal fiber tracts) and functional level (correlations in time series) and interact dynamically (Engel et al., 2013; Uhlhaas, 2013). Currently, available techniques to measure brain connectivity non-invasively are based on a process of interference. This enables us to measure brain connections in living human subjects. Thus, permitting the creation of a comprehensive whole-brain connection map, the so-called 'connectome', which may elucidate the architecture of large-scale networks connecting sets of brain regions (Behrens and Sporns, 2012). The term 'connectome' refers to a comprehensive structural description of the network of elements and connections forming the human brain (Sporns et al., 2005). Three scales of organization may be distinguished: the 'microscale' of single neurons and synapses, the 'macroscale' of anatomically distinct brain regions and pathways, and the 'mesoscale' of neuronal populations and their interconnecting circuitry (Sporns et al., 2005).

The knowledge of connectivity between different brain areas is also of importance in order to understand the pathophysiology of neurological and psychiatric diseases. It can be thus speculated, that diseases can be reappraised based on the network pathology. Several studies support the

understanding that various neurological and psychiatric diseases are at least partly reflected by impairments of connectivities and thereby could be named ‘connectopathies’ or ‘disconnectivity’ or ‘dysconnectivity syndromes’ (Friston and Frith, 1995; Harrison, 1999; McGlashan and Hoffman, 2000; Peled). The term ‘dysconnectivity’ highlights the involvement of both reduced and increased interactions in extended cortical circuits in schizophrenia (Uhlhaas, 2013): on the microscale, neurons differentiated out of induced pluripotent stem cells of patients with schizophrenia showed diminished neuronal connectivity in conjunction with a decreased neurite number compared to neurons from healthy subjects (Brennand et al., 2011).

Furthermore, autism should be mentioned which is associated with abnormalities of information integration that is linked with a reduction in the connectivity between specialized local neuronal networks in the brain on the mesoscale and possible overconnectivity within the isolated individual neuronal assemblies (Brock et al., 2002; Rippon et al., 2007).

Also in AD, the topological architecture of the ‘connectome’ is disrupted. Neurophysiological studies in AD showed abnormal fronto-parietal long-range synchrony in the alpha and beta band (Babiloni et al., 2004). Besides, in AD a global loss of network connectivity and altered synchronizability in most frequency bands occurs (de Haan et al., 2012). This disruption is already present in amnestic mild cognitive impairment, the prodromal stage of AD (Wang et al., 2013),again offering the potential for using connectome-based metrics as a disease biomarker. Accordingly, sensing technologies of fluctuating pathological network activity may enable us to apply therapies more precisely (Little et al., 2013) and a more personalized and specific treatment of patients may be possible through novel therapeutic strategies. Besides, such novel concepts might enable us to define predictors of disease progression, which will help to diagnose diseases at an earlier stage.

Also in basal ganglia disease these considerations include the functional organization and long-range connectivity of wide-spread neuronal integrators: Although neurodegeneration of dopaminergic cells in the substantia nigra pars

compacta is considered crucial for PD motor symptoms, it is conceivable and supported by our findings that the motor symptoms stand in parallel with wide-spread deregulation of the large-scale motor network that exceeds a focal nuclear dysfunction. Interestingly, some network characteristics in PD are transient in nature (and thereby potentially match clinical motor fluctuations). PD patients in the motor ‘off state’ had significantly decreased functional MRI connectivity in the supplementary motor area, left dorsal lateral prefrontal cortex and left putamen, and increased functional connectivity in the left cerebellum, left primary motor cortex, and left parietal cortex compared to normal subjects. This abnormal functional connectivity of motor network in the baseline state is possibly an important factor contributing to some motor deficits in PD, e.g. akinesia (Wu et al., 2009). Administration of L-Dopa in part normalized the pattern of functional connectivity in PD patients, and functional connectivity in most regions of the motor network correlated with motor symptoms (Wu and Hallett, 2005).

In PD, beta band synchronizations (which are suspected to be rather antikinetic) predominate over the (rather prokinetic) gamma band synchronizations in the subthalamo-cortical network. These lower frequency oscillations facilitate slow idling rhythms in the motor areas of the cortex leading to motor inhibition, whereas synchronization at high frequency restores dynamic task-related cortical ensemble activity in the gamma band (Brown, 2003). Recently, sensing technologies of fluctuating pathological network activity was used to apply neurostimulation more precisely (Little et al., 2013), and this may promote more stratified and context-dependent therapy, thereby potentially facilitating efficacy and tolerability.

To conclude, our study adds to the converging evidence that defective or maladaptive neuronal connectivity contributes to the pathophysiology of a large spectrum of neuropsychiatric diseases. Noting that the journey towards a more comprehensive understanding of the brain and its diseases will be challenging, then again, a great potential of strategies integrating anatomy, function and connectivity is apparent and will improve medical diagnostics and therapy.

5 Summary

On the one hand, the neuronal circuitry and connectivity of the large-scale motor network play an important role in many human cognitive functions, i. e. in implicit motor learning. On the other hand, alterations in connectivity of the motor network are also a hallmark in the pathophysiology of a variety of psychological and neurological diseases, such as Parkinson's disease.

Here, we set out to study the motor network activity (more exactly the cortical and spinal aspects of it) under two different aspects: in healthy controls during implicit motor learning and in Parkinson's disease patients in the conditions 'stimulation off' and 'stimulation on'. To this end, 12 healthy controls and 20 Parkinson's disease patients performed externally paced right finger movements with simultaneous recordings of a 64-channel EEG and EMG of the forearm muscles. The healthy controls performed the serial reaction time task. Parkinson's disease patients conducted the baseline of this task with only random trials in the two conditions 'stimulation off' and 'stimulation on '. Cortical and muscular activity was analyzed by time-frequency movement-related spectral perturbations and by power spectral density and corticospinal synchronization was assessed by time-frequency cross-spectra coherence.

Clinically, Parkinson's disease patients improved significantly with deep brain stimulation, assessed by the Unified Parkinson's Disease Rating Scale III score, the reaction time and the error ratio. Deep brain stimulation lead to an increased cortical beta-band movement-related desynchronization, which was topographically spread over a wider cortical area. Besides, in 'stimulation off' after finger tap we found a premature beta-band rebound of the corticomuscular coherence to the extensor digitorum over the primary sensorimotor cortex, which was suppressed with stimulation on.

The healthy controls presented with significantly reduced reaction times in the 'sequence blocks' compared to 'random blocks'. In 'sequence blocks', power spectral density increased mainly over the right posterior parietal cortex but also over a larger left-hemispheric cortical area in alpha and low beta band. Alpha

and beta band movement-related desynchronization presented most pronounced over the bilateral prefrontal, fronto-central and central channels. The movement-related desynchronization was significantly modulated over the course of implicit motor learning.

The present findings reveal the impressive modulation of the motor network activity including cortical activations and corticospinal synchronizations introduced by deep brain stimulation therapy of the subthalamic nucleus in Parkinson’s disease.

6 Deutsche Zusammenfassung

Einerseits spielen neuronale Kreisläufe und Konnektivität des weitverteilten motorischen Netzwerkes eine wichtige Rolle bei vielen menschlichen kognitiven Funktionen, beispielsweise beim impliziten motorischen Lernen. Andererseits sind Veränderungen in der Konnektivität des motorischen Netzwerks auch ein Kennzeichen der Pathophysiologie einer Vielzahl von psychischen und neurologischen Erkrankungen, wie Parkinson.

In dieser Studie untersuchten wir die motorische Netzwerkaktivität (genauer gesagt die kortikalen und spinalen Bestandteile davon) unter zwei unterschiedlichen Aspekten: Bei gesunden Probanden während des impliziten motorischen Lernens und bei Parkinsonpatienten unter den zwei Konditionen Tiefe Hirnstimulation des Nucleus subthalamicus „an“ und „aus“. Dafür führten 12 gesunde Probanden sowie 20 Parkinsonpatienten extern getriggerte Bewegungen der Finger der rechten Hand aus, begleitet von der simultanen Aufzeichnung eines 64-Kanal-EEGs sowie EMG-Ableitungen der Unterarmmuskeln Flexor und Extensor digitorum. Die gesunden Probanden absolvierten eine Reaktionszeitaufgabe (Serial Reaction Time Task). Die Parkinsonpatienten absolvierten die aus zufällig auftretenden Stimuli bestehende Baseline der Aufgabe. Wir analysierten die kortikale und muskuläre Aktivität an Hand von der bewegungsbezogenen spektralen Zeit-Frequenz-Pertubation sowie der spektralen Leistungsdichte und die kortikospinale Synchronisationen an Hand der kortikomuskulären Zeit-Frequenz-Kreuzspektrumskohärenz.

Klinisch besserten sich die Parkinsonpatienten signifikant mit tiefer Hirnstimulation, bewertet durch den Unified Parkinson’s Disease Rating Scale III Wert, die Reaktionszeit und die Fehlerratio. Die tiefe Hirnstimulation führte zu einer signifikant verstärkten bewegungsbezogenen kortikalen Betabanddesynchronisation, die außerdem über ein weiteres kortikales Areal verbreitet war. Desweiteren fanden wir in der Kondition Stimulation „aus“ eine verfrühte Betabanderholung der kortikomuskulären Kohärenz zum Extensor

digitorums über dem primärmotorischen Kortex, welche mit Stimulation „an“ unterdrückt wurde.

Die gesunden Probanden zeigten eine signifikant reduzierte Reaktionszeit in den Sequenzblöcken verglichen mit den Blocks mit zufällig auftretenden Stimuli. In den Sequenzblöcken nahm die spektrale Leistungsdichte hauptsächlich über dem rechten posterioparietalen Kortex zu, aber auch über einem größeren linkshemisphärischen kortikalen Areal im Alpha- und Betaband. Die bewegungsbezogene Alpha- und Betabanddesynchronisation zeigte sich am ausgeprägtesten über den bilateralen präfrontalen, frontozentralen und zentralen Kanälen. Die bewegungsbezogene Desynchronisation wurde signifikant moduliert während des impliziten motorischen Lernens.

Diese Ergebnisse zeigen die beeindruckende Modulation der motorischen Netzwerkaktivität einschließlich der kortikalen Aktivität sowie der kortikospinalen Synchronisation durch tiefe Hirnstimulationstherapie des Nucleus subthalamicus bei Parkinson auf.

7 Reference list

Akimoto, Y., Kanno, A., Kambara, T., Nozawa, T., Sugiura, M., Okumura, E., Kawashima, R., 2013. Spatiotemporal dynamics of high-gamma activities during a 3-stimulus visual oddball task. PLoS One. 8**,** e59969.

Ashe, J., Lungu, O.V., Basford, A.T., Lu, X., 2006. Cortical control of motor sequences. Current Opinion in Neurobiology. 16**,** 213-221.

Babiloni, C., Ferri, R., Moretti, D.V., Strambi, A., Binetti, G., Dal Forno, G., Ferreri, F., Lanuzza, B., Bonato, C., Nobili, F., Rodriguez, G., Salinari, S., Passero, S., Rocchi, R., Stam, C.J., Rossini, P.M., 2004. Abnormal fronto-parietal coupling of brain rhythms in mild Alzheimer's disease: a multicentric EEG study. European Journal of Neuroscience. 19**,** 2583-2590.

Baker, S.N., Olivier, E., Lemon, R.N., 1997. Coherent oscillations in monkey motor cortex and hand muscle EMG show task-dependent modulation. J Physiol. 501 (Pt 1)**,** 225-41.

Behrens, T.E., Sporns, O., 2012. Human connectomics. Curr Opin Neurobiol. 22**,** 144-53.

Ben-Shaul, Y., Drori, R., Asher, I., Stark, E., Nadasdy, Z., Abeles, M., 2004. Neuronal activity in motor cortical areas reflects the sequential context of movement. J Neurophysiol. 91**,** 1748-62.

Benabid, A.L., Pollak, P., Louveau, A., Henry, S., de Rougemont, J., 1987. Combined (thalamotomy and stimulation) stereotactic surgery of the VIM thalamic nucleus for bilateral Parkinson disease. Appl Neurophysiol. 50**,** 344-6.

Benabid, A.L., Pollak, P., Hommel, M., Gaio, J.M., de Rougemont, J., Perret, J., 1989. [Treatment of Parkinson tremor by chronic stimulation of the ventral intermediate nucleus of the thalamus]. Rev Neurol (Paris). 145**,** 320-3.

Benazzouz, A., Hallett, M., 2000. Mechanism of action of deep brain stimulation. Neurology. 55**,** S13-6.

Benjamini, Y., Hochberg, Y., 1995. Controlling the false discovery rate: a practical and powerful approach to multiple testing. Journal of the Royal Statistical Society. Series B (Methodological). 289-300.

Benjamini, Y., Drai, D., Elmer, G., Kafkafi, N., Golani, I., 2001. Controlling the false discovery rate in behavior genetics research. Behav Brain Res. 125**,** 279-84.

Berg, D., Niwar, M., Maass, S., Zimprich, A., Moller, J.C., Wuellner, U., Schmitz-Hubsch, T., Klein, C., Tan, E.K., Schols, L., Marsh, L., Dawson, T.M., Janetzky, B., Muller, T., Woitalla, D., Kostic, V., Pramstaller, P.P., Oertel, W.H., Bauer, P., Krueger, R., Gasser, T., Riess, O., 2005. Alpha-synuclein and Parkinson's disease: implications from the screening of more than 1,900 patients. Mov Disord. 20**,** 1191-4.

Berger, H., 1929. Über das elektrenkephalogramm des menschen. European Archives of Psychiatry and Clinical Neuroscience. 87**,** 527-570.

Bertolasi, L., Priori, A., Tinazzi, M., Bertasi, V., Rothwell, J.C., 1998. Inhibitory action of forearm flexor muscle afferents on corticospinal outputs to antagonist muscles in humans. The Journal of Physiology. 511**,** 947-956.

Betarbet, R., Sherer, T.B., MacKenzie, G., Garcia-Osuna, M., Panov, A.V., Greenamyre, J.T., 2000. Chronic systemic pesticide exposure reproduces features of Parkinson's disease. Nat Neurosci. 3**,** 1301-6.

Beurrier, C., Bioulac, B., Audin, J., Hammond, C., 2001. High-frequency stimulation produces a transient blockade of voltage-gated currents in subthalamic neurons. J Neurophysiol. 85**,** 1351-6.

Boiten, F., Sergeant, J., Geuze, R., 1992. Event-related desynchronization: the effects of energetic and computational demands. Electroencephalography and Clinical Neurophysiology. 82**,** 302-309.

Boucai, L., Cerquetti, D., Merello, M., 2004. Functional surgery for Parkinson's disease treatment: a structured analysis of a decade of published literature. Br J Neurosurg. 18**,** 213-22.

Brennand, K.J., Simone, A., Jou, J., Gelboin-Burkhart, C., Tran, N., Sangar, S., Li, Y., Mu, Y., Chen, G., Yu, D., McCarthy, S., Sebat, J., Gage, F.H., 2011. Modelling schizophrenia using human induced pluripotent stem cells. Nature. 473**,** 221-225.

Brock, J., Brown, C.C., Boucher, J., Rippon, G., 2002. The temporal binding deficit hypothesis of autism. Development and psychopathology. 14**,** 209-224.

Brown, P., Marsden, C.D., 1999. Bradykinesia and impairment of EEG desynchronization in Parkinson's disease. Mov Disord. 14**,** 423-9.

Brown, P., Marsden, J., Defebvre, L., Cassim, F., Mazzone, P., Oliviero, A., Altibrandi, M.G., Di Lazzaro, V., Limousin-Dowsey, P., Fraix, V., Odin, P., Pollak, P., 2001. Intermuscular coherence in Parkinson's disease: relationship to bradykinesia. Neuroreport. 12**,** 2577-81.

Brown, P., Kupsch, A., Magill, P.J., Sharott, A., Harnack, D., Meissner, W., 2002. Oscillatory local field potentials recorded from the subthalamic nucleus of the alert rat. Exp Neurol. 177**,** 581-5.

Brown, P., 2003. Oscillatory nature of human basal ganglia activity: relationship to the pathophysiology of Parkinson's disease. Movement Disorders. 18**,** 357-363.

Brown, P., 2007. Abnormal oscillatory synchronisation in the motor system leads to impaired movement. Curr Opin Neurobiol. 17**,** 656-64.

Brown, R., Dowsey, P.L., Brown, P., Jahanshahi, M., Pollak, P., Benabid, A., Rodriguez-Oroz, M., Obeso, J., Rothwell, J., 1999. Impact of deep brain stimulation on upper limb akinesia in Parkinson's disease. Annals of neurology. 45**,** 473-488.

Brucke, C., Bock, A., Huebl, J., Krauss, J.K., Schonecker, T., Schneider, G.H., Brown, P., Kuhn, A.A., 2013. Thalamic gamma oscillations correlate with reaction time in a Go/noGo task in patients with essential tremor. NeuroImage. 75**,** 36-45.

Burbulla, L., Fitzgerald, J., Stegen, K., Westermeier, J., Thost, A., Kato, H., Mokranjac, D., Sauerwald, J., Martins, L., Woitalla, D., 2014. Mitochondrial proteolytic stress induced by loss of mortalin function is rescued by Parkin and PINK1. Cell death & disease. 5**,** e1180.

Cassim, F., Monaca, C., Szurhaj, W., Bourriez, J.L., Defebvre, L., Derambure, P., Guieu, J.D., 2001. Does post-movement beta synchronization reflect an idling motor cortex? Neuroreport. 12**,** 3859-63.

Castrioto, A., Lozano, A.M., Poon, Y.-Y., Lang, A.E., Fallis, M., Moro, E., 2011. Ten-year outcome of subthalamic stimulation in Parkinson disease: a blinded evaluation. Archives of neurology. 68**,** 1550-1556.

Chawla, H., Walia, S., Behari, M., Noohu, M.M., 2014. Effect of type of secondary task on cued gait on people with idiopathic Parkinson's disease. Journal of neurosciences in rural practice. 5**,** 18.

Chen, C.C., Litvak, V., Gilbertson, T., Kuhn, A., Lu, C.S., Lee, S.T., Tsai, C.H., Tisch, S., Limousin, P., Hariz, M., Brown, P., 2007. Excessive synchronization of basal ganglia neurons at 20 Hz slows movement in Parkinson's disease. Exp Neurol. 205**,** 214-21.

Chen, R., Yaseen, Z., Cohen, L.G., Hallett, M., 1998. Time course of corticospinal excitability in reaction time and self-paced movements. Ann Neurol. 44**,** 317-25.

Cohen, A., Ivry, R.I., Keele, S.W., 1990. Attention and structure in sequence learning. Journal of Experimental Psychology: Learning, Memory, and Cognition. 16**,** 17-30.

Costa, R.M., Cohen, D., Nicolelis, M.A., 2004. Differential corticostriatal plasticity during fast and slow motor skill learning in mice. Curr Biol. 14**,** 1124-34.

Crone, N.E., Miglioretti, D.L., Gordon, B., Lesser, R.P., 1998. Functional mapping of human sensorimotor cortex with electrocorticographic spectral analysis. II. Event-related synchronization in the gamma band. Brain. 121 (Pt 12)**,** 2301-15.

Dayan, E., Cohen, Leonardo G., 2011. Neuroplasticity Subserving Motor Skill Learning. Neuron. 72**,** 443-454.

de Haan, W., van der Flier, W.M., Wang, H., Van Mieghem, P.F., Scheltens, P., Stam, C.J., 2012. Disruption of functional brain networks in Alzheimer's disease: what can we learn from graph spectral analysis of resting-state magnetoencephalography? Brain Connect. 2**,** 45-55.

De Rijk, M., Launer, L., Berger, K., Breteler, M., Dartigues, J., Baldereschi, M., Fratiglioni, L., Lobo, A., Martinez-Lage, J., Trenkwalder, C., 1999. Prevalence of Parkinson's disease in Europe: A collaborative study of population-based cohorts. Neurologic Diseases in the Elderly Research Group. Neurology. 54**,** S21-3.

Defebvre, L., Derambure, P., Bourriez, J.L., Destee, A., Guieu, J.D., 1999. [Event-related desynchronization and Parkinson disease. Importance in the analysis of the phase of preparation for movement]. Neurophysiol Clin. 29**,** 71-89.

Del Tredici, K., Rüb, U., de Vos, R.A., Bohl, J.R., Braak, H., 2002. Where does parkinson disease pathology begin in the brain? Journal of Neuropathology & Experimental Neurology. 61**,** 413-426.

Delorme, A., Makeig, S., 2004. EEGLAB: an open source toolbox for analysis of single-trial EEG dynamics including independent component analysis. J Neurosci Methods. 134**,** 9-21.

Delorme, A., Sejnowski, T., Makeig, S., 2007. Enhanced detection of artifacts in EEG data using higher-order statistics and independent component analysis. NeuroImage. 34**,** 1443-1449.

Derambure, P., Bourriez, J.L., Defebvre, L., Cassim, F., Josien, E., Duhamel, A., Destee, A., Guieu, J.D., 1997. Abnormal cortical activation during planning of voluntary movement in patients with epilepsy with focal motor seizures: event-related desynchronization study of electroencephalographic mu rhythm. Epilepsia. 38**,** 655-62.

Deuschl, G., Schade-Brittinger, C., Krack, P., Volkmann, J., Schafer, H., Botzel, K., Daniels, C., Deutschlander, A., Dillmann, U., Eisner, W., Gruber, D., Hamel, W., Herzog, J., Hilker, R., Klebe, S., Kloss, M., Koy, J., Krause, M., Kupsch, A., Lorenz, D., Lorenzl, S., Mehdorn, H.M., Moringlane, J.R., Oertel, W., Pinsker, M.O., Reichmann, H., Reuss, A., Schneider, G.H., Schnitzler, A., Steude, U., Sturm, V., Timmermann, L., Tronnier, V., Trottenberg, T., Wojtecki, L., Wolf, E., Poewe, W., Voges, J., 2006. A randomized trial of deep-brain stimulation for Parkinson's disease. N Engl J Med. 355**,** 896-908.

Devos, D., Labyt, E., Cassim, F., Bourriez, J.L., Reyns, N., Touzet, G., Blond, S., Guieu, J.D., Derambure, P., Destee, A., Defebvre, L., 2003a. Subthalamic stimulation influences postmovement cortical somatosensory processing in Parkinson's disease. Eur J Neurosci. 18**,** 1884-8.

Devos, D., Labyt, E., Derambure, P., Bourriez, J.L., Cassim, F., Guieu, J.D., Destee, A., Defebvre, L., 2003b. Effect of L-Dopa on the pattern of movement-related (de)synchronisation in advanced Parkinson's disease. Neurophysiol Clin. 33**,** 203-12.

Devos, D., Labyt, E., Derambure, P., Bourriez, J.L., Cassim, F., Reyns, N., Blond, S., Guieu, J.D., Destee, A., Defebvre, L., 2004. Subthalamic nucleus stimulation modulates motor cortex oscillatory activity in Parkinson's disease. Brain. 127**,** 408-19.

Diekelmann, S., Born, J., 2010. The memory function of sleep. Nature Reviews Neuroscience. 11**,** 114-126.

Diener, H.-C., 2012. Leitlinien für Diagnostik und Therapie in der Neurologie: Herausgegeben von der Kommission" Leitlinien" der DGN, Vol., Georg Thieme Verlag.

Dirnberger, G., Frith, C.D., Jahanshahi, M., 2005. Executive dysfunction in Parkinson's disease is associated with altered pallidal–frontal processing. NeuroImage. 25**,** 588-599.

Dostrovsky, J.O., Levy, R., Wu, J.P., Hutchison, W.D., Tasker, R.R., Lozano, A.M., 2000. Microstimulation-induced inhibition of neuronal firing in human globus pallidus. J Neurophysiol. 84**,** 570-4.

Doyon, J., Ungerleider, L.G., 2002. Functional anatomy of motor skill learning. Neuropsychology of memory. 3**,** 225-238.

Dudai, Y., 2004. The neurobiology of consolidations, or, how stable is the engram? Annu. Rev. Psychol. 55**,** 51-86.

Dujardin, K., Derambure, P., Defebvre, L., Bourriez, J.L., Jacquesson, J.M., Guieu, J.D., 1993. Evaluation of event-related desynchronization (ERD) during a recognition task: effect of attention. Electroencephalography and Clinical Neurophysiology. 86**,** 353-356.

Dujardin, K., Bourriez, J.L., Guieu, J.D., 1995. Event-related desynchronization (ERD) patterns during memory processes: effects of aging and task difficulty. Electroencephalogr Clin Neurophysiol. 96**,** 169-82.

Dujardin, K., Defebvre, L., Krystkowiak, P., Blond, S., Destee, A., 2001. Influence of chronic bilateral stimulation of the subthalamic nucleus on cognitive function in Parkinson's disease. Journal of neurology. 248**,** 603-611.

Engel, A.K., Gerloff, C., Hilgetag, C.C., Nolte, G., 2013. Intrinsic coupling modes: multiscale interactions in ongoing brain activity. Neuron. 80**,** 867-886.

Eusebio, A., Thevathasan, W., Doyle Gaynor, L., Pogosyan, A., Bye, E., Foltynie, T., Zrinzo, L., Ashkan, K., Aziz, T., Brown, P., 2011. Deep brain stimulation can suppress pathological synchronisation in parkinsonian patients. J Neurol Neurosurg Psychiatry. 82**,** 569-73.

Feige, B., Aertsen, A., Kristeva-Feige, R., 2000. Dynamic synchronization between multiple cortical motor areas and muscle activity in phasic voluntary movements. Journal of neurophysiology. 84**,** 2622-2629.

Ferraro, F.R., Balota, D.A., Connor, L.T., 1993. Implicit memory and the formation of new associations in nondemented Parkinson's disease individuals and individuals with senile dementia of the Alzheimer type: a serial reaction time (SRT) investigation. Brain Cogn. 21**,** 163-80.

Florin, E., Erasmi, R., Reck, C., Maarouf, M., Schnitzler, A., Fink, G.R., Timmermann, L., 2013. Does increased gamma activity in patients suffering from Parkinson's disease counteract the movement inhibiting beta activity? Neuroscience. 237**,** 42-50.

Floyer-Lea, A., Matthews, P.M., 2004. Changing brain networks for visuomotor control with increased movement automaticity. J Neurophysiol. 92**,** 2405-12.

Frensch, P.A., Lin, J., Buchner, A., 1998. Learning versus behavioral expression of the learned: The effects of a secondary tone-counting task on implicit learning in the serial reaction task. Psychological Research. 61**,** 83-98.

Friston, K.J., Frith, C.D., 1995. Schizophrenia: a disconnection syndrome. Clin Neurosci. 3**,** 89-97.

Garcia, L., Audin, J., D'Alessandro, G., Bioulac, B., Hammond, C., 2003. Dual Effect of High-Frequency Stimulation on Subthalamic Neuron Activity. The Journal of Neuroscience. 23**,** 8743-8751.

George, J.S., Strunk, J., Mak-McCully, R., Houser, M., Poizner, H., Aron, A.R., 2013. Dopaminergic therapy in Parkinson's disease decreases cortical beta band coherence in the resting state and increases cortical beta band power during executive control. NeuroImage: Clinical. 3**,** 261-270.

Gerloff, C., Richard, J., Hadley, J., Schulman, A.E., Honda, M., Hallett, M., 1998a. Functional coupling and regional activation of human cortical motor areas during simple, internally paced and externally paced finger movements. Brain. 121 (Pt 8)**,** 1513-31.

Gerloff, C., Uenishi, N., Hallett, M., 1998b. Cortical activation during fast repetitive finger movements in humans: dipole sources of steady-state movement-related cortical potentials. J Clin Neurophysiol. 15**,** 502-13.

Gerloff, C., Braun, C., Staudt, M., Hegner, Y.L., Dichgans, J., Krageloh-Mann, I., 2006. Coherent corticomuscular oscillations originate from primary motor cortex: evidence from patients with early brain lesions. Hum Brain Mapp. 27**,** 789-98.

Ghilardi, M., Ghez, C., Dhawan, V., Moeller, J., Mentis, M., Nakamura, T., Antonini, A., Eidelberg, D., 2000. Patterns of regional brain activation associated with different forms of motor learning. Brain Res. 871**,** 127-45.

Gibb, W.R., Lees, A.J., 1988. The relevance of the Lewy body to the pathogenesis of idiopathic Parkinson's disease. Journal of Neurology, Neurosurgery & Psychiatry. 51**,** 745-752.

Gomez-Beldarrain, M., Garcia-Monco, J.C., Rubio, B., Pascual-Leone, A., 1998. Effect of focal cerebellar lesions on procedural learning in the serial reaction time task. Exp Brain Res. 120**,** 25-30.

Grafton, S.T., Mazziotta, J.C., Presty, S., Friston, K.J., Frackowiak, R.S., Phelps, M.E., 1992. Functional anatomy of human procedural learning determined with regional cerebral blood flow and PET. J Neurosci. 12**,** 2542-8.

Grafton, S.T., Hazeltine, E., Ivry, R.B., 1998. Abstract and effector-specific representations of motor sequences identified with PET. J Neurosci. 18**,** 9420-8.

Gross, J., Tass, P.A., Salenius, S., Hari, R., Freund, H.J., Schnitzler, A., 2000. Cortico-muscular synchronization during isometric muscle contraction in humans as revealed by magnetoencephalography. J Physiol. 527 Pt 3**,** 623-31.

Guieu, J., Bourriez, J., Derambure, P., Defebvre, L., Cassim, F., 1999. Temporal and spatial aspects of event-related desynchronization and movement-related cortical potentials. Event-Related Desynchronization. Handbook of Electroencephalography and Clinical Neurophysiology. 6**,** 279-290.

Halliday, D.M., Conway, B.A., Farmer, S.F., Rosenberg, J.R., 1998. Using electroencephalography to study functional coupling between cortical activity and electromyograms during voluntary contractions in humans. Neurosci Lett. 241**,** 5-8.

Hari, R., Salenius, S., 1999. Rhythmical corticomotor communication. Neuroreport. 10**,** R1.

Harrison, P.J., 1999. The neuropathology of schizophrenia A critical review of the data and their interpretation. Brain. 122**,** 593-624.

Hashimoto, T., Elder, C.M., Okun, M.S., Patrick, S.K., Vitek, J.L., 2003. Stimulation of the Subthalamic Nucleus Changes the Firing Pattern of Pallidal Neurons. The Journal of Neuroscience. 23**,** 1916-1923.

Hebb, D.O., 2002. The organization of behavior: A neuropsychological theory, Vol., Psychology Press.

Herz, D.M., Siebner, H.R., Hulme, O.J., Florin, E., Christensen, M.S., Timmermann, L., 2013. Levodopa reinstates connectivity from prefrontal to premotor cortex during externally paced movement in Parkinson's disease. NeuroImage.

Hjorth, B., 1980. Source derivation simplifies topographical EEG interpretation. Vol. 20, ed.^eds. American Society of Electroneurodiagnostic Technologists, US, pp. 121-132.

Honda, M., Deiber, M.P., Ibanez, V., Pascual-Leone, A., Zhuang, P., Hallett, M., 1998. Dynamic cortical involvement in implicit and explicit motor sequence learning. A PET study. Brain. 121 (Pt 11)**,** 2159-73.

Hotermans, C., Peigneux, P., Noordhout, D., Maertens, A., Moonen, G., Maquet, P., 2008. Repetitive transcranial magnetic stimulation over the primary motor cortex disrupts early boost but not delayed gains in performance in motor sequence learning. European Journal of Neuroscience. 28**,** 1216-1221.

Hughes, A.J., Daniel, S.E., Lees, A.J., 2001. Improved accuracy of clinical diagnosis of Lewy body Parkinson's disease. Neurology. 57**,** 1497-9.

Hummel, F.C., Gerloff, C., 2006. Interregional long-range and short-range synchrony: a basis for complex sensorimotor processing. Prog Brain Res. 159**,** 223-36.

Hunot, S., Hartmann, A., Hirsch, E.C., 2001. The inflammatory response in the Parkinson brain. Clinical Neuroscience Research. 1**,** 434-443.

Huo, X., Xiang, J., Wang, Y., Kirtman, E.G., Kotecha, R., Fujiwara, H., Hemasilpin, N., Rose, D.F., Degrauw, T., 2010. Gamma oscillations in the primary motor cortex studied with MEG. Brain Dev. 32**,** 619-24.

Jackson, G.M., Jackson, S.R., Harrison, J., Henderson, L., Kennard, C., 1995. Serial reaction time learning and Parkinson's disease: evidence for a procedural learning deficit. Neuropsychologia. 33**,** 577-93.

Jahanshahi, M., 2013. Effects of deep brain stimulation of the subthalamic nucleus on inhibitory and executive control over prepotent responses in Parkinson's disease. Frontiers in Systems Neuroscience. 7**,** 118.

Jankovic, J., 2008. Parkinson's disease: clinical features and diagnosis. J Neurol Neurosurg Psychiatry. 79**,** 368-76.

Jenkins, I., Brooks, D., Nixon, P., Frackowiak, R., Passingham, R., 1994. Motor sequence learning: a study with positron emission tomography. The Journal of Neuroscience. 14**,** 3775-3790.

Jenner, P., 2003. Oxidative stress in Parkinson's disease. Ann Neurol. 53 Suppl 3**,** S26-36; discussion S36-8.

Jurkiewicz, M.T., Gaetz, W.C., Bostan, A.C., Cheyne, D., 2006. Post-movement beta rebound is generated in motor cortex: Evidence from neuromagnetic recordings. NeuroImage. 32**,** 1281-1289.

Karni, A., Meyer, G., Jezzard, P., Adams, M.M., Turner, R., Ungerleider, L.G., 1995. Functional MRI evidence for adult motor cortex plasticity during motor skill learning. Nature. 377**,** 155-8.

Keele, S.W., Jennings, P., Jones, S., Caulton, D., Cohen, A., 1995. On the Modularity of Sequence Representation. Journal of Motor Behavior. 27**,** 17-30.

Kilner, J., Baker, S., Salenius, S., Jousmäki, V., Hari, R., Lemon, R., 1999. Task-dependent modulation of 15-30 Hz coherence between rectified EMGs from human hand and forearm muscles. The Journal of Physiology. 516**,** 559-570.

Kilner, J.M., Baker, S.N., Salenius, S., Hari, R., Lemon, R.N., 2000. Human cortical muscle coherence is directly related to specific motor parameters. J Neurosci. 20**,** 8838-45.

Kleiner-Fisman, G., Herzog, J., Fisman, D.N., Tamma, F., Lyons, K.E., Pahwa, R., Lang, A.E., Deuschl, G., 2006. Subthalamic nucleus deep brain stimulation: summary and meta-analysis of outcomes. Mov Disord. 21 Suppl 14**,** S290-304.

Krack, P., Pollak, P., Limousin, P., Hoffmann, D., Xie, J., Benazzouz, A., Benabid, A.L., 1998. Subthalamic nucleus or internal pallidal stimulation in young onset Parkinson's disease. Brain. 121 (Pt 3), 451-7.

Krack, P., Batir, A., Van Blercom, N., Chabardes, S., Fraix, V., Ardouin, C., Koudsie, A., Limousin, P.D., Benazzouz, A., LeBas, J.F., Benabid, A.L., Pollak, P., 2003. Five-year follow-up of bilateral stimulation of the subthalamic nucleus in advanced Parkinson's disease. N Engl J Med. 349, 1925-34.

Kristeva, R., Patino, L., Omlor, W., 2007. Beta-range cortical motor spectral power and corticomuscular coherence as a mechanism for effective corticospinal interaction during steady-state motor output. NeuroImage. 36, 785-92.

Kuhn, A.A., Kupsch, A., Schneider, G.H., Brown, P., 2006. Reduction in subthalamic 8-35 Hz oscillatory activity correlates with clinical improvement in Parkinson's disease. Eur J Neurosci. 23, 1956-60.

Kuhn, A.A., Kempf, F., Brucke, C., Gaynor Doyle, L., Martinez-Torres, I., Pogosyan, A., Trottenberg, T., Kupsch, A., Schneider, G.H., Hariz, M.I., Vandenberghe, W., Nuttin, B., Brown, P., 2008a. High-frequency stimulation of the subthalamic nucleus suppresses oscillatory beta activity in patients with Parkinson's disease in parallel with improvement in motor performance. J Neurosci. 28, 6165-73.

Kuhn, A.A., Kempf, F., Brucke, C., Gaynor Doyle, L., Martinez-Torres, I., Pogosyan, A., Trottenberg, T., Kupsch, A., Schneider, G.H., Hariz, M.I., Vandenberghe, W., Nuttin, B., Brown, P., 2008b. High-Frequency Stimulation of the Subthalamic Nucleus Suppresses Oscillatory Activity in Patients with Parkinson's Disease in Parallel with Improvement in Motor Performance. Journal of Neuroscience. 28, 6165-6173.

Kühn, A.A., Kupsch, A., Schneider, G.-H., Brown, P., 2006. Reduction in subthalamic 8-35 Hz oscillatory activity correlates with clinical improvement in Parkinson's disease. European Journal of Neuroscience. 23, 1956-1960.

LEES, A.J., SMITH, E., 1983. COGNITIVE DEFICITS IN THE EARLY STAGES OF PARKINSON'S DISEASE. Brain. 106, 257-270.

Leocani, L., Toro, C., Manganotti, P., Zhuang, P., Hallett, M., 1997. Event-related coherence and event-related desynchronization/synchronization in the 10 Hz and 20 Hz EEG during self-paced movements. Electroencephalogr Clin Neurophysiol. 104, 199-206.

Leocani, L., Locatelli, M., Bellodi, L., Fornara, C., Henin, M., Magnani, G., Mennea, S., Comi, G., 2001a. Abnormal pattern of cortical activation associated with voluntary movement in obsessive-compulsive disorder: an EEG study. Am J Psychiatry. 158, 140-2.

Leocani, L., Toro, C., Zhuang, P., Gerloff, C., Hallett, M., 2001b. Event-related desynchronization in reaction time paradigms: a comparison with event-related potentials and corticospinal excitability. Clin Neurophysiol. 112, 923-30.

Limousin, P., Krack, P., Pollak, P., Benazzouz, A., Ardouin, C., Hoffmann, D., Benabid, A.L., 1998. Electrical stimulation of the subthalamic nucleus in advanced Parkinson's disease. N Engl J Med. 339, 1105-11.

Little, S., Pogosyan, A., Neal, S., Zavala, B., Zrinzo, L., Hariz, M., Foltynie, T., Limousin, P., Ashkan, K., FitzGerald, J., 2013. Adaptive deep brain stimulation in advanced Parkinson disease. Annals of neurology. 74, 449-457.

Litvak, V., Eusebio, A., Jha, A., Oostenveld, R., Barnes, G., Foltynie, T., Limousin, P., Zrinzo, L., Hariz, M.I., Friston, K., Brown, P., 2012. Movement-related changes in local and long-range synchronization in Parkinson's disease revealed by simultaneous magnetoencephalography and intracranial recordings. J Neurosci. 32, 10541-53.

Magnani, G., Cursi, M., Leocani, L., Volonte, M.A., Comi, G., 2002. Acute effects of L-dopa on event-related desynchronization in Parkinson's disease. Neurol Sci. 23**,** 91-7.

Manganotti, P., Gerloff, C., Toro, C., Katsuta, H., Sadato, N., Zhuang, P., Leocani, L., Hallett, M., 1998. Task-related coherence and task-related spectral power changes during sequential finger movements. Electroencephalogr Clin Neurophysiol. 109**,** 50-62.

Maris, E., Oostenveld, R., 2007. Nonparametric statistical testing of EEG-and MEG-data. Journal of neuroscience methods. 164**,** 177-190.

Marsden, C.D., 1982. The mysterious motor function of the basal ganglia: the Robert Wartenberg Lecture. Neurology. 32**,** 514-39.

Marsden, J., Limousin-Dowsey, P., Fraix, V., Pollak, P., Odin, P., Brown, P., 2001. Intermuscular coherence in Parkinson's disease: effects of subthalamic nucleus stimulation. Neuroreport. 12**,** 1113-7.

Marusiak, J., Jaskolska, A., Budrewicz, S., Koszewicz, M., Jaskolski, A., 2011. Increased muscle belly and tendon stiffness in patients with Parkinson's disease, as measured by myotonometry. Mov Disord. 26**,** 2119-22.

McFarland, D.J., Miner, L.A., Vaughan, T.M., Wolpaw, J.R., 2000. Mu and beta rhythm topographies during motor imagery and actual movements. Brain Topography. 12**,** 177-186.

McGlashan, T.H., Hoffman, R.E., 2000. Schizophrenia as a disorder of developmentally reduced synaptic connectivity. Archives of General Psychiatry. 57**,** 637-648.

McIntyre, C.C., Savasta, M., Kerkerian-Le Goff, L., Vitek, J.L., 2004. Uncovering the mechanism(s) of action of deep brain stimulation: activation, inhibition, or both. Clin Neurophysiol. 115**,** 1239-48.

McKeown, M.J., Palmer, S.J., Au, W.L., McCaig, R.G., Saab, R., Abu-Gharbieh, R., 2006. Cortical muscle coupling in Parkinson's disease (PD) bradykinesia. J Neural Transm Suppl. 31-40.

Mendez-Balbuena, I., Naranjo, J.R., Wang, X., Andrykiewicz, A., Huethe, F., Schulte-Monting, J., Hepp-Reymond, M.C., Kristeva, R., 2013. The strength of the corticospinal coherence depends on the predictability of modulated isometric forces. J Neurophysiol. 109**,** 1579-88.

Meunier, S., Pol, S., Houeto, J.-L., Vidailhet, M., 2000. Abnormal reciprocal inhibition between antagonist muscles in Parkinson's disease. Brain. 123**,** 1017-1026.

Mima, T., Hallett, M., 1999. Corticomuscular coherence: a review. J Clin Neurophysiol. 16**,** 501-11.

Montgomery, E.B., Jr., Baker, K.B., 2000. Mechanisms of deep brain stimulation and future technical developments. Neurol Res. 22**,** 259-66.

Murthy, V.N., Fetz, E.E., 1992. Coherent 25- to 35-Hz oscillations in the sensorimotor cortex of awake behaving monkeys. Proc Natl Acad Sci U S A. 89**,** 5670-4.

Nenadic, I., Gaser, C., Volz, H.P., Rammsayer, T., Hager, F., Sauer, H., 2003. Processing of temporal information and the basal ganglia: new evidence from fMRI. Exp Brain Res. 148**,** 238-46.

Neuper, C., Pfurtscheller, G., 1996. Post-movement synchronization of beta rhythms in the EEG over the cortical foot area in man. Neurosci Lett. 216**,** 17-20.

Neuper, C., Pfurtscheller, G., 2001. Event-related dynamics of cortical rhythms: frequency-specific features and functional correlates. International Journal of Psychophysiology. 43**,** 41-58.

Nissen, M.J., Bullemer, P., 1987. Attentional requirements of learning: Evidence from performance measures. Cognitive Psychology. 19**,** 1-32.

Nitsche, M.A., Schauenburg, A., Lang, N., Liebetanz, D., Exner, C., Paulus, W., Tergau, F., 2003. Facilitation of implicit motor learning by weak transcranial

direct current stimulation of the primary motor cortex in the human. J Cogn Neurosci. 15**,** 619-26.

Nutt, J.G., Bloem, B.R., Giladi, N., Hallett, M., Horak, F.B., Nieuwboer, A., 2011. Freezing of gait: moving forward on a mysterious clinical phenomenon. The Lancet Neurology. 10**,** 734-744.

Oldfield, R.C., 1971. The assessment and analysis of handedness: the Edinburgh inventory. Neuropsychologia. 9**,** 97-113.

Oostenveld, R., Fries, P., Maris, E., Schoffelen, J.M., 2011. FieldTrip: Open source software for advanced analysis of MEG, EEG, and invasive electrophysiological data. Comput Intell Neurosci. 2011**,** 156869.

Ozkurt, T.E., Butz, M., Homburger, M., Elben, S., Vesper, J., Wojtecki, L., Schnitzler, A., 2011. High frequency oscillations in the subthalamic nucleus: a neurophysiological marker of the motor state in Parkinson's disease. Exp Neurol. 229**,** 324-31.

Parkinson, J., 1817. An essay on the shaking palsy, Vol., Printed by Whittingham and Rowland for Sherwood, Neely, and Jones.

Pascual-Leone, A., Grafman, J., Clark, K., Stewart, M., Massaquoi, S., Lou, J.S., Hallett, M., 1993. Procedural learning in Parkinson's disease and cerebellar degeneration. Ann Neurol. 34**,** 594-602.

Pascual-Leone, A., Grafman, J., Hallett, M., 1994. Modulation of cortical motor output maps during development of implicit and explicit knowledge. Science. 263**,** 1287-9.

Pascual-Leone, A., Grafman, J., Hallett, M., 1995. Procedural learning and prefrontal cortex. Ann N Y Acad Sci. 769**,** 61-70.

Pascual-Leone, A., Wassermann, E.M., Grafman, J., Hallett, M., 1996. The role of the dorsolateral prefrontal cortex in implicit procedural learning. Exp Brain Res. 107**,** 479-85.

Peled, A., Brain “Globalopathies” cause mental disorders. Medical Hypotheses. 81**,** 1046-1055.

Pfurtscheller, G., Aranibar, A., 1979. Evaluation of event-related desynchronization (ERD) preceding and following voluntary self-paced movement. Electroencephalogr Clin Neurophysiol. 46**,** 138-46.

Pfurtscheller, G., 1981. Central beta rhythm during sensorimotor activities in man. Electroencephalogr Clin Neurophysiol. 51**,** 253-64.

Pfurtscheller, G., Berghold, A., 1989. Patterns of cortical activation during planning of voluntary movement. Electroencephalogr Clin Neurophysiol. 72**,** 250-8.

Pfurtscheller, G., 1992. Event-related synchronization (ERS): an electrophysiological correlate of cortical areas at rest. Electroencephalogr Clin Neurophysiol. 83**,** 62-9.

Pfurtscheller, G., Neuper, C., 1992. Simultaneous EEG 10 Hz desynchronization and 40 Hz synchronization during finger movements. Neuroreport. 3**,** 1057-60.

Pfurtscheller, G., Stancak, A., Jr., Neuper, C., 1996. Post-movement beta synchronization. A correlate of an idling motor area? Electroencephalogr Clin Neurophysiol. 98**,** 281-93.

Pfurtscheller, G., Pichler-Zalaudek, K., Ortmayr, B., Diez, J., Reisecker, F., 1998a. Postmovement beta synchronization in patients with Parkinson's disease. J Clin Neurophysiol. 15**,** 243-50.

Pfurtscheller, G., Zalaudek, K., Neuper, C., 1998b. Event-related beta synchronization after wrist, finger and thumb movement. Electroencephalogr Clin Neurophysiol. 109**,** 154-60.

Pfurtscheller, G., Andrew, C., 1999. Event-Related changes of band power and coherence: methodology and interpretation. J Clin Neurophysiol. 16**,** 512-9.

Pfurtscheller, G., Lopes da Silva, F.H., 1999. Event-related EEG/MEG synchronization and desynchronization: basic principles. Clin Neurophysiol. 110**,** 1842-57.

Pirozzolo, F.J., Hansch, E.C., Mortimer, J.A., Webster, D.D., Kuskowski, M.A., 1982. Dementia in Parkinson disease: A neuropsychological analysis. Brain and Cognition. 1**,** 71-83.

Poewe, W., 2008. Non-motor symptoms in Parkinson's disease. European Journal of Neurology. 15**,** 14-20.

Poldrack, R.A., 2000. Imaging brain plasticity: conceptual and methodological issues--a theoretical review. NeuroImage. 12**,** 1-13.

Polymeropoulos, M.H., Lavedan, C., Leroy, E., Ide, S.E., Dehejia, A., Dutra, A., Pike, B., Root, H., Rubenstein, J., Boyer, R., Stenroos, E.S., Chandrasekharappa, S., Athanassiadou, A., Papapetropoulos, T., Johnson, W.G., Lazzarini, A.M., Duvoisin, R.C., Di Iorio, G., Golbe, L.I., Nussbaum, R.L., 1997. Mutation in the alpha-synuclein gene identified in families with Parkinson's disease. Science. 276**,** 2045-7.

Qassim, Y.T., Cutmore, T.R., James, D.A., Rowlands, D.D., 2013. Wavelet coherence of EEG signals for a visual oddball task. Comput Biol Med. 43**,** 23-31.

Raoul, S., Roualdes, V., Deligny, C., Leduc, D., Lamy, J.-C., Lackmy-Vallée, A., N'Guyen, J.-P., Damier, P., Katz, R., 2012. Subthalamic nucleus stimulation reverses spinal motoneuron activity in parkinsonian patients. Brain. 135**,** 139-147.

Rappelsberger, P., Pfurtscheller, G., Filz, O., 1994. Calculation of event-related coherence--a new method to study short-lasting coupling between brain areas. Brain Topography. 7**,** 121-7.

Rippon, G., Brock, J., Brown, C., Boucher, J., 2007. Disordered connectivity in the autistic brain: Challenges for the 'new psychophysiology'. International Journal of Psychophysiology. 63**,** 164-172.

Robertson, E.M., Tormos, J.M., Maeda, F., Pascual-Leone, A., 2001. The role of the dorsolateral prefrontal cortex during sequence learning is specific for spatial information. Cereb Cortex. 11**,** 628-35.

Rocchi, L., Chiari, L., Horak, F.B., 2002. Effects of deep brain stimulation and levodopa on postural sway in Parkinson's disease. J Neurol Neurosurg Psychiatry. 73**,** 267-74.

Rodriguez-Oroz, M.C., Obeso, J.A., Lang, A.E., Houeto, J.L., Pollak, P., Rehncrona, S., Kulisevsky, J., Albanese, A., Volkmann, J., Hariz, M.I., Quinn, N.P., Speelman, J.D., Guridi, J., Zamarbide, I., Gironell, A., Molet, J., Pascual-Sedano, B., Pidoux, B., Bonnet, A.M., Agid, Y., Xie, J., Benabid, A.L., Lozano, A.M., Saint-Cyr, J., Romito, L., Contarino, M.F., Scerrati, M., Fraix, V., Van Blercom, N., 2005. Bilateral deep brain stimulation in Parkinson's disease: a multicentre study with 4 years follow-up. Brain. 128**,** 2240-9.

Romano, J.C., Howard, J.H., Jr., Howard, D.V., 2010. One-year retention of general and sequence-specific skills in a probabilistic, serial reaction time task. Memory. 18**,** 427-41.

Rosenkranz, K., Kacar, A., Rothwell, J.C., 2007. Differential modulation of motor cortical plasticity and excitability in early and late phases of human motor learning. The Journal of Neuroscience. 27**,** 12058-12066.

Salenius, S., Portin, K., Kajola, M., Salmelin, R., Hari, R., 1997. Cortical control of human motoneuron firing during isometric contraction. J Neurophysiol. 77**,** 3401-5.

Salenius, S., Avikainen, S., Kaakkola, S., Hari, R., Brown, P., 2002. Defective cortical drive to muscle in Parkinson's disease and its improvement with levodopa. Brain. 125**,** 491-500.

Salmelin, R., Hámáaláinen, M., Kajola, M., Hari, R., 1995. Functional Segregation of Movement-Related Rhythmic Activity in the Human Brain. NeuroImage. 2**,** 237-243.

Sampaio-Baptista, C., Khrapitchev, A.A., Foxley, S., Schlagheck, T., Scholz, J., Jbabdi, S., DeLuca, G.C., Miller, K.L., Taylor, A., Thomas, N., Kleim, J., Sibson, N.R., Bannerman, D., Johansen-Berg, H., 2013. Motor Skill Learning Induces Changes in White Matter Microstructure and Myelination. The Journal of Neuroscience. 33**,** 19499-19503.

Schiesling, C., Kieper, N., Seidel, K., Kruger, R., 2008. Review: Familial Parkinson's disease--genetics, clinical phenotype and neuropathology in relation to the common sporadic form of the disease. Neuropathol Appl Neurobiol. 34**,** 255-71.

Schoffelen, J.M., Oostenveld, R., Fries, P., 2005. Neuronal coherence as a mechanism of effective corticospinal interaction. Science. 308**,** 111-3.

Schuepbach, W.M., Rau, J., Knudsen, K., Volkmann, J., Krack, P., Timmermann, L., Halbig, T.D., Hesekamp, H., Navarro, S.M., Meier, N., Falk, D., Mehdorn, M., Paschen, S., Maarouf, M., Barbe, M.T., Fink, G.R., Kupsch, A., Gruber, D., Schneider, G.H., Seigneuret, E., Kistner, A., Chaynes, P., Ory-Magne, F., Brefel Courbon, C., Vesper, J., Schnitzler, A., Wojtecki, L., Houeto, J.L., Bataille, B., Maltete, D., Damier, P., Raoul, S., Sixel-Doering, F., Hellwig, D., Gharabaghi, A., Kruger, R., Pinsker, M.O., Amtage, F., Regis, J.M., Witjas, T., Thobois, S., Mertens, P., Kloss, M., Hartmann, A., Oertel, W.H., Post, B., Speelman, H., Agid, Y., Schade-Brittinger, C., Deuschl, G., 2013. Neurostimulation for Parkinson's disease with early motor complications. N Engl J Med. 368**,** 610-22.

Schwab, R.S., Chafetz, M.E., Walker, S., 1954. Control of two simultaneous voluntary motor acts in normals and in parkinsonism. AMA Arch Neurol Psychiatry. 72**,** 591-8.

Schwarb, H., Schumacher, E.H., 2010. Implicit sequence learning is represented by stimulus-response rules. Mem Cognit. 38**,** 677-88.

Seitz, R.J., Roland, E., Bohm, C., Greitz, T., Stone-Elander, S., 1990. Motor learning in man: a positron emission tomographic study. Neuroreport. 1**,** 57-60.

Seitz, R.J., Roland, P.E., 1992. Learning of Sequential Finger Movements in Man: A Combined Kinematic and Positron Emission Tomography (PET) Study. Eur J Neurosci. 4**,** 154-165.

Serrien, D.J., Brown, P., 2002. The functional role of interhemispheric synchronization in the control of bimanual timing tasks. Exp Brain Res. 147**,** 268-72.

Sherer, T.B., Kim, J.H., Betarbet, R., Greenamyre, J.T., 2003. Subcutaneous rotenone exposure causes highly selective dopaminergic degeneration and alpha-synuclein aggregation. Exp Neurol. 179**,** 9-16.

Silberstein, P., Pogosyan, A., Kuhn, A.A., Hotton, G., Tisch, S., Kupsch, A., Dowsey-Limousin, P., Hariz, M.I., Brown, P., 2005. Cortico-cortical coupling in Parkinson's disease and its modulation by therapy. Brain. 128**,** 1277-91.

Sporns, O., Tononi, G., Kötter, R., 2005. The human connectome: a structural description of the human brain. PLoS computational biology. 1**,** e42.

Stancak, A., Jr., Pfurtscheller, G., 1996a. The effects of handedness and type of movement on the contralateral preponderance of mu-rhythm desynchronisation. Electroencephalogr Clin Neurophysiol. 99**,** 174-82.

Stancak, A., Jr., Pfurtscheller, G., 1996b. Mu-rhythm changes in brisk and slow self-paced finger movements. Neuroreport. 7**,** 1161-4.

Sterman, M.B., Kaiser, D., Veigel, B., 1996. Spectral analysis of event-related EEG responses during short-term memory performance. Brain Topography. 9**,** 21-30.

Sulzer, D., 2007. Multiple hit hypotheses for dopamine neuron loss in Parkinson's disease. Trends Neurosci. 30**,** 244-50.

Sun, F.T., Miller, L.M., Rao, A.A., D'Esposito, M., 2007. Functional connectivity of cortical networks involved in bimanual motor sequence learning. Cerebral Cortex. 17**,** 1227-1234.

Swerdlow, N.R., Braff, D., Geyer, M., 2000. Animal models of deficient sensorimotor gating: what we know, what we think we know, and what we hope to know soon. Behavioural pharmacology. 11**,** 185-204.

Swerdlow, R.H., Parks, J.K., Miller, S.W., Tuttle, J.B., Trimmer, P.A., Sheehan, J.P., Bennett, J.P., Jr., Davis, R.E., Parker, W.D., Jr., 1996. Origin and functional consequences of the complex I defect in Parkinson's disease. Ann Neurol. 40**,** 663-71.

Tai, C.H., Boraud, T., Bezard, E., Bioulac, B., Gross, C., Benazzouz, A., 2003. Electrophysiological and metabolic evidence that high-frequency stimulation of the subthalamic nucleus bridles neuronal activity in the subthalamic nucleus and the substantia nigra reticulata. Faseb J. 17**,** 1820-30.

Thatcher, R., McAlaster, R., Lester, M., Horst, R., Cantor, D., 1983. Hemispheric EEG asymmetries related to cognitive functioning in children. Cognitive processing in the right hemisphere. 125-146.

Toro, C., Deuschl, G., Thatcher, R., Sato, S., Kufta, C., Hallett, M., 1994. Event-related desynchronization and movement-related cortical potentials on the ECoG and EEG. Electroencephalogr Clin Neurophysiol. 93**,** 380-9.

Torriero, S., Oliveri, M., Koch, G., Caltagirone, C., Petrosini, L., 2004. Interference of left and right cerebellar rTMS with procedural learning. J Cogn Neurosci. 16**,** 1605-11.

Troche, M.S., Okun, M.S., Rosenbek, J.C., Altmann, L.J., Sapienza, C.M., 2014. Attentional resource allocation and swallowing safety in Parkinson's disease: A dual task study. Parkinsonism & related disorders. 20**,** 439-443.

Uhlhaas, P.J., Singer, W., Neural Synchrony in Brain Disorders: Relevance for Cognitive Dysfunctions and Pathophysiology. Neuron. 52**,** 155-168.

Uhlhaas, P.J., 2013. Dysconnectivity, large-scale networks and neuronal dynamics in schizophrenia. Current Opinion in Neurobiology. 23**,** 283-290.

Volgushev, M., Chistiakova, M., Singer, W., 1998. Modification of discharge patterns of neocortical neurons by induced oscillations of the membrane potential. Neuroscience. 83**,** 15-25.

von der Malsburg, C., Schneider, W., 1986. A neural cocktail-party processor. Biol Cybern. 54**,** 29-40.

von Stein, A., Sarnthein, J., 2000. Different frequencies for different scales of cortical integration: from local gamma to long range alpha/theta synchronization. International Journal of Psychophysiology.

Wang, H.C., Lees, A.J., Brown, P., 1999. Impairment of EEG desynchronisation before and during movement and its relation to bradykinesia in Parkinson's disease. J Neurol Neurosurg Psychiatry. 66**,** 442-6.

Wang, J., Zuo, X., Dai, Z., Xia, M., Zhao, Z., Zhao, X., Jia, J., Han, Y., He, Y., 2013. Disrupted Functional Brain Connectome in Individuals at Risk for Alzheimer's Disease. Biological Psychiatry. 73**,** 472-481.

Warner, T.T., Schapira, A.H., 2003. Genetic and environmental factors in the cause of Parkinson's disease. Ann Neurol. 53 Suppl 3**,** S16-23; discussion S23-5.

Wassermann, E.M., McShane, L.M., Hallett, M., Cohen, L.G., 1992. Noninvasive mapping of muscle representations in human motor cortex. Electroencephalography and Clinical Neurophysiology/Evoked Potentials Section. 85**,** 1-8.

Weaver, F.M., Follett, K., Stern, M., Hur, K., Harris, C., Marks, W.J., Jr., Rothlind, J., Sagher, O., Reda, D., Moy, C.S., Pahwa, R., Burchiel, K., Hogarth, P., Lai, E.C., Duda, J.E., Holloway, K., Samii, A., Horn, S., Bronstein, J., Stoner, G.,

Heemskerk, J., Huang, G.D., 2009. Bilateral deep brain stimulation vs best medical therapy for patients with advanced Parkinson disease: a randomized controlled trial. JAMA. 301**,** 63-73.

Weiss, D., Govindan, R.B., Rilk, A., Wachter, T., Breit, S., Zizlsperger, L., Haarmeier, T., Plewnia, C., Kruger, R., Gharabaghi, A., 2011. Central oscillators in a patient with neuropathic tremor: evidence from intraoperative local field potential recordings. Mov Disord. 26**,** 323-7.

Weiss, D., Breit, S., Hoppe, J., Hauser, A.K., Freudenstein, D., Kruger, R., Sauseng, P., Govindan, R.B., Gerloff, C., 2012. Subthalamic nucleus stimulation restores the efferent cortical drive to muscle in parallel to functional motor improvement. Eur J Neurosci. 35**,** 896-908.

Weiss, D., Walach, M., Meisner, C., Fritz, M., Scholten, M., Breit, S., Plewnia, C., Bender, B., Gharabaghi, A., Wächter, T., 2013. Nigral stimulation for resistant axial motor impairment in Parkinson's disease? A randomized controlled trial. Brain. 136**,** 2098-2108.

Williams, D., Kuhn, A., Kupsch, A., Tijssen, M., van Bruggen, G., Speelman, H., Hotton, G., Loukas, C., Brown, P., 2005. The relationship between oscillatory activity and motor reaction time in the parkinsonian subthalamic nucleus. Eur J Neurosci. 21**,** 249-58.

Willingham, D.B., Nissen, M.J., Bullemer, P., 1989. On the development of procedural knowledge. J Exp Psychol Learn Mem Cogn. 15**,** 1047-60.

Willingham, D.B., 1998. A neuropsychological theory of motor skill learning. Psychol Rev. 105**,** 558-84.

Womelsdorf, T., Schoffelen, J.M., Oostenveld, R., Singer, W., Desimone, R., Engel, A.K., Fries, P., 2007. Modulation of neuronal interactions through neuronal synchronization. Science. 316**,** 1609-12.

Wu, T., 2005. A functional MRI study of automatic movements in patients with Parkinson's disease. Brain. 128**,** 2250-2259.

Wu, T., Hallett, M., 2005. A functional MRI study of automatic movements in patients with Parkinson's disease. Brain. 128**,** 2250-9.

Wu, T., Wang, L., Chen, Y., Zhao, C., Li, K., Chan, P., 2009. Changes of functional connectivity of the motor network in the resting state in Parkinson's disease. Neuroscience Letters. 460**,** 6-10.

Wu, X., Li, W., Shen, S., Zheng, X., Zhang, Y., Hou, W., 2013. Corticomuscular coherence modulation with the pattern of finger force coordination. IEEE Trans Neural Syst Rehabil Eng. 21**,** 812-9.

Yang, Y., Lisberger, S.G., 2013. Interaction of plasticity and circuit organization during the acquisition of cerebellum-dependent motor learning. eLife. 2**,** e01574.

Zhuang, P., Toro, C., Grafman, J., Manganotti, P., Leocani, L., Hallett, M., 1997. Event-related desynchronization (ERD) in the alpha frequency during development of implicit and explicit learning. Electroencephalogr Clin Neurophysiol. 102**,** 374-81.

Ziemann, U., Iliać, T.V., Pauli, C., Meintzschel, F., Ruge, D., 2004. Learning modifies subsequent induction of long-term potentiation-like and long-term depression-like plasticity in human motor cortex. The Journal of Neuroscience. 24**,** 1666-1672.

8 Erklärung zum Eigenanteil der Dissertationsschrift

Die Konzeption der Studie erfolgte in Zusammenarbeit mit Dr. med. Daniel Weiß, Prof. Dr. med. Rejko Krüger, Dr. med. Tobias Wächter und Prof. Dr. med. Alireza Gharabaghi.

Sämtliche Versuche wurden von mir nach Einarbeitung eigenständig durchgeführt und dokumentiert.

Die statistische Auswertung habe ich mit Unterstützung durch Dr. med. Daniel Weiß, Rathinaswamy Govindan, Dr. biol. hum. Christoph Meißner durchgeführt.

Ich versichere, die Dissertationsschrift selbständig verfasst zu haben und keine weiteren als die von mir angegebenen Quellen verwendet zu haben.

Heidelberg, den

Parts of this work have been published elsewhere:

Weiss, D.; Klotz, R.; Govindan, R.; Scholten, M.; Naros, G.; Ramos-Murguialday, A.; Bunjes, F.; Meisner, C.; Plewnia, C.; Krüger, R.; Gharabaghi, A. Subthalamic stimulation modulates cortical motor network activity and synchronization in Parkinson's Disease. BRAIN [in press]

9 Acknowledgement

Ich möchte mich herzlich bei allen bedanken, die zum Gelingen dieser Dissertation beigetragen haben.

Insbesondere danke ich Herrn Dr. med. Daniel Weiss für seine unermüdliche Unterstützung bei allen Arbeitsschritten dieser Dissertation, aber besonders bei der Bearbeitung und Analyse des umfangreichen und komplexen Datenmaterials. Seine Geduld, Kompetenz und Erfahrung waren unverzichtbar.

Durch den intensiven wissenschaftlichen Austausch innerhalb der „Lab meetings“ der Arbeitsgruppe für „Deep brain Stimulation“ unter Leitung von Prof. Dr. med. Reijko Krüger habe ich sehr viel gelernt. Deshalb bedanke ich mich für die anregenden und interessanten Diskussionen bei der gesamten Arbeitsgruppe und besonders bei Herrn Prof. Dr. med. Reijko Krüger vielmals.

Weiterhin möchte ich mich ausdrücklich bedanken bei Dr. med. Tobias Wächter für seine kompetente Unterstützung bezüglich des SRTT-Paradigmas und der Analysen sowie bei Dr. med. Georgius Naros, der bei den Messungen ein wichtiger Ansprechpartner war. Ebenso danke ich Herrn Dr. rer. nat. Friedemann Bunjes, Herrn Rathinaswamy B. Govindan, Herrn Ander Ramos-Murguialday und Herrn Christoph Meißner für ihre unkomplizierte und kompetente Hilfe beim Programmieren und der Statistik.

Von ganzem Herzen danke ich außerdem meinen Eltern, meiner Schwester und allen meinen Freunden, die mich über die Jahre begleitet und durch ihren Zuspruch motiviert und gestärkt und so das Gelingen dieser Arbeit ermöglicht haben.